JOURNAL OF ADVANCES IN

ENGINEERING AND TECHNOLOGY

VOLUME 1, ISSUE 1
SEPTEMBER 2022

ISSN 2950 - 7138 (PRINTED)
ISSN 2961 - 5410 (ONLINE)

ivil Engineering | Electrical and Electronic Engineering | Materials Engineering | Mechanical Engineering | Mechatronics Engineering | Quantity Surveying

About the Journal of Advances in Engineering and Technology

The Journal of Advances in Engineering and Technology (JAET) is an international, open access, double blind peer-reviewed journal. It is published by the Faculty of Engineering of Sri Lanka Institute of Information Technology (SLIIT). The JAET aims at fostering research and development work in Engineering and Technology and bringing researchers on to a common platform. Furthermore, JAET will also accept review articles on appropriate subject areas including concept papers of academic opinions, book reviews, etc. for publication therein.

The views and opinions expressed by the authors are their own and would not necessarily reflect the views of the Faculty of Engineering. The research articles submitted to JAET have not been nor envisaged to be published elsewhere and will not simultaneously be published elsewhere. It is also stated that at time of acceptance to publish an article submitted to JAET, the authors agree that the copyright for their accepted articles is transferred to JAET. The copyright covers the exclusive right to reproduce and distribute the article in any form by JAET without the permission of the author.

Notes for the authors: Please see page VI

All correspondence should be addressed to:

Editor-in-Chief
Journal of Advances in Engineering and Technology
Faculty of Engineering
SLIIT
Kandy Road, Malabe, 10115
Sri Lanka

Email: **jaet@sliit.lk**

Official website: **https://jaet.sliit.lk**

ISSN 2950-7138 (Printed)

ISSN 2961 - 5410 (Online)

Randhi Printers: No. 22 Sesatha Watta, Waduramulla, Panadura

Journal of Advances in Engineering and Technology (JAET)

Volume 1 Issue (1)-2022

Sri Lanka Institute of Information Technology
Malabe, Sri Lanka

Journal of Advances in Engineering and Technology

Volume 01, Issue 01, 2022

Contents

Faculty of Engineering

Sri Lanka Institute of Information Technology (SLIIT)

Malabe, 10115, Sri Lanka

EDITORIAL TEAM

Notes to the Authors

Journal of Advances in Engineering and Technology (JAET) is a biannual peer review journal which aims at publishing original, theoretical and practice-oriented research papers related to Engineering and Technology. This journal provides a forum for researchers, scholars, academicians, and practitioners in the field of Engineering at international level to discuss and disseminate their findings in advanced and emerging technologies in Engineering.

Articles/ contributions should be sent to:

Editor-in-Chief
Journal of Advances in Engineering and Technology (JAET)
Faculty of Engineering
SLIIT , New Kandy Road, Malabe, Sri Lanka
E – mail: jaet@sliit.lk

- Your article will be subjected to a double-blind review process by two reviewers who are experts in their relevant field. In order to facilitate anonymous review process, you are requested to provide the title page separately.
- The title page should include the title of the article, your full name, affiliation, address, email and telephone/ mobile number.
- Recommendations of two reviewers are necessary for the publication of your article.
- The article should not exceed 6,000 words.
- Abstract should be between 150-200 words with 4-5 keywords.
- Article should include the following:
- Introduction to the research statement/ background to the research/ rationale
- Methods and Material
- Results and Discussion
- Conclusions and Recommendations
- References
- Footnotes can be numbered and given at the end of the article.
- Referencing should conform to the APA style.
- Tables/ graphs should be included in the appropriate places. Longer tables should be added at the end of the article as annexes.
- Use Times New Roman Fonts - Abstract 11pt; Article 11pt; Spacing Single

Message from the Chancellor

I am very happy to note the launch of the journal by the Faculty of Engineering on 'Advances in Engineering and Technology" which is a timely subject providing a new level of knowledge in an area where constant development in theories and methodologies transpire. This is a collective effort to broaden the scope and coverage that researchers across the institute that can contribute to the publication.

It is an integral part of our education culture at SLIIT to encourage our budding researchers to publish their research output in the form of journal articles. SLIIT is the largest private university in the country consisting of research scholars, postgraduate, and undergraduate students and our aim is to provide the students a platform to publish their research work. Therefore, journal publications of this caliber will certainly cover all aspects of Engineering and affiliated fields and inculcate innovative ideas among the participants paving way for more greater academic research in the future.

Publication of a journal benefits the university in many ways as much as it does the participants. Students can share new innovations, methodologies, research, and development amongst the fraternity which contributes to the overall growth of the community and society at large. We wish to see this momentum continue and expect greater results from participants as they embark into the future of the Engineering and Technological world.

I would like to thank and congratulate all the contributors, and the Editorial team for bringing out this Journal and wish all the success in future publications as well.

Prof. Lakshman Ratnayake
Chancellor / SLIIT

Message from the Vice Chancellor

We are pleased to announce the publication of the inaugural volume of the "Journal of Advances in Engineering and Technology," a new research journal launched by the Faculty of Engineering and devoted to advancing engineering and technological disciplines, providing researchers with a platform from which to disseminate their valuable research findings and the opportunity to network with their peers in both the local and international research communities.

Research is a fundamental component and a responsibility of a university that will ultimately benefit the society as a whole. Hence it is indeed a timely initiative taken by the Faculty of Engineering to launch this journal and website to spread knowledge created by the researchers which is rich yet vivid. Our goals in launching this journal are twofold: to become the preeminent provider in Sri Lanka for Research Findings from the ever-expanding field of Engineering and Technology, and to provide a high-quality publication platform for cutting-edge research which are contemporary and impactful for the same fields.

And while I applaud the researchers in the Faculty of Engineering for their tireless efforts to boost the Faculty and SLIIT's research profile, volume, and influence, I am confident that this new initiative will yield even greater benefits and positive exposure for the institution. This journal will forge one of the key pillars envisioned by SLIIT's strategic plan for fostering a conducive landscape for high-end research.

I would like to extend my sincere appreciation to the Dean of the Faculty, Editor-in-Chief and the Editorial Committee for their dedication. We hope you enjoy reading the first of many issues to come, and we invite you and your colleagues to contribute to the subsequent issues of JAET. I would like to wish the "Journal of Advances in Engineering and Technology" all the success in its mission to serve as a definitive resource for ground-breaking research in the fields of Engineering and Technology.

Professor Lalith Gamage
Vice-Chancellor / CEO - SLIIT

Message from the Deputy Vice Chancellor

It gives me great pleasure to send this congratulatory message to the SLIIT Faculty of Engineering on the occasion of launching the inaugural issue of the Journal of Advances in Engineering and Technology. Since its inception, the Faculty of Engineering at SLIIT has demonstrated a solid commitment to research and dissemination of knowledge. It is, therefore, natural for the Faculty to launch a research journal to establish its leadership position in research and international collaboration. The Faculty has also launched an international conference to enhance its profile, promote collaboration and attract full-length papers to the journal.

Under the leadership of Prof. Saman Thilakasiri, Dean of the Faculty of Engineering, the research activities have grown. I am pleased to note that several scholars from engineering are included in the AD International Research Ranking. Funding has been secured from the World Bank, European Union and other partners to strengthen research and attract research students. Many initiatives are underway to enhance the research stature and output further. Launching this journal will provide opportunities for the Faculty to grow research partnerships and broaden its research network. I am confident that the journal will attract high-quality international papers and establish itself as a premier journal in the region in due course. It also has a high potential to become an indexed journal based on the published papers and the editorial team's reputation.

The journal is a timely and strategic initiative of the Faculty of Engineering. I wish the Editors and the Editorial Board continued success with the journal.

Professor Nimal Rajapakse
Deputy Vice-Chancellor / SLIIT

Message from the Dean, Faculty of Engineering

I give this congratulatory message to the inaugural volume of the research journal of the Faculty of Engineering, named the "Journal of Advances in Engineering and Technology" with immense pleasure.

At the outset, I thank the Editorial board members of the Journal for the excellent job they did by reviewing the submitted research papers using the double-blind review process and getting the other publication requirements of the first volume of the journal successfully. This will be a beginning of new era and this Journal will be published bi-annually, once in parallel with the SICET conference conducted by the faculty.

In parallel with the development of undergraduate programs of the faculty, we developed our Postgraduate research programs leading up to MPhil and PhD degrees, for which we were given permission by Ministry of Higher Education (MoH), Sri Lanka in 2015 after a thorough inspection of our capabilities. We take a genuine effort to disseminate our research in indexed journal and conference proceedings, and have a very good publication record over the past few years. We started this Journal with the idea of developing further research collaborations with the industry and other research institutions. I believe this Journal gives an excellent opportunity to achieve these objectives and I give my warm wishes for its future success!

Professor Saman Thilakasiri
Dean, Faculty of Engineering / SLIIT

Message from the Editor – in- Chief, Faculty of Graduate Studies and Research

I am extremely pleased and honored to be appointed as the Editor-in-Chief of the Journal of Advances in Engineering and Technology (JAET) of the Faculty of Engineering of the Sri Lanka Institute of Information Technology (SLIIT) and extend this message in its inaugural Issue. As the Editor-in-Chief, I am also proud of being associated with an outstanding and dedicated editorial committee. Furthermore, I am also honored to be engaged with a globally represented and recognized team representing the Advisory Board of JAET.

Our team will endeavor in ensuring the research published in JAET would encompass the work representing diverse parts of the globe highlighting the key developments in Engineering and Technology and potentially of multi-disciplinary nature. Furthermore, we recognize the emphasis that the authors place on high quality, transparent peer reviewing process in a timely manner. The editorial committee has engaged a well experienced, efficient and dedicated reviewing team to ensure this high quality, transparent and timely reviewing process.

We believe that this research journal would not only designate a landmark in the research landscape of the Faculty of Engineering but would also assist positioning the Sri Lanka Institute of Information Technology to higher elevations.

I am truly excited to have been assigned to steer this very important and new task of the Faculty of Engineering envisioning a change in the dynamics of its research culture. I would like to sincerely thank the leadership of SLIIT, the Chancellor, Vice-Chancellor and Deputy Vice Chancellor (Academic) and also the Dean of the Faculty of Engineering for all the encouragement and support extended in this regard. My sincere appreciations are also presented to the contributing authors to this first issue and the Editorial Committee for all its untiring efforts in bringing this first issue into realization.

Professor Rahula Attalage
Editor-in-Chief - Faculty of Graduate Studies and Research / SLIIT

Application of Sentinel-2 Satellite Data to Map Forest Cover in Southeast Sri Lanka through the Random Forest Classifier

Thakshila Gunawansa
School of Surveying and Built Environment, University of Southern Queensland,
West Street, Toowoomba, 4350 QLD, Australia
Department of Engineering Technology, Faculty of Technological Studies,
Uva Wellassa University, Passara Road, Badulla, Sri Lanka.
u1129332@umail.usq.edu.au, thakshila@uwu.ac.lk

Kithsiri Perera
School of Surveying and Built Environment, University of Southern Queensland,
West Street, Toowoomba, 4350 QLD, Australia
Kithsiri.Perera@usq.edu.au

Armando Apan
School of Surveying and Built Environment, University of Southern Queensland,
West Street, Toowoomba, 4350 QLD, Australia
Armando.Apan@usq.edu.au

Nandita Hettiarachchi
Department of Mechanical and Manufacturing Engineering, Faculty of Engineering,
University of Ruhuna, Hapugala, Galle, Sri Lanka
nandita@mme.ruh.ac.lk

ABSTRACT

Sentinel-2 satellite data has been used for forest cover monitoring for almost five years. Mapping with Sentinel data will be a cost-effective solution for Sri Lanka, where the lack of updated land cover maps with high spatial resolution is a significant challenge in the land resource management of the country. A study area of about 5,000 km2 located in southeast Sri Lanka was selected for this study. Agricultural lands, forests including Yala national park, and villages with perennial crops make up the region. A Level-2A Sentinel-2 image with less than 10 percent cloud cover was used in the European Space Agency's (ESA) SNAP software version 8.0.0 for image processing and the forest cover of the study area was mapped through the Random Forest classifier (RFC). Normalized Difference Vegetation Index (NDVI) is also calculated as a Sentinel product to support RFC output. For RFC, ground truth data were collected through the reference of Google Earth high-resolution data. The classification accuracy was assessed using the Google Earth image as the reference dataset. Furthermore, RFC results were compared with NVDI greenness values. The classification accuracy was calculated using a confusion matrix (error matrix) through randomly selected 100 sample points. The overall accuracy of the land cover map was 85 percent, with a 96 percent accuracy for forest cover identification. The study found RFC as an effective method to isolate forest cover in Sri Lanka.

KEYWORDS: *Sentinel-2, Random Forest Classifier, Land cover classification, Land cover mapping, Normalized Difference Vegetation Index.*

1 INTRODUCTION

Humans rely on forests for necessities such as livelihoods, shelter, food, and energy. Beyond these, the forest ecosystem is essential for biogeochemical cycle regulation, carbon sequestration, climate, and support services needed to maintain waste management and detoxification (Aznar-Sánchez et al., 2018; Sheeren et al., 2016). The global land cover has been rapidly changing due to urbanization, agricultural expansion, fire, fuelwood gathering, invasive species, and climate changes (Murayama & Ranagalage, 2020). Adverse impacts include biodiversity loss, decreasing land productivity, and changing climate conditions. Due to these changes impacting human life, effective monitoring

mechanisms ensure that natural resources are used correctly. As a result, accurate and up-to-date forest cover mapping has become a valuable resource for agriculture monitoring, land policy development, land cover assessment, forest monitoring and management, scientific research, urban planning, and conservation (Grabska et al., 2019; Thanh Noi & Kappas, 2017). Several studies have been conducted globally on deforestation, degradation, and interventions (Ranagalage et al., 2020).

South Asia is an economically developing region with a rapidly growing population. Sri Lanka is a 65,525 km2 tropical island in the Indian Ocean, located between 5◦55'–9◦51' N latitude and 79◦52'–81◦51' E longitude. Sri Lanka has a unique and diversified ecosystem due to its central hilly topography and extensive waterways. As a result, the geographical patterns of wind, rainfall, temperature, relative humidity, and other climatic components are influenced by topographical variances of diverse regions, such as the central highlands and lowland plains extending to the coastline zone. The country's annual rainfall ranges from less than 1000 mm per year in the southeast and northwest to more than 2500 mm per year in the central mountains.

Population growth has increased in Sri Lanka's agriculture sector activities, particularly in rural areas. The rural population has increased dramatically from 14.1 million in 1990 to 17.8 million in 2020 with the advancement of the country's free healthcare system (Rural population Sri Lanka, 2021). Population and agriculture growth have put tremendous pressure on land utilization (Perera & Tateishi, 2012). Due to the open economic policy implemented in the late 1970s, socio-economic and political changes occurred, and many development projects began. These projects included the development of the Mahaweli river basin, transportation and highway, and rural urbanization (Rathnayake et al., 2020). From 1980 to 2009, Sri Lanka has suffered a civil war, particularly in the North and the East (Höglund & Svensson, 2009). Unfortunately, land cover mapping records for these periods are limited.

Forest loss in Sri Lanka has escalated in the last few decades. It shows that 23,217 km2 of forests in 1976 decreased to 21,936 km2 in 2014, a net loss of 1281 km2 (5.5%) in four decades (Nisansala et al., 2020; Sudhakar Reddy et al., 2017). However, to understand the patterns of forest cover changes and their drivers, Sri Lanka needs comprehensive studies that use robust analytical techniques and available data (Rathnayake et al., 2020). The demand for reliable information on the county's forest cover has grown in the past decades. Furthermore, the available studies are highly localized ,obsolete and restricted to bitemporal comparisons (Rathnayake et al., 2020).

Remote sensing is the technology of detecting and monitoring the physical characteristics of an area by measuring its reflected and emitted radiation at a distance (typically from a satellite or an aircraft). Unique cameras collect remotely sensed images, which help researchers "sense" things about the Earth. Furthermore, remote sensing is an effective method for collecting spatially explicit information on the Earth's surface, such as forests (Belgiu & Drăgu, 2016).

The Sentinel-2 multispectral products produced by the ESA and the European Union (EU) as a part of the Copernicus Programme have contributed to effectively monitoring the Earth's surface. Sentinel-2 satellites contain multispectral scanners onboard and are the second constellation of the ESA Sentinel missions. Sentinel-2's main objective is to deliver high-resolution satellite data for spatial planning, agricultural and environmental monitoring, water monitoring, forest and vegetation monitoring, land carbon monitoring, natural resource monitoring, and global crop monitoring (SUHET, 2015). In addition, many research studies on land cover/use classification have used Sentinel-2 pictures since the launch of the Sentinel-2 multispectral detectors in 2015. In addition, Sentinel-2 can map and monitor forest regions and measure biophysical structures of vegetation (Askar et al., 2018).

Sentinel-2 is regularly used to map forests in many research studies. Table 1 presents the Sentinel-2 product types. Sentinel-2 satellite data shows ample potential for improving forest classification at medium to large scales because of the availability of high spatial resolution.

Sentinel-2 sensed data used to determine the status of Sri Lanka's southeast forest cover and forecast future changes. Also, land cover mapping with Sentinel data will be a cost-effective solution for Sri Lanka, where the lack of updated land cover maps is a significant challenge in land resource management.

RFC is a powerful machine learning classifier that produces multiple decision trees using a randomly selected subset of training samples and variables. It provides an algorithm for estimating missing values and flexibility in classification and regression problems (Belgiu & Drăgu, 2016; Rodriguez-Galiano et al., 2012). Higher classification accuracy and the ability to measure variable importance in land-cover mapping are two advantages of RFC (Jin et al., 2018).

Table 1. Sentinel-2 product types

Name	Description
Level-0	Not released to users, compressed raw image data in Instrument Source Packet (ISP) format
Level-1A	Not released to users, obtained by decompressing the Level-0 raw image data. A geometric model is developed, allowing any pixel in the image to be located
Level-1B	Not released to users, provides radiometrically corrected imagery with top-of-atmosphere radiance values, and the product includes the refined geometry used to produce the user accessed Level-1C products
Level-1C	Available to users, top-of-atmospheric reflectance are the most commonly used products in land cover/use mapping, systematic generation, and online distribution
Level-2A	Available to users, provides bottom-of-atmospheric reflectance, is the most commonly used product in land cover/use mapping, systematic generation, and online distribution and generation on the user side (using Sentinel-2 Toolbox)

The present study prepared a forest cover map of a selected area in the southeast Sri Lanka using Sentinel-2 satellite data through the RFC to investigate the accuracy of the forest map.

2 DATA AND METHODS

2.1 Study Area

Figure 1 shows the study area (approximately 5,000 km2) in the southeast of Sri Lanka. The region mainly accounts for Yala national park, agricultural lands, forests, and villages with perennial plants. Yala national park covers a vast proportion of the selected area.

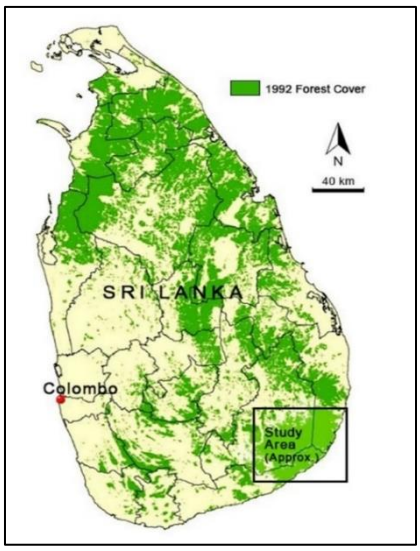

Figure 1. The study area (base map source: www.fao.org)(Sathurusinghe A, 2017)

2.2 Sentinel-2 Data Collection and Pre-processing

Sentinel-2 has 13 spectral bands, three spatial resolution levels of 10 m, 20 m, and 60 m (ESA. Sentinel-2 Missions-Sentinel Online; ESA: Paris, France, 2014), a 290 km swath, a radiometric resolution of 12 bits, and five days of revisit times two satellites (SUHET, 2015). The remainder of the

study was focused on 10m bands. Table 2 illustrates the characteristics of ESA Sentinel-2 satellite images.

Table 2. Characteristics of ESA Sentinel-2 satellite images

Spatial resolution (m)	**Bands**	**Wavelength (nm)**
10	Band 2 – Blue	490
	Band 3 – Green	560
	Band 4 – Red	665
	Band 8 – NIR	842
20	Band 5 – Red Edge	705
	Band 6 – Red Edge	740
	Band 7 – Red Edge	783
	Band 8A – Narrow NIR	865
	Band 11 – SWIR	1610
	Band 12 – SWIR	2190
60	Band 1 – Coastal Aerosol	443
	Band 9 – Water Vapour	940
	Band 10 – Cirrus	1375

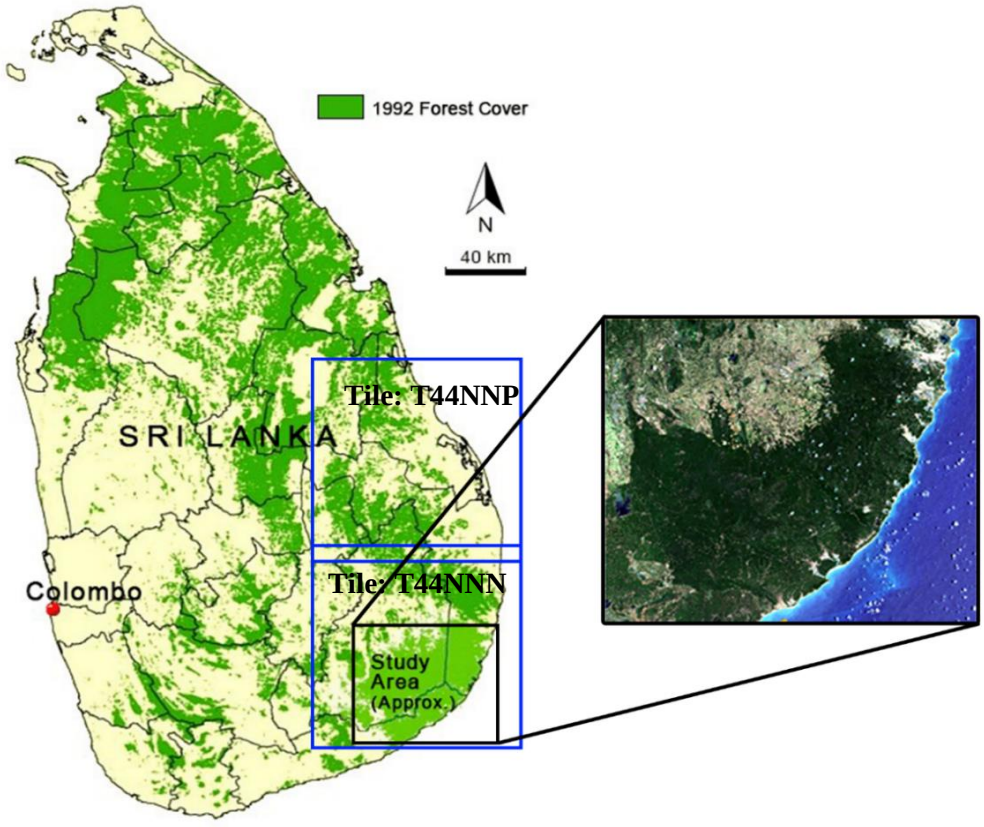

Figure 2. Sentinel-2 imagery of study area

In this study, a Level-2A Sentinel-2 image (20200402T080805) from image tile T44NNN was downloaded to retrieve the bottom of atmosphere reflectance in Sen2Cor's cartographic geometry. Copernicus Open Access Hub is a map browser that allows users to download data from all operational Sentinel missions using the ESA's graphical user interface. Less than 10 percent cloud cover over the entire area and full tile coverage was considered for this study. Figure 2 shows the Sentinel-2 imagery of the study area.

The data were pre-processed using the ESA SNAP version 8.0.0 software developed by ESA. The downloaded image opened in ESA SNAP with profile as Sentinel-2 Multispectral Instrument (MSI) natural colours, responsible for standard RGB composition of the image bands by assigning corresponding spectral bands to the red, blue, and green composition were explored further.

Sentinel-2 photos have varied pixel sizes (10, 20, and 60 meters) based on the spectral band. Resampling is to adjust the pixel size of an image to the required size. Thus, it enables uniform presentation and processing of data with a varying spatial resolution. In addition, most of the functions in the ESA SNAP software require the exact spatial resolution of every band in the source image. The ESA SNAP software was resampled at 10m, and a B2 reference band from the source product was used.

Sentinel data cover large areas, which negatively affects the processing time. As a result, the ESA SNAP program allows users to limit the data's geographic range or select the required bands for processing. The subset image will only show the selected bands that have been chosen. As a result, the area of interest and size of the image was limited to forest boundaries. To generate a subset, one enters the subset range in the geocoordinate section and selects the required bands for the band subset. For this study, B2, B3, B4, and B8 were selected.

2.3 Data Processing

Data processing was based on the training and validation of polygons of Sentinel-2 imagery. Vector data is essential to identify training sites for the RFC. Therefore, training data sites had to be defined and located on the map for the classification. Table 3 summarizes the land cover classification schemes used in this study.

Table 3. Land cover classification schemes

Classification Scheme	**Description**
Crop Land	The land planted for crops, including cultivated land
Forest	The land grow trees, bushes, covered by natural, newly forested, or planted forests
Residential Land	Land used for townships, and rural settlements
Sea	Sea and lagoon
Inland water	Reservoirs, ponds, and tanks
Clouds	Clouds
Other	Coastal areas and bear land

2.3.1 Random Forest Classifier

Classification of the individual trees is the output in RFC. Therefore, the number of training samples and the number of trees to generate are the required input parameters for RFC. The number of training samples and the number of trees used in this study to generate RFC were fixed at 5000 and 1000, respectively.

2.3.2 Normalized Difference Vegetation Index

According to a variety of sources, NDVI is the most widely utilized index for vegetation monitoring. The computation equation was derived from the ESA SNAP algorithm requirements. Red corresponds to the B4 band, while near-infrared (NIR) corresponds to the B8 band.

$$NDVI = \frac{NIR-Red}{NIR+Red} = \frac{B8-B4}{B8+B4} \quad (1)$$

2.4 Accuracy Assessment

For the study, a measure of validation of each classified map was provided by constructing a confusion matrix between the training areas and the RFC maps. A confusion matrix (or error matrix) is usually used as the quantitative method to calculate image classification accuracy. One hundred ground truth data (pixels) was used and manually digitized an image recorded to build the confusion matrix. Google Earth imagery is an open source and offers a clear view of land cover and land use features with details and can be best utilized for field verifications. In addition, Google Earth also provides ground information such as sharp longitude/latitude readings and elevation data. In this study, Google Earth image was used as the source of ground truth data collection. Figure 3 shows the flow chart of the methodology.

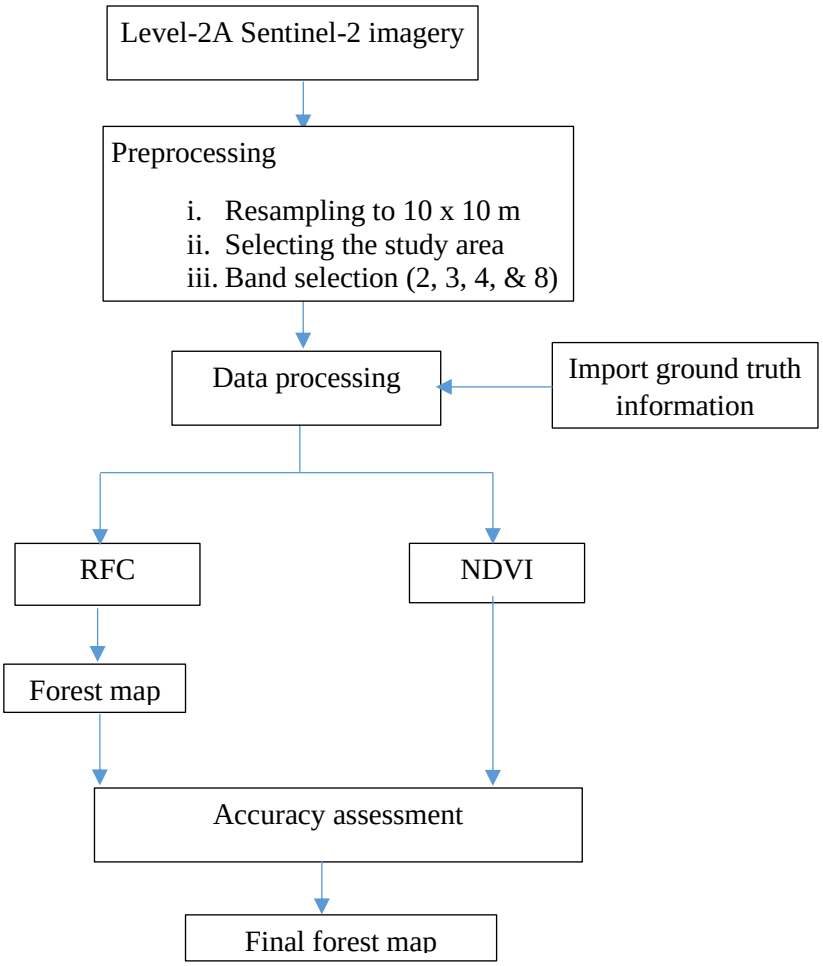

Figure 3. Flowchart of the methodology applied in the study

3 RESULTS

Accuracy assessment of the random forest classified image was verified by comparing the randomly developed dataset with 100 ground truth points. Figure 4 presents the forest cover in the southeast Sri Lanka derived using the RFC and Table 4 illustrates the confusion matrix of the RFC with Google Earth images (figure 5). This visual interpretation was coupled with the expert and prior knowledge of the study area's features. The accuracy assessment was essential for determining the quality of the classified cultivated area derived through the RFC in remote sensing.

For each classification scheme, the overall accuracy (OA) was calculated as the classifier performance estimators. The OA was defined as,

$$OA = \frac{\sum Correct\ predictions}{Total\ number\ of\ predictions} \quad (2)$$

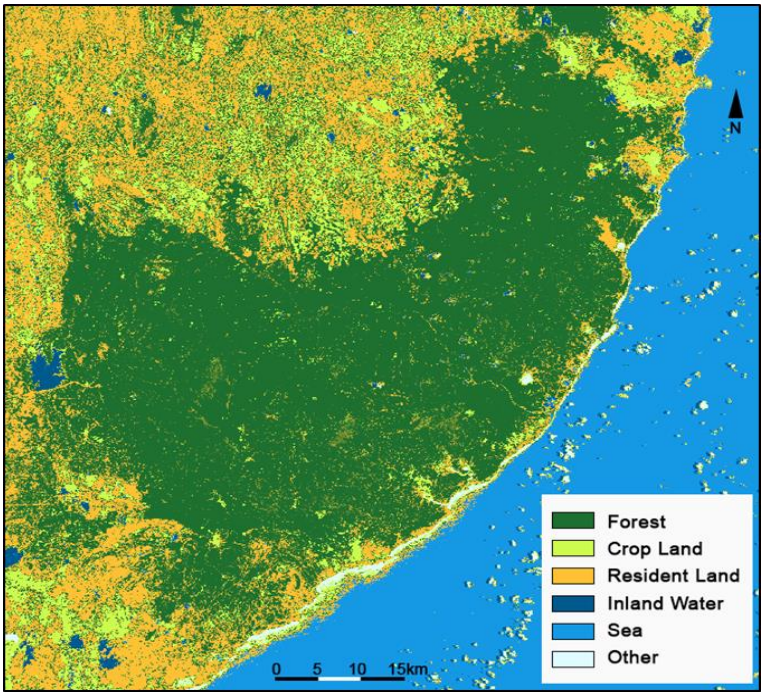

Figure 4. Forest cover in southeast Sri Lanka derived using the RFC

Table 4. Confusion matrix of the RFC with Google Earth images

		Reference Image (Google Earth)							
		Forest	**Crop land**	**Resident land**	**Sea**	**Inland water**	**Clouds**	**Other**	**Total**
Classified Image (RFC Map)	**Forest**	48	2	0	0	0	0	0	50
	Crop land	1	12	1	0	0	0	0	14
	Resident land	1	0	3	0	0	0	3	7
	Sea	0	0	0	15	0	0	0	15
	Inland water	0	1	0	0	5	0	0	6
	Clouds	0	0	0	5	0	0	0	5
	Other	0	0	0	0	1	0	2	3
	Total	50	15	4	20	6	0	5	N=100

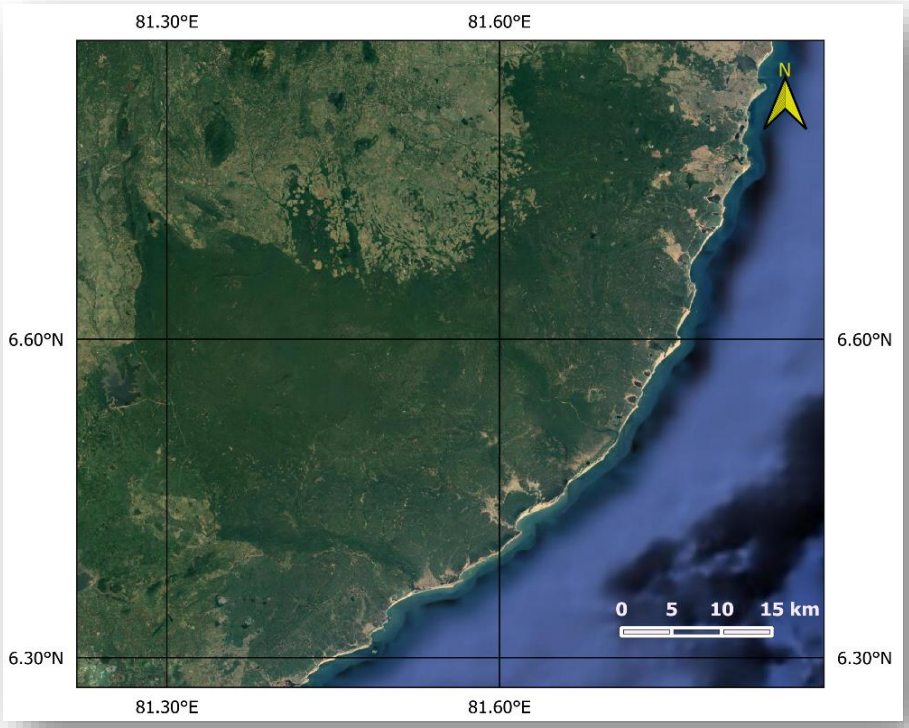

Figure 5. Map of the study area (sky view source: Google map)

The accuracy of the land cover map was 85 percent, with a 96 percent higher accuracy of forest cover identification. The accuracy of residential land area and cropland was 43 percent and 86 percent, respectively. During the analysis, the inland water resulted in an 83 percent accuracy. The study found RFC to be an effective method for isolating forest cover in the southeast Sri Lanka.

Figure 6 shows the level sliced NDVI result of the study area. The values of more than 0.6575 of the legend indicate the forest's maximum possible areas. NDVI is used to check the accuracy of RFC and is used only as a supporting product to validate where the forest is.

4 CONCLUSIONS

This study examines the performance of RFC using Sentinel-2 satellite data to produce enhanced quality forest cover mapping for Sri Lanka. Sri Lanka's southeast land cover map was downloaded with less than 10 percent cloud cover, and a land cover classification with 7 land cover categories was performed using RFC. Furthermore, randomly selected 100 ground truth points were compared with super-resolution Google Earth images. The super-resolution Google Earth images were used as reference datasets to assess the classification accuracy of forest cover identification. The results show that RFC gives an overall classification accuracy of 85 percent in forest identification. RFC also has 83 percent and 86 percent performances corresponding for inland water and cropland, respectively. The result of RFC is compared to the NDVI to verify the accuracy of the forest cover. NDVI images produced from the same dataset have values more than 0.6575 in NDVI indicate the forest pixels with a higher probability. In the study, RFC was determined to be an efficient method for identifying forest cover in Sri Lanka.

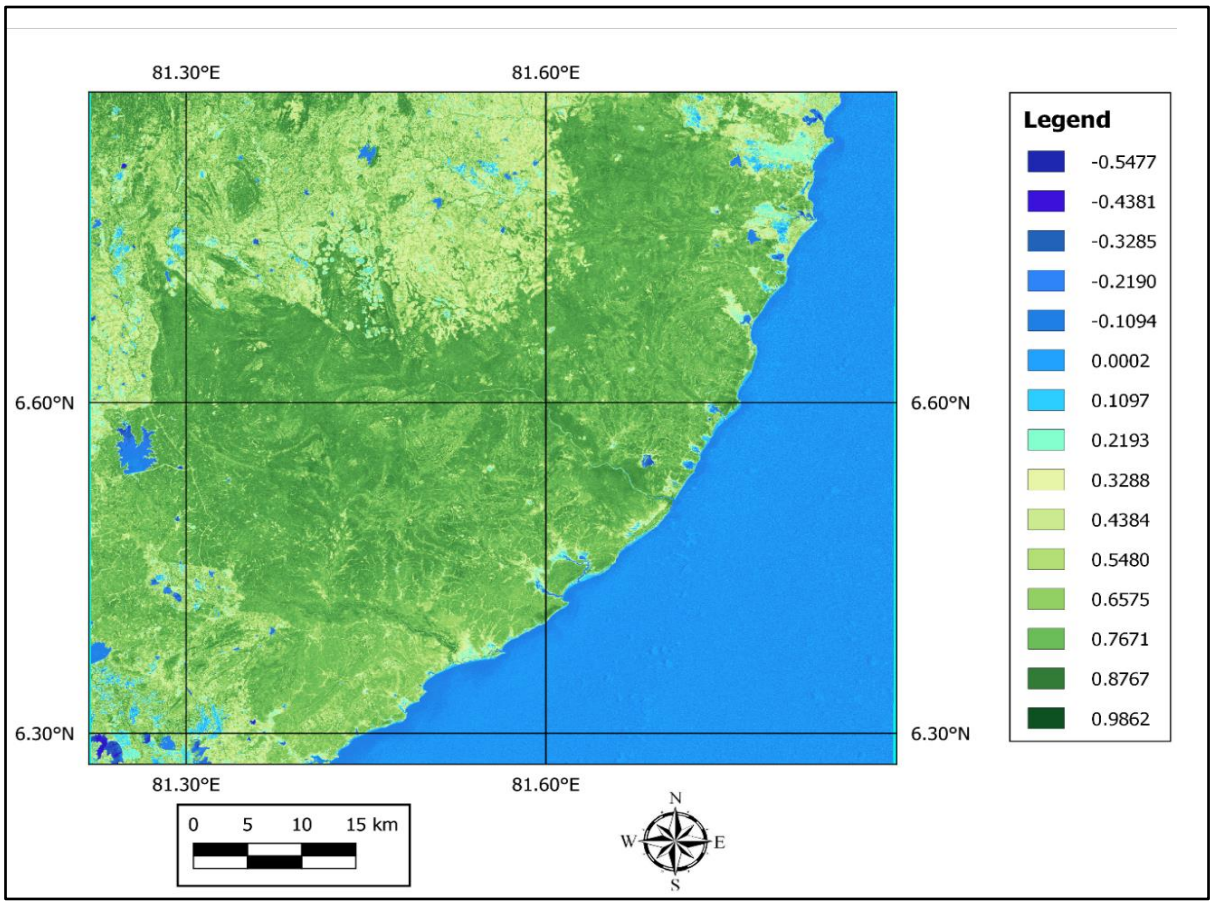

Figure 6. Level sliced NDVI result of the study area

5 ACKNOWLEDGEMENTS

The first author is indebted to the University of Southern Queensland Australia for offering an international Ph.D. fees scholarship. Moreover, the first author acknowledged the institutional facilities from the University of Ruhuna and the Uva Wellassa University of Sri Lanka to carry out this study.

REFERENCES

Askar, Nuthammachot, N., Phairuang, W., Wicaksono, P., & Sayektiningsih, T. (2018). Estimating aboveground biomass on private forest using sentinel-2 imagery. *Journal of Sensors*, *2018*. https://doi.org/10.1155/2018/6745629

Assessment, M. E. (2005). Ecosystems and Human Well-Being. *United States of America: Island Press*, *5*, 563. http://www.bioquest.org/wp-content/blogs.dir/files/2009/06/ecosystems-and-health.pdf

Aznar-Sánchez, J. A., Belmonte-Ureña, L. J., López-Serrano, M. J., & Velasco-Muñoz, J. F. (2018). Forest ecosystem services: An analysis of worldwide research. *Forests*, *9*(8). https://doi.org/10.3390/f9080453

Belgiu, M., & Drăgu, L. (2016). Random forest in remote sensing: A review of applications and future directions. *ISPRS Journal of Photogrammetry and Remote Sensing*, *114*, 24–31. https://doi.org/10.1016/j.isprsjprs.2016.01.011

Grabska, E., Hostert, P., Pflugmacher, D., & Ostapowicz, K. (2019). Forest stand species mapping using the sentinel-2 time series. *Remote Sensing*, *11*(10), 1–24. https://doi.org/10.3390/rs11101197

Höglund, K., & Svensson, I. (2009). Mediating between tigers and lions: Norwegian peace diplomacy in Sri Lanka's civil war. *Contemporary South Asia*, *17*(2), 175–191. https://doi.org/10.1080/09584930902870792

Jin, Y., Liu, X., Chen, Y., & Liang, X. (2018). Land-cover mapping using Random Forest classification and incorporating NDVI time-series and texture: a case study of central Shandong. *International*

Journal of Remote Sensing, *39*(23), 8703–8723. https://doi.org/10.1080/01431161.2018.1490976

Murayama, Y., & Ranagalage, M. (2020). remote sensing Sentinel-2 Data for Land Cover / Use Mapping : A Review. *Remote Sensing*, *2291*(12), 14.

Nisansala, W. D. S., Abeysingha, N. S., Islam, A., & Bandara, A. M. K. R. (2020). Recent rainfall trend over Sri Lanka (1987–2017). *International Journal of Climatology*, *40*(7), 3417–3435. https://doi.org/10.1002/joc.6405

Perera, K., & Tateishi, R. (2012). Supporting elephant conservation in Sri Lanka through MODIS imagery. *Land Surface Remote Sensing*, *8524*(February), 85241N. https://doi.org/10.1117/12.979382

Ranagalage, M., Gunarathna, M. H. J. P., Surasinghe, T. D., Dissanayake, D., Simwanda, M., Murayama, Y., Morimoto, T., Phiri, D., Nyirenda, V. R., Premakantha, K. T., & Sathurusinghe, A. (2020). Multi-decadal forest-cover dynamics in the tropical realm: Past trends and policy insights for forest conservation in Dry Zone of Sri Lanka. *Forests*, *11*(8), 1–24. https://doi.org/10.3390/F11080836

Rathnayake, C. W. M., Jones, S., & Soto-Berelov, M. (2020). Mapping land cover change over a 25-year period (1993-2018) in Sri Lanka using landsat time-series. *Land*, *9*(1). https://doi.org/10.3390/land9010027

Rodriguez-Galiano, V. F., Ghimire, B., Rogan, J., Chica-Olmo, M., & Rigol-Sanchez, J. P. (2012). An assessment of the effectiveness of a random forest classifier for land-cover classification. *ISPRS Journal of Photogrammetry and Remote Sensing*, *67*(1), 93–104. https://doi.org/10.1016/j.isprsjprs.2011.11.002

Rural population-Sri Lanka. (2021). The World Bank Group. https://data.worldbank.org/indicator/SP.RUR.TOTL.ZS?locations=LK

Sathurusinghe A. (2017, May 25). *Forests and poverty alleviation in Sri Lanka*. Forests and Poverty Alleviation in Sri Lanka. https://www.fao.org/fileadmin/templates/rap/files/meetings/2017/2_Day1.pdf

Sheeren, D., Fauvel, M., Josipovíc, V., Lopes, M., Planque, C., Willm, J., & Dejoux, J. F. (2016). Tree species classification in temperate forests using Formosat-2 satellite image time series. *Remote Sensing*, *8*(9), 1–29. https://doi.org/10.3390/rs8090734

Sudhakar Reddy, C., Manaswini, G., Jha, C. S., Diwakar, P. G., & Dadhwal, V. K. (2017). Development of National Database on Long-term Deforestation in Sri Lanka. *Journal of the Indian Society of Remote Sensing*, *45*(5), 825–836. https://doi.org/10.1007/s12524-016-0636-8

SUHET. (2015). Microbial Adaptation. In *Sentinel-2 User Handbook: Vol. Rev 2* (2nd ed., Issue 1). European Space Agency. https://doi.org/10.1021/ie51400a018

Thanh Noi, P., & Kappas, M. (2017). Comparison of Random Forest, k-Nearest Neighbor, and Support Vector Machine Classifiers for Land Cover Classification Using Sentinel-2 Imagery. *Sensors (Basel, Switzerland)*, *18*(1). https://doi.org/10.3390/s18010018

Understanding the Characteristics of the Heatwaves using Temperature as the Only Variable – A Case Study on the Heatwaves in 1994 in South Korea

Sewwandhi S. K. Chandrasekara[1, 2]
[1] Department of Agricultural Engineering
Faculty of Agriculture, University of Peradeniya 20400, Sri Lanka.
sewwandhich@agri.pdn.ac.lk

Hyun-Han Kwon[2]
[2] Department of Civil and Environmental Engineering
Sejong University, Seoul 05006, South Korea.
hkwon@sejong.ac.kr

ABSTRACT

Acutely warm weather coupled with extreme weather variables or latent cooling due to a deficit of soil moisture could generate heatwaves. South Korea is highly susceptible to heatwaves that occur annually in different intensities and cause devastating impacts. This study aimed to identify the characteristics of the heatwaves, especially focusing on one of the most severe heatwaves observed in 1994 in South Korea using only temperature as a variable. The summer season, June to September (JJAS), was selected for the study because heatwaves were prominent during the summer in South Korea. The maximum and minimum daily temperatures were collected from the 67 meteorological stations located in South Korea. The mean daily 95th percentiles of the temperatures were assessed to identify the heatwave durations and the intensities. In 1994, the 15 stations recorded their highest heatwave durations, and durations varied between 48 to 66 days in the JJAS season. *Busan* station recorded the highest heatwave duration in 1994, which persisted for 66 days or throughout half of the season. Further, it was interesting to identify that coastal meteorological stations were most vulnerable to heatwaves in South Korea. However, the relationship between temperature intensities and heatwave duration for coastal cities showed statistically low significance. Furthermore, it is identified that the daily maximum temperature was most influential in the occurrence of heatwaves in both the coastal and mainland meteorological stations, except for *Pohang* and *Ulleungdo*. Therefore, the characteristics of heatwaves observed in 1994 in South Korea were identified using temperature as the only variable. Furthermore, a study on the dynamic atmospheric oscillations due to heated waves in coastal regions of South Korea over characteristics of heatwaves observed in South Korea is suggested.

KEYWORDS: *Heatwaves, South Korea, Temperature, 95th percentile.*

1 INTRODUCTION

A heatwave is one of the extreme events observed as a result of excessively hot weather, which is coupled with high temperature, high humidity, and low rainfall (Mueller and Seneviratne, 2013; Quesada et al., 2012). Furthermore, latent cooling due to high temperature-influenced soil moisture depletion could also cause heatwaves in some instances. In addition, the blocking highs in the Northern hemisphere due to moisture deficit cause heatwaves in mid-latitudes (Quesada et al., 2012; Pfahl and Wernli, 2012; Hirschi et al., 2011). The recurrent high-amplitude Rossby wave for the hemisphere (Kornhuber et al., 2020) and the oceanic oscillations such as El-Nino Southern Oscillation (ENSO) and North Atlantic Oscillation could cause heatwaves too. (Hsu et al., 2017; Loughran et al., 2017; Grotjahn et al., 2015). Unfortunately, anthropogenic activities leading to the emission of urban heat in the cities and the emission of greenhouse gasses aggravate heatwaves as well. (Ramamurthy et al., 2017; Jaeger et al., 2008).

The definitions for heatwaves vary globally due to the temperature threshold levels used to define heatwaves. The globally applicable generalized definition for a heatwave is provided by the World Meteorological Organization (WMO) as the presence of warming air, in which the daily maximum temperature (T_{Max}) is higher than the mean temperature (i.e., between 1961 and 1990) by 5°C

or more for 5 or more consecutive days and destroy routine human activities (Frich et al., 2002). Nonetheless, WMO noted that a heatwave differs from warm spells, since a warm spell is defined based on 90th or 95th percentiles of daily T_{Max}. Furthermore, a warm spell can be observed at any time of the year, whereas heatwaves can only be observed during the warm season. Some countries have their criteria to identify heatwaves as shown in Table 1.

Table 2. The criteria to declare heatwaves in different countries

Country	**Criterion**	**Source**
Netherlands, Belgium, and Luxemburg	T_{Max} in De Bilt, Utrecht, Netherlands exceeds 25°C or 30°C for consecutive five days or consecutive three days, respectively	Seveno, 2020.
Denmark	average T_{Max} exceeds 28° C for at least three days over 50% of the country	Scanpix, 2018.
Australia	both the T_{Max} and minimum temperatures (T_{Min}) unusually hot over 3 consecutive days	Commonwealth of Australia, 2021.
South Korea	daily T_{Max} exceeds 33°C for consecutive two days	Lim et al., 2019; Yoon et al., 2018

2 SOUTH KOREA AND ITS SUSCEPTIBILITY TO HEATWAVES

The expansion of the Western North Pacific subtropical high (WNPSH) and anticyclone circulation over the East Asian–northwestern pacific region are the main origins of a heatwave in South Korea (Park and Schubert, 1997; Garcia-Herrera et al., 2010). Furthermore, the Foehn effect acts as a cause of heatwaves in the southeastern parts of South Korea (Kim and Lee, 2007; Lee, 2003), and the impact of the Foehn effect over the western hills of South Korea was identified by Byun et al. (2006) and Lee (2003).

According to the statistics, the duration of the heatwave has increased from 10.1 days to a maximum of 31.5 days from 1981 to 2010, and the mentioned maximum value was observed in 2018 (Kim et al., 2020). Even though the highest daily T_{Max} was recorded as 41°C in *Hongcheon* in 2018 and was identified as the highest recorded T_{Max} after 111 years, the heatwave that occurred between July and August in 1994 over South Korea had a devastating impact on South Korea, causing more than 3000 deaths (Kysely and Kim, 2009). Nonetheless, due to the high susceptibility to heatwaves in South Korea, a surveillance system was developed by The Korea Center for Disease Control and Prevention (KCDC) in 2011 to monitor the deaths and hospitalizations related to the diseases caused by annual heatwaves (Na et al., 2013). Later in 2018, the South Korean Government declared heatwaves a natural disaster, and the government is liable to compensate the victims (Lee, 2018). Furthermore, Kim et al. (2006) identified that the daily mortality rate would increase from 6.7% to 16.3% if the daily temperature increases by 1°C from the threshold level.

Temperature changes could intensify the occurrence of heatwaves in a country. Kwon (2005) identified that the emission of greenhouse gasses and urbanization increased the mean temperature of South Korea by 1.5°C and continuous anthropogenic activities altered the climate in South Korea drastically (Im et al., 2008). Furthermore, Boo et al. (2004 and 2006) stated that the projected daily temperature of Korea would increase by 6°C during 2071–2100 compared to the observed daily temperature during 1971–2000.

The intensified and prolonged duration of heatwaves could couple with other natural disasters such as droughts and could cause a massive impact on a nation such as inadequate water in the reservoirs leading

to losses in agriculture, inefficacy in domestic and industrial water supply, damages to the economy and wellbeing of the society.

Therefore, it is a timely need to understand the duration and intensity of the heatwaves observed in South Korea. In this context, the study primarily aims to identify the temporal and spatial distributions of T_{Max} and T_{Min} in South Korea and, to understand the heatwaves observed in 1994 in South Korea.

3 METHODOLOGY

3.1 The Temperature in South Korea – The Study Area

South Korea is a temperate country located between 34°N–38°N and 126°E–130°E. The climate of South Korea depends on the land–air–oceanic impacts of the nearby large landmass in the Northeastern Asia and the Pacific Ocean (Ghafouri-Azar and Bae, 2020). The temperature of South Korea is governed by two mechanisms: a) Pacific high pressure governs the summer season temperature, and the average temperature varies from 22–25°C, b) Elevation difference governs the winter temperature, and the average temperature ranges from -5°C to -3°C. Figure 1a illustrates the distribution of the mean monthly T_{Max} and T_{Min} in South Korea, and both the T_{Max} and T_{Min} are at their highest in August, which decreases during the summer season.

Nonetheless, 70% of the annual rainfall occurs during the summer season, which is commonly called the rainy season (i.e., Changma in the Korean language) (Figure 1b). There are two foremost mechanisms that govern the rainfall during the summer season: a) The local convention govern the Changma season b) Tropical cyclones (typhoons) govern the Post–Changma season (Lee et al., 2016; Choi et al., 2017). A part of the Changma season delivers heavy rainfall to the southern parts of South Korea starting from the end of June and moving northward across the country, continuing for nearly one month. Despite that, June to September (JJAS) was selected as a reference season for the study because many heatwaves are observed in the mentioned season, and it is beneficial to understand the behaviors of T_{Max} and T_{Min} during the summer season in South Korea.

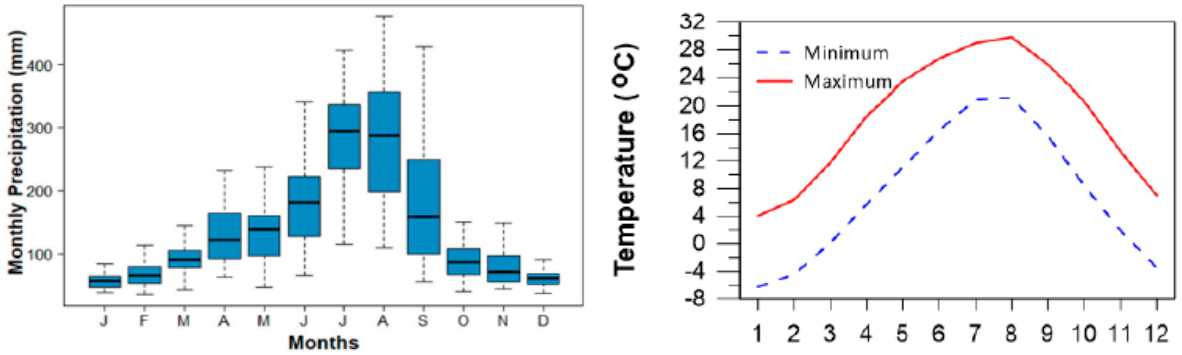

Figure 2. The distributions of a) mean monthly maximum and minimum temperatures (Left), and mean monthly precipitation (Right) in South Korea*

Source: a) Ghafouri-Azar and Bae, 2020. and b) Alcantara and Ahn, 2020.

* The X axis represents the months of the year in both figures.

3.2 Data

Two main data types – daily T_{Max} and T_{Min} data from 67 ASOS (Automated Surface or Synoptic Observing System) were used for the study (Figure 2). The 14 stations consist of data from 1960 to 2019 (i.e., 60 years), and the rest of the stations have data series between 32 years and 59 years.

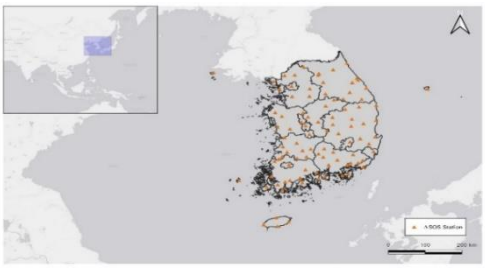

Figure 2. The location of KMA-managed ASOS stations used for the study

3.3 Use of 95th percentiles to identify the heatwaves

The heatwave episodes were identified using the methodology developed by Kuglitsch et al. (2010) with slight modifications. The daily time series of T_{Max} and T_{Min} for the JJAS season was plotted for each year and for each station. The long-term daily 95th percentiles were calculated using the daily T_{Max} and T_{Min} from May to October, which was the calculation procedure developed by Della-Marta et al. (2007). Firstly, the mean daily T_{Max} and T_{Min} series for the period of May to October for each station was calculated. In this process, the mean temperature of a specific day was calculated by averaging the temperature of a given day for the total of selected years. Secondly, the 95th percentile of a specific day was calculated based on the sample of 15 days (i.e., seven days on either side of the particular day). The 95th percentiles for each day between May to October were calculated for both the T_{Max} and T_{Min} time series. Finally, the heatwave is identified where both the daily T_{Max} and T_{Min} exceed their 95th percentiles by plotting the daily climatologies of T_{Max}, T_{Min}, and 95th percentiles of T_{Max} and T_{Min}. Based on the methodology adopted by Della-Marta et al. (2007), a heatwave is identified as a period of three or more consecutive hot days and nights not interrupted by more than a non-hot day or night. Specifically, in this study, the duration is not specified to identify the heatwave, but the consecutive days of temperature which exceed both the 95th percentiles of T_{Max} and T_{Min} are identified as the presence of a heatwave phenomenon or a heatwave duration.

The intensities of daily T_{Max} and T_{Min} were developed using temperatures and their respective heat wave durations. Thereafter, the intensities were plotted against the number of days identified as the presence of heatwaves within a year to identify the correlation between the intensities and the days which had heatwaves annually.

4 RESULTS AND DISCUSSION

4.1 The heatwave in 1994 – the longest heatwave duration observed in South Korea

As discussed in the previous paragraphs, intensified or long-duration heatwaves can lead to the occurrence of droughts. South Korea observed severe droughts in 1994 and 2018 due to the severe heatwaves during the mentioned years. Nevertheless, in 1994 it was recorded that there were 29 consecutive days in which daily T_{Max} exceeded 33°C which was a remarkable record for the longest duration heatwave observed in South Korea (Lee and Lee, 2016). Ahn (2019) presented that the droughts observed between 1994 and 1995 depleted the reservoir levels and impacted agriculture, drinking water, and industrial water in South Korea.

Out of 67 stations, 15 stations (i.e., the third-highest number of stations) recorded their highest heatwave duration (days) in 1994. The heat wave durations for those 15 stations varied between 48 – 66 days for the JJAS season. The highest heatwave duration in 1994 is observed in *Busan* station, and it is 66 days out of 122 days in the JJAS season (Figure 3a). The *Ulleungdo* station on *Ulleungdo* Island, which is located in the east of the mainland, had the second longest heatwave duration (i.e., 65 days) in 1994 (Figure 3b). Therefore, both regions experienced heatwaves during almost half of the JJAS season in 1994.

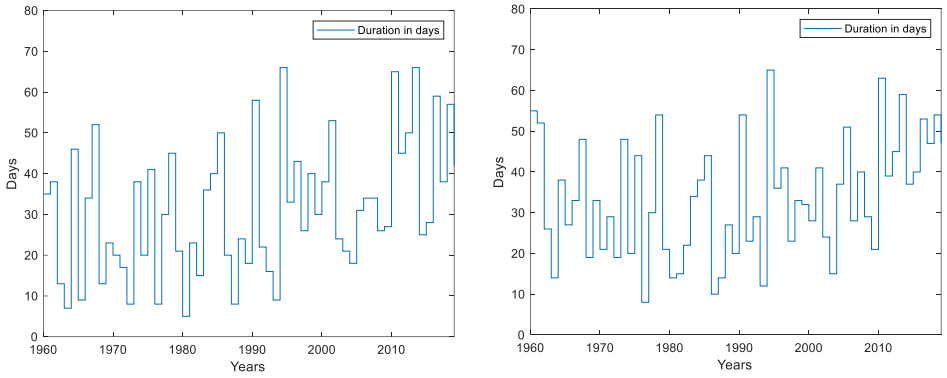

Figure 3. The distribution of heatwave durations* for a) *Busan* station (Left) and b) *Ulleungdo* station (Right)

*The blue line represents the duration in days

It is interesting to observe that heatwaves in *Busan* and *Ulleungdo* stations continued from the beginning of July to the beginning of August, where the daily T_{Max} and T_{Min} exceeded both their respective 95th percentiles (Figure 4a and 4b). However, the persisting heatwaves stopped for a few days and resumed and lasted till the beginning of September (Figure 4a and 4b). Choi et al. (2012) showed that the end of the Changma season in mid-July could trigger the occurrence of a heatwave in South Korea.

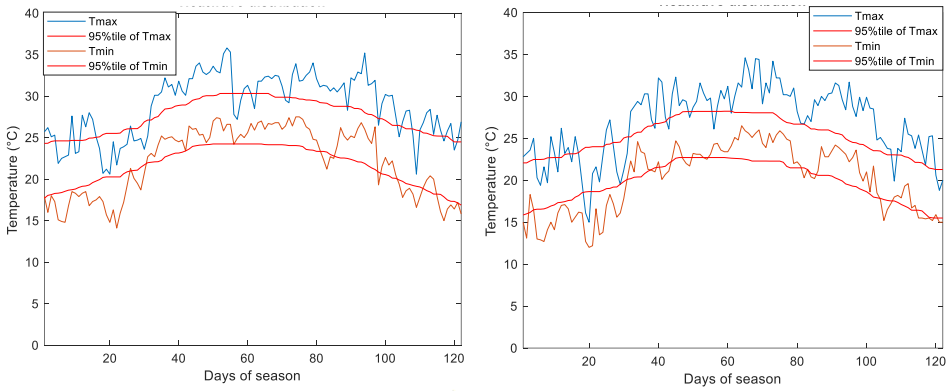

Figure 4. Time series distribution of daily T_{Max} and T_{Min} and respective 95th percentiles* for a) *Busan* station (Left) and b) *Ulleungdo* station (Right)

*The blue and brown lines represent the T_{Max} and $T_{Min,}$ respectively. The red line represents the 95th percentiles for each temperature distribution.

4.2 Changes in temperature intensities during the heatwaves

During JJAS in 1994, the diurnal difference in daily T_{Max} and T_{Min} intensities for *Busan* station is insignificant, where T_{Max} was 2.7078°C/day, and T_{Min} was 2.0488°C. However, it is noteworthy that in 1992 and 1993, the daily T_{Min} intensity was higher compared to the T_{Max} intensity for the *Busan* station (Figure 5a). Therefore, it could be due to the increase in the daily mean T_{Min}, i.e., the temperature at night during the summer season is significantly higher than the variation in T_{Max} during daytime. This scenario may have occurred due to the increased humidity levels in the nighttime and, it could be because there was no time lapse to reduce the increased humidity levels in the daytime due to the heatwaves, and increased humidity levels continued for the night, causing disastrous heat impact in the night. Further, this phenomenon could be intensified in the coming days. Even though *Ulleungdo* station

had the second-longest heatwave duration in 1994, T_{Min} intensity did not exceed the T_{Max} intensity (Figure 5b). Therefore, the main reason could be that the breezes may have reduced the heat generated during the daytime and decreased the temperature in the nighttime for *Ulleungdo* Island compared to the *Busan* station.

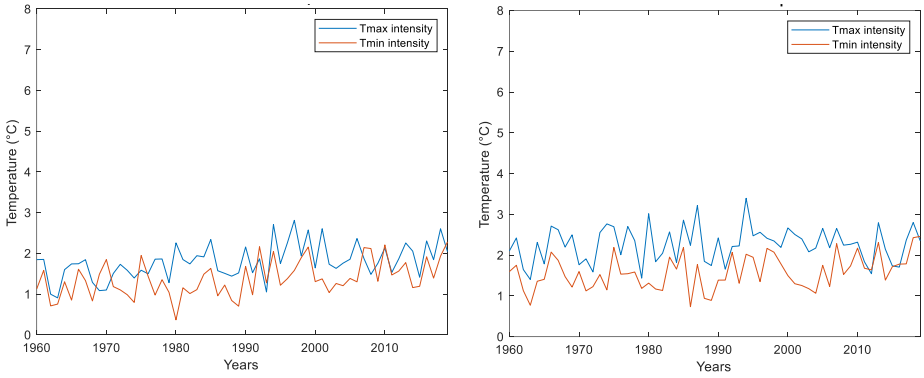

Figure 5. Time series distribution of intensities of daily T_{Max} and T_{Min}* a) *Busan* station (Left) and b) *Ulleungdo* station (Right)

*The blue line represents the T_{Max} intensity and the red line represents the T_{Min} intensity.

A higher correlation between both the temperature intensities and the durations of heatwaves was observed for *Busan* station compared to *Ulleungdo* station (Table 1). The correlation resulted in most of the coastal cities, including *Busan*, *Ulleungdo*, *Seosan*, *Pohang*, *Mokpo*, *Tongyeong*, and *Jinju that were* impacted by the deadly heatwaves in 1994. However, the relationship between heatwave duration and the temperature intensities for stations located in coastal cities showed statistically low significance. This could be due to the dynamic changes in surface temperature in coastal cities because of the land-sea breezes. This could have caused vigorous changes in the behavior of the heated air in the atmosphere. Furthermore, Park and Schubert (1997) suggested that the orographic and zonal wind over the Tibetan Plateau could change the atmospheric oscillations over South Korea and result in extreme heat in 1994. Consequently, it is recommended to study the teleconnection between the oceanic and atmospheric oscillations over temperature variation or the generation of a heatwave in South Korea.

Furthermore, the inland stations such as *Icheon*, *Cheonan*, *Geumsan*, and *Yeongju* were also severely affected in 1994. For the Pohang station, the daily T_{Min} is highly influenced by heatwave intensity and duration (Table 1). Interestingly, correlation resulted in daily T_{Max} being statistically more influential for the duration of heatwave compared to daily T_{Min} for stations on the mainland.

Table 2. The correlation between the duration of a heatwave (days) and the temperature (T_{Max} and T_{Min}) intensities for relevant durations for selected stations.

Location of the station	**Station Name**	**Correlation**	
		T_{Max}	**T_{Min}**
Near to coast or coastal cities	Busan	0.596	0.581
	Ulleungdo	0.327	0.577
	Seosan	0.523	0.211
	Pohang	0.180	0.699
	Mokpo	0.563	0.473
	Jinju	0.635	0.447
Mainland	Icheon	0.618	0.411
	Geumsan	0.544	0.388
	Yeongju	0.512	0.342

4.3 Evidence of absence of heatwave impacts in 1994

As mentioned previously, the longest duration of heatwave observed at *Busan* station in 1994 was 66 days. In addition, the study identified some stations which had longer heatwave durations in different years where there was no evidence for declared occurrences of heatwaves. The *Jeju* and *Seogwipo* stations on *Jeju* Island, South Korea, had the longest heatwave duration in 2017 and 2014, about 74 days and 72 days, respectively, for the period 1960 to 2019. South Korea is geographically and temporally highly diverse within the country. Therefore, it is helpful to identify the teleconnections between temperature and other weather variables which would lead to heatwaves in South Korea.

5 CONCLUSION

South Korea is prone to heatwave-induced devastations which have an impact on the economic, social, and environmental status of South Korea. Therefore, identification of the occurrence of heatwaves would be advantageous. Therefore, this study attempted to identify heatwaves in South Korea using only temperature as a variable such as daily maximum and minimum temperatures and their 95^{th} percentiles and focused on the occurrence of severe heatwave incidents observed in 1994.

The study identified that *Busan* and *Ulleungdo* stations showed the longest durations of a heatwave during 1994. Further, the heatwaves were identified from the beginning of July to the beginning of August for both stations. Nonetheless, there was an intermittent break in between August, and the heatwave lasted until September. Some researchers argued that the end of the Changma season in mid-July could prompt the occurrence of a heatwave in South Korea.

Further, the correlation between temperature intensities and the heatwave durations showed that mainland stations had a higher correlation with the T_{Max} compared to the coastal stations. The coastal stations may have been influenced by land-sea breezes over temperature changes. For some instances, T_{Min} intensities exceeded the T_{Max} intensities because the heated air persisted until night and caused the heatwave impacts in the nighttime.

Some stations were not impacted by the heatwaves observed in 1994, but they had the longest heatwave durations in different years based on the method used in this study. It may be due to the presence of geographically wide variations in South Korea.

The study suggests further studies on the teleconnections between land-atmospheric circulations with regard to the occurrence of heatwaves in South Korea.

6 ACKNOWLEDGEMENTS

This work was funded by the Korea Meteorological Administration Research and Development Program under Grant KMI 2018-07010.

REFERENCES

Ahn, H. (2019). Disaster management in Rep. of Korea. Especially in drought management. *2019 KOICA-UN ESCAP Capacity Building on Drought Monitoring and Early Warning*. 23-28 September, 2019, Bangkok, Thailand.

Alcantara, A.L., & Ahn, K-H. (2020). Probability distribution and characterization of daily precipitation related to tropical cyclones over the Korean Peninsula, *Water*, *12*(4), 1214: https://doi.org/10.3390/w12041214.

Boo, K.O., Kwon, W.T., & Baek, H.J. (2006). Change of extreme events of temperature and precipitation over Korea using regional projection of future climate change, *Geophysical Research Letters, 33*: L01701, DOI: 10.1029/2005JD006290.

Boo, K.O., Kwon, W.T., Oh, J.K., & Baek, H.J. (2004). Response of global warming in regional climate change over Korea: an experiment with the MM% model, *Geophysical Research Letters, 31*: L21206, DOI: 10.1029/2014GL021171.

Byun, H. R., Hwang, H. S., & Go, H. Y. (2006). Characteristics and synoptic causes on the abnormal heat occurred at Miryang in 2004, *Atmosphere*, *16*(3), 187–201.

Choi, J-W., Cha, Y., & Kim, H-D. (2017). Interdecadal variation of precipitation days in Augustin the Korean Peninsula, *Dynamics of Atmospheres and Oceans, 77*: 74-88. http://dx.doi.org/10.1016/j.dynatmoce.2016.10.003

Choi, K.S., Wang, B., & Kim, D.W. (2012). Changma onset definition in Korea using the available water resources index and its relation to the Antarctic oscillation, *Climate Dynamics, 38*:547-562.

Commonwealth of Australia. (2021, November 18). *Understanding heatwaves*. Bureau of Meteorology in Australian Government. www.bom.gov.au/australia/heatwave/knowledge-centre/understanding.shtml.

Della-Marta, P. M., Haylock, M. R., Luterbacher, J., & Wanner, H. (2007). Doubled length of western European summer heat waves since 1880, *Journal of Geophysical Research, 112*, D15103. https://doi.org/10.1029/2007JD008510

Frich, P., Alexander, L.V., Della-Marta, P., Gleason, B., Haylock, M., Klein Tank, A.M.G., & Peterson, T. (2002). Observed coherent changes in climatic extremes during the second half of the twentieth century, *Climate Research, 19*: 193-212.

Garcia-Herrera, R., Diaz, J., Trigo, R.M., Luterbacher, J., & Fischer, E.M. (2010). A review of the European summer heat wave of 2003, *Critical Reviews in Environmental Science and Technology, 40*(4): 267-306. https://doi.org/10.1080/10643380802238137

Ghafouri-Azar, M., & Bae, D-H. (2020).The impacts of water cycle components on streamflow in a changing climate of Korea: Historical and future trends, *Sustainability, 12*(10), 4260: https://doi.org/10.3390/su12104260

Grotjahn, R., Black, R., Leung, R., Wehner, M. F., Barlow, M., Bosilovich, M., et al. (2015). North American extreme temperature events and related large scale meteorological patterns: A review of statistical methods, dynamics, modeling, and trends, *Climate Dynamics, 46*, 1–34. https://doi.org/10.1007/s00382-015-2638-6

Hirschi, M., Seneviratne, S. I., Alexandrov, V., Boberg, F., Boroneant, C., Christensen, O. B., et al. (2011). Observational evidence for soil-moisture impact on hot extremes in southeastern Europe, *Nature Geoscience, 4*(1), 17–21.

Hsu, P.-C., Lee, J.-Y., Ha, K.-J., & Tsou, C.-H. (2017). Influences of boreal summer intraseasonal oscillation on heat waves in monsoon Asia, *Journal of Climate, 30*, 7191–7211.

Im, E.S., Ahn, J.B., Kwon, W.T., & Giorgi, F. (2008). Multi-decadal scenario simulation over Korea using a one-way double-nested regional climate model system. Part 2. Future climate projection (2021-2050), *Climate Dynamics, 30*: 329-254.

Jaeger, C. C., Krause, J., Haas, A., Klein, R., & Hasselmann, K. (2008). A method for computing the fraction of attributable risk related to climate damages, *Risk Analysis, 28*(4), 815–823. https://doi.org/10.1111/j.1539-6924.2008.01070.x

Kim, D-W., Kwon, C., Kim, J., & Lee, J-S. (2020). Characteristics of heat waves from a disaster perspective, *Journal of Prevention Medicine & Public Health, 53*: 26-28. https://doi.org/10.3961/jpmph.19.315

Kim, H., Ha, J. S., & Park, J. (2006). High temperature, heat index, and mortality in 6 major cities in South Korea, *Archives of Environmental & Occupational Health, 61*(6), 265–270. https://doi.org/10.3200/AEOH.61.6.265-270

Kim, J., & Lee, S. (2007). The distribution of heat waves and its cause in South Korea, *Journal of the Korean Geographical Society, 42*(3), 332–343.

Kornhuber, K., Coumou, D., Vogel, E., et al. (2020). Amplified Rossby waves enhance risk of concurrent heatwaves in major breadbasket regions, *Nature Climate Change, 10*(1), 48–53. https://doi.org/10.1038/s41558-019-0637-z

Kuglitsch, F.G., Toreti, A., Xoplaki, E., Della-Marta, P.M., Zerefos, C.S., Turkes, M., & Luterbacher, J. (2010). Heat wave change in the eastern Mediterranean since 1960, *Geophysical Research Letters, 37*, L04802, DOI: 10.1029/2009GL041841.

Kwon, W.T. (2005). Current status and perspectives of climate change science, *Journal of Korean Meteorological Society, 41*: 325-336 [in Korean with English abstract].

Kysely, J., & Kim, J. (2009). Mortality during heat waves in South Korea, 1991 to 2005: How exceptional was the 1994 heat wave?, *Climate Research, 38*(2), 105-116. https://www.jstor.org/stable/24870402

Lee, S. (2003). Difference of air temperature between the west and east coast regions of Korea, *Asia-Pacific Journal of Atmospheric Sciences, 39*(1), 43–57.

Lee, S-J. (2018). *Heat wave victims to be eligible for natural disaster subsidies of up to W10m*. The Korea Herald, Dec 3, 2018, p 1.

Lee, W-S., & Lee, M-I. (2016). Interannual variability of heat waves in South Korea and their connection with large-scale atmospheric circulation patterns, *International Journal of Climatology, 36*(15): 4815-4830. https://doi.org/10.1002/joc.4671

Lim, Y-H., Lee, K-S., Bae, H-J., Kim, D., Yoo, H., Park, S., & Hong, Y-C. (2019). Estimation of heat-related deaths during heat wave episodes in South Korea (2006-2017), *International Journal of Biometeorology, 63*(12), 1621-1629. https://doi.org/10.1007/s00484-019-01774-2

Loughran, T. F., Perkins-Kirkpatrick, S. E., & Alexander, L. V. (2017). Understanding the spatio-temporal influence of climate variability on Australian heatwaves, *International Journal of Climatology*, *37*(10), 3963–3975. https://doi.org/10.1002/joc.4971

Mueller, B., & Seneviratne, A. S. I. (2013). Hot days induced by precipitation deficits at the global scale. *Proceedings of the National Academy of Sciences of the United States of America, 109* (12), 398–12, 403

Na, W., Jang, J-Y., Lee, K.E., Kim, H., Jun, B., Kwon, J-W., & Jo, S-N. (2013). The effects of temperature on heat-related illness according to the characteristics of patients during the summer of 2012 in the Republic of Korea, *Journal of Preventive Medicine and Public Health, 46*(1):19–27. https://doi.org/10.3961/jpmph.2013.46.1.19

Park, C-K., & Schubert, S. D. (1997). On the nature of the 1994 East Asian summer drought, *Journal of Climate, 10*(5), 1056–1070. https://doi.org/10.1175/1520-0442(1997)010<1056:OTNOTE>2.0.CO;2

Pfahl, S., & Wernli, H. (2012). Quantifying the relevance of atmospheric blocking for co-located temperature extremes in the Northern Hemisphere on (sub-) daily time scales, *Geophysical Research Letters, 39*, L12807. https://doi.org/10.1029/2012GL052261

Quesada, B., Vautard, R., Yiou, P., Hirschi, M., & Seneviratne, S. I. (2012). Asymmetric European summer heat predictability from wet and dry southern winters and springs, *Nature Climate Change, 2*, 736–741.

Ramamurthy, P., González, J., Ortiz, L., Arend, M., & Moshary, F. (2017). Impact of heatwave on a megacity: An observational analysis of New York City during July 2016, *Environmental Research Letters, 12*(5), 054011. https://doi.org/10.1088/1748-9326/aa6e59

Scanpix. R. (2018, July 23). *Danish 'heatwave and tropical nights' forecast*. The Local, Denmark's news in English, The Local Europe AB, Sweden, https://www.thelocal.dk/20180723/danish-heatwave-and-trpical-nights-forecast/

Seveno, V. (2020, August 10). *The Netherlands swelters in first official heatwave of 2020*. IamExpat, IamExpat Media, https://www.iamexpat.nl/expat-info/dutch-expat-news/netherlands-swelters-first-official-heatwave-2020

Yoon, D., Cha, D-H., Lee, G., Park, C., Lee, M-I., & Min, K-H. (2018). Impacts of synoptic and local factors on heat wave events over southern region of Korea in 2015, *Journal of Geophysical Research: Atmospheres, 123*, 12081-12096. https://doi.org/10.1029/2018JD029247

Factors Affecting Red-Light Running of Pedestrians at Signalized Intersections

Chamara Herath, Niranga Amarasingha
Department of Civil Engineering, Sri Lanka Institute of Information Technology,
New Kandy Road, Malabe, 10115, Sri Lanka
nadunchamara39@gmail.com, niranga.a@sliit.lk

ABSTRACT

Hundreds of pedestrians have died and many have been injured in the past decades as a result of Red Light Running (RLR) infractions. According to the United States Department of Transportation, 846 pedestrians have died and 143,000 have been injured in 2019 due to RLR violations. The majority of previous studies have focused on pedestrian behavior at an intersection, whereas only a few have looked into pedestrian RLR violations. The main objectives of this research are to find the pedestrians' RLR rate in Sri Lanka and to find ways to reduce the RLR rate of pedestrians at the signalized crossing. Video observation surveys were conducted to collect data at three signalized intersections within Kandy city limits during weekdays for two hours per site. Pedestrian demographic variables such as gender and age; crossing characteristics such as crossing type, direction, crossing speed etc; and site characteristics such as crossing length, pedestrian green time, etc. were recorded. Chi-square and binary logistic regression tests were done. Results showed that out of 178 females, 130 had compliance with signal phases and out of 386 males, only 215 had compliance with RLR of a pedestrian. Furthermore, other independent variables such as age, crossing type, direction etc. were also associated with compliance RLR of pedestrians under Chi-square results. Based on the results of binary logistic regression, the variables such as gender, crossing type, number of traffic lanes, and pedestrian speed are significant when decreasing the log of probability -0.658, -3.040, -1.022 and -2.556 of compliance for RLR respectively. Variables that crosswalk utilization are also significant when increasing the log of probability of RLR 1.406 of compliance for RLR. The results would help develop safer pedestrian infrastructures and engineering countermeasures as well as assist the researchers and practitioners in better understanding pedestrian crossing behavior at signalized intersections.

KEYWORDS: *Pedestrian's violation, Road safety, Signalized crosswalk, Red-light running.*

1 INTRODUCTION

Globally, about 1.24 million lives are lost annually due to road traffic accidents (WHO, 2018). According to the United States (US) National Highway Traffic Safety Administration's (NHTSA), Fatality Analysis Reporting System (FARS), the number of pedestrian fatalities in the US has increased by 53%, from 4,109 in 2009 to 6,283 deaths in 2018 and compared with other traffic fatalities which had only increased by +2% during that period as shown in Table 1(Retting, 2019). According to the National Police Agency (NPA) examination of data from traffic accidents in multiple nations between 2016 and 2018, pedestrians account for around 36% of fatalities in Japan (Sasaki et al, 2019). In the same year, the number of pedestrian fatalities in the United Kingdom is around 25% (IIHS, 2020), and in the US and France are both around 16% (Retting, 2019). In addition, based on World Health Organization (WHO) statistics, road traffic fatalities in Sri Lanka reached 3,590 or 2.82% of total fatalities and ranked 96th in the world in 2018 (WHO, 2018).

It is very important to investigate pedestrians' RLR violations at signalized intersections. In this research, pedestrian crossing behavior is investigated using a video observation survey with the objectives of (a) quantifying the RLR rate at the selected signalized intersections; (b) suggesting recommendations which can be used to develop education programmes about the safety of pedestrians for school children and it will help them to be safe on road as pedestrians; (c) giving some recommendations which can be used to reduce the RLR.

Table 1: Pedestrian fatalities and percentage out of total fatalities in the US: 2009-2018

Year	Pedestrian Fatalities	All other traffic fatalities (Excluding pedestrian fatalities)	Total traffic fatalities	
			Number	Percentage
2009	4,109	29,774	33,883	12%
2010	4,302	28,697	32,999	13%
2011	4,457	28,022	32,479	14%
2012	4,818	28,964	33,782	14%
2013	4,779	28,114	32,893	15%
2014	4,910	27,834	32,744	15%
2015	5,494	29,990	35,484	15%
2016	6,080	31,726	37,806	16%
2017	6,075	31,398	37,473	16%
2018	6,283	30,277	36,560	17%
% change from 2009 to 2018	+53%	+2%	+8%	

Source: (Retting, 2019)

Motorized vehicles, non-motorized vehicles, and pedestrians should refrain from driving or walking in front of red traffic lights, according to the traffic safety law of Sri Lanka (Amarasingha and Ilhaam, 2019). Thus, all traffic that passes the red traffic light can be defined as RLR violations. It is not considered a violation, if the traffic passes the traffic light before it turns red. Pedestrian signal phases/colors have been categorized into three: green, amber, and red. When the 'green' light is pedestrians can cross the road, while the 'flash green/ amber light is on, pedestrians can cross but they cannot start to cross. Also, when the 'red' light is on, pedestrians cannot cross the road. Besides, pedestrian cycle length has also been defined using signal phases. It starts from green then amber and ends with red. In addition, RLR violators should be considered as one of the main contributing factors for pedestrian crashes (Johnson, 2011). Pedestrian RLR violators are of two types: 'opportunists' and 'risk takers'. Opportunist pedestrians cross the road even if the red signal is on if there is no vehicle in sight, risk takers cross the road when the color is amber (Amarasingha and Ilhaam, 2019).

According to Sri Lankan police-reported crash data, over time pedestrian crashes have increased in Sri Lanka even though it is still a developing country in the world. Some pedestrians on Sri Lankan roads seem to be aggressive while not obeying the rules and regulations (Jayasinghe and Amarasingha, 2019). The majority of Sri Lankans do not have their own vehicles when compared with people who live in developed countries. Therefore, most Sri Lankans travel by foot. Due to the high number of pedestrians, there is a high probability of accidents. In Japan, people generally use public transportation for travelling as they do not like to use their own vehicles for inefficient travel (Yudhistira et al, 2015). Japanese pedestrians obey traffic rules. Even when there are no cars on the road, pedestrians remain in the proper place at the edge of the sidewalk and wait the traffic light to turn green.

Road injuries have a major impact on a country's public health. Unfortunately, only about one-third of countries have a government-endorsed national road safety strategy that includes specific objectives, as well as funds allocated for its implementation (WHO, 2018). In addition, due to the increase in the number of road collisions, lives and property damages have also increased and it negatively affects society as well as the economy. Pavement qualities, road characteristics, geometric features, traffic characteristics, vehicle design, driver characteristics, road user behavior, and environmental features are some sub factors that contribute to the probability of road pedestrian accidents occurrence. It is difficult to identify pedestrian crossing behavior due to the complexity of multiple parameters such as personal, environmental and traffic attributes at signalized intersections (Marisamynathan et al, 2014). Because of the noncompliance behavior of pedestrians with traffic signals, vehicular-pedestrian interactions may occur at signalized intersections, and it is also highly likely for pedestrians to be injured in traffic accidents as a group at high risk of traveling on the road.

Over time, signal lights have been developed to control the interaction between vehicles and pedestrians at crosswalks. But accidents occur every day. One main reason for this issue may be pedestrians' violation of traffic regulations.

2 LITERATURE REVIEW

Wang et al. (2019) investigated RLR infringement of pedestrians in Hong Kong. According to that pedestrians were accountable for 62% of road fatalities in 2017(Transport Department, 2018). The purpose of this study was to investigate the factors that impact pedestrian red-light infractions and the severity of pedestrian injuries at signalized intersections. A significant non-compliance with traffic laws, especially among walkers, was found. The data used in this study's statistical analysis is from the Transport Department's Traffic Accident Database System (TRADS) and the Hong Kong Police Force. A binary logit model was applied to investigate the elements to find the severity of accident injuries and pre-crash violation behavior. The data was separated according to whether violated (N=1364) or not (N=388). The percentage of fatal/serious injuries that were caused that happened as a result of pedestrian RLR violations (28.39 %) did not vary from that of serious injuries that did not occur as a result of pedestrian RLR violations (25.29 %). Consequently, several models based on the random parameter probit approach were used to study pedestrian red-light infractions and injury severity.

Dommes et al. (2015) investigated RLR violation by adult pedestrians and other safety-related behaviors at signalized crosswalks. According to the Organization for Economic Cooperation and Development (OECD), over 20,000 pedestrian deaths occurred in its member nations in 2011 and ranged from 8% to 37% of all road fatalities. According to national figures, 30% of traffic collision has occurred on signalized crosswalks in France. An observation grid, location of observation, and questionnaires were used to collect data. Observational data with questionnaires administered among the 680 observed pedestrians, answered by 422 pedestrians (221 women and 201 men) of French adult pedestrians were observed. The functions of certain contextual, demographical, and mobility-related variables were investigated and a total of 13 observed behavioral indicators were extracted (twelve before, while crossing, and red-light violation). Subsequently, they were able to find, the distribution of participants' age groups: very elderly pedestrians (>75 years), elderly pedestrians (65-74 years), mature pedestrians (50-64 years), middle-aged pedestrians (30-49 years), young pedestrians (18-29 years) who make up 19% , 24%, 17%, 23%, and 17% of the sample, respectively, with nearly equal proportions of males and females in each age group, with the exception of the 18-29-year-old group (more women). The findings of logistic regression analysis conducted on each of the twelve behavioral variables that were observed prior to and during crossing revealed that gender had no significant effect, but that age did, with older pedestrians exhibiting more conservative behaviors. The results can help develop pedestrian safety as well as infrastructures.

Besides, Guo et al. (2011) did a study to identify the RLR of pedestrian activities at signalized crosswalks. In 2006, pedestrian deaths were nearly 26% of all traffic fatalities in China (23,285 pedestrians) and pedestrian injuries reported as 19% of all traffic injuries (82,391 pedestrians) as reported by the Ministry of Public Security of People's Republic of China (MPSPRC, 2007). The hazards-based duration model approach and video observation method were used for analysis. The assessment was carried out at seven crosswalks in Beijing, China. Video cameras were placed in each area to collect data. Peak hours (from 8:00 a.m. to 9:00 a.m. or from 5:00 p.m. to 6:00 p.m.) and off-peak hours (from 2:00 p.m. to 4:00 p.m.) data were included in the survey. Guo et al. (2011) were able to find that, of 1497 pedestrian observations, pedestrians had violated traffic laws in 597 cases (39.88 percent of 100). Per sample, there was an average waiting time of 17.1 seconds, with a standard deviation of 9.2 seconds. The violating crossing had an average waiting time of 15.9 seconds, whereas the normal crossing had an average waiting time of 18.2 seconds.

Marisamynathan et al. (2014) examined pedestrian crossing behavior in mixed traffic conditions such as the crossing speed, signal compliance, and pedestrian-vehicle contact and found contributing factors using statistical tests while designing signalized intersections. Pedestrian crossing speed was a considerable parameter under that study. According to the Indian Road Congress (IRC), the walking speed of pedestrians was estimated as 1.2 m/s at crosswalks. All possible parameters which influence pedestrian crossing behavior at crosswalks were identified using

SPSS 16.0 software. Noncompliance logistic model was developed using 775 completed samples. Only 434 pedestrians were in noncompliance with traffic lights and signals. There were 141 pedestrians, who interacted with vehicles directly. Males had higher odds of non-compliance rate and interaction with vehicles than female pedestrians. Old pedestrians and children had much higher odds of interaction than adult pedestrians (8.074).

Xie et al, (2017) explored pedestrian jaywalking at signalized crosswalks. The most prevalent type of intersection in Hong Kong was signalized intersections. Pedestrian vehicle collisions at signalized intersections had decreased by 35% in the last 5 years, although 387 pedestrian-vehicle collisions were recorded, accounting for approximately 25% of all accidents at signalized intersections. The following methods were used to analyze collected data: Basic binary logit model, Random parameter binary logit model, Random effect binary logit model and Goodness-of-fit. Observational surveys were conducted at seven crosswalks in Hong Kong, and pedestrian data and site condition data were integrated into a database. The modified pseudo R^2 value was in the range of 0.26 - 0.29, three models were produced, and an acceptable overall fit was obtained. The AIC values of the random parameter and random effect binary logit models were lower than the basic binary logit model and Mac Fadden's modified Pseudo R^2 values were higher.

Gong et al, (2019) conducted a study which characterized pedestrian violation crossing behavior of the Anning District of Lanzhou City. Pedestrian road deaths accounted for nearly 25 percent of all deaths, as 10 percent in Beijing and 19 percent in Chengdu happened at intersections. Several characteristics that potentially impact the violation rate were determined from the video observation method and field records using questionnaires. A total of 617 violations were involved at random from a total of 2852 legitimate pedestrian crossing samples at signalized junctions. The findings revealed that the rate of infraction crossing among older pedestrians was higher among other age groups with males slightly higher than that of females. The percentage of violations was 21.6 percent. Finally, age, headway, crosswalk length, the time it took to cross the road, gender, countdown display, red light duration, and companions were found as factors causing infractions. It has been found that pedestrians' walking speed, gender, traffic flow, the condition of the crosswalk, and the location of road significantly affect the probability of jaywalking.

Based on literature reviews, the number of pedestrian crash proportion is high. Therefore, countermeasures should be taken to increase traffic safety. Unfortunately, available studies have been done using information concerning pedestrian crossing behavior (Dommes et al, 2015; Wang et al, 2017; Xie et al, 2017, Jayasinghe and Amarasingha, 2019, Egodawatta, and Amarasingha, 2019), road and traffic characteristics (Sisiopiku et al, 2003; Wang et al, 2011) and vehicle interaction (Avineri et al, 2012). Many authors have identified both internal human factors as well as external environment's effects such as weather to understand RLR violation in pedestrian crossing, only a few research studies have been done on pedestrians' crossing behavior at signalized intersections in the world, while very few studies in Sri Lanka (Jayasinghe and Amarasingha, 2019) and they do not focus on RLR violations. This study investigates all possible variables and parameters that influence the crossing behavior of pedestrians at crosswalks in Kandy, Sri Lanka with a particular focus on the impact of gender on RLR violations.

However, most of the past safety research has been focused on vehicles rather than pedestrians. Transportation engineers and planners should be concerned about the behavior of pedestrians to improve their walking ability and reduce the interaction between vehicles and pedestrians under mixed traffic conditions at signalized intersections. This research attempts to identify the RLR violation rate of pedestrians in Sri Lanka. This would be helpful in taking measures to reduce pedestrian traffic fatalities.

3 METHODOLOGY

3.1 Study Area

To identify the pedestrian RLR violation, quantitative data were collected through video observation at three crosswalks which are located near 4-way junctions in the Kandy city area as

shown in Figure 1 near the sub-post office Crosswalk (SPOC), in front of café 210, and Bowatte Beheth Shalawa Crosswalk (BBSC).

a) Map b) Street view

Site 1: Near sub-post office Crosswalk (SPOC)

b) Map b) Street view

Site 2: In front of café 210 Crosswalk

a) Map b) Street view

Site 3: Kandy,Bowatte Beheth Shalawa Crosswalk (BBSC)

Figure 1: Maps and the street views of the study sites

3.2 Data collection

The main characteristics of the selected sites are shown in Table 2. The video camera was set up at selected crosswalks for 1-hour in the morning peak hours (from 7 am to 8am) and 1 hour in the evening peak hours (from 4pm to 5 pm). In other words, data collection was done for 2 hours per site.

Table 2: Characteristics of crosswalks in the study

Site Information	**Site 1**	**Site 2**	**Site 3**
Crosswalk Location	Sub post office, Kandy/ Kandy Jaffna Hwy A9(SPOC)	Sub post office, Kandy/ Kandy Jaffna Hwy A9 (café 210 crosswalk)	4-way junction/ Bowatte- Beheth-Shalawa/ Yatinuwara-Street (BBSC)
Pedestrian waiting time (For one cycle)	1 min and 55 secs	1 min and 55 secs	1 min and 8 secs
Pedestrian green time	20 secs	20 secs	25 secs
Crossing length	Approximately 8m	Approximately 10m	Approximately 8m
Vehicle flow rate	1675 Veh/hr	2420 Veh/hr	1120 Veh/hr
Number of traffic lanes	One-way road - three lanes	Two-way road	One-way road - three lanes
Date of data collection	14/06 & 15/06/2021	15/06 & 16/06/2021	16/06 & 17/06/2021

Even though the site characteristics are different, pedestrian demographic data can be considered together. Information about pedestrian crossing behavior such as running or walking, alone or accompanied by a companion or group; pedestrians' demographics details such as mainly

gender and age; other factors such as pedestrian crossing time, the crossing location (whether crosswalk is used or not), phase time pedestrian (crossing in non-green or green phase), traffic flow rate, number of lanes, and vehicle-pedestrian interaction at crosswalk were considered during the survey. To avoid lighting, visibility, and weather condition considerations, daytime during sunny days was chosen to get the video recording.

3.3 Data analysis

Video recordings were observed, and the variables needed for the study were manually recorded. Data collected using the video observations along with the variable definition are shown in Table 3. The total number of pedestrians observed was 564. Out of the 186 (32.98%) were in SPOC crossing and 277 (49.11%) were in café 210 and 101 (17.91%) were in BBSC.

Table 3: Variable Definitions and Collected Data

Variable	Definition	Observations
Gender	If the pedestrian is female, Gender= 0	178
	If the pedestrian is male, Gender= 1	386
Age	If the pedestrian's age is <20 years, Age= 0	72
	If the pedestrian's age is 20-60 years, Age= 1	316
	If the pedestrian's age is > 60 years, Age= 2	176
Crossing type	Crossing the road running = 0	67
	Crossing the road walking = 1	497
Accompanying pedestrians	If the pedestrian is alone, Accom. ped. =0	374
	If the pedestrian with one companion, Accom. ped. =1	43
	If it is a group of pedestrians, Accom. ped. =2	147
Carrying an item	If the pedestrian crosses with baggage, Item= 0	284
	If the pedestrian crosses with an umbrella, Item= 1	11
	If the pedestrian crosses with a heavy item, Item= 2	5
	If the pedestrian crosses without any item, Item= 3	264
Direction	If the pedestrian crosses upstream traffic and then downstream =0	244
	If the pedestrian crosses downstream traffic and then upstream =1	320
Crosswalk utilization	If the pedestrian crosses on the marked crosswalk =0	440
	If the pedestrian does not cross on the marked crosswalk =0	124
Crossing pattern	If the pedestrian crosses the road walking diagonally =0	431
	If the pedestrian crosses the road walking straight =1	86
	If the pedestrian crosses the road walking within the marked crosswalk lines =2	47
Compliance	Non-compliance with the signal phase =0	222
	Compliance with the signal phase =1	342
Mobile phone use while crossing	If the pedestrian uses a mobile phone while crossing =0	28
	If the pedestrian does not use a mobile phone while crossing =1	536

In addition to the categorical data collected for variables in Table 2, waiting endurance time and the crossing speed (the time pedestrians waited to cross during non-green phases) for each pedestrian were collected. The mean values were 18.3 seconds and 0.71 m/s respectively.

Chi-square test and binary logistic regression are utilized in this research. The Chi-Square Test is a statistical approach for determining whether an observed distribution is likely to have arisen randomly. It looks at how well the observed data distribution matches the anticipated distribution if the variables were independent (Heiberger et al, 2015). The Chi-square test is often known as the 'Goodness of Fit' test because of this. As a result, the Chi-square test does not operate with continuous

or parametric data. A Chi-square test's null hypothesis usually states that no statistical difference exists between observed and predicted counts of a particular variable in the population. By comparing with the observed and predicted counts at each level of category variable, Chi-square statistic for the Goodness of fit testing can be obtained. The decision can be made on whether to reject the null hypothesis at a predefined significance level. If the prediction is satisfied, the null hypothesis should be rejected. Otherwise, it will not be rejected. As an example, compliance varies with gender, assuming the following,

- Gender and compliance are independent, Null Hypothesis (H0)
- Gender and compliance are not independent, Alternative Hypothesis (H1)

Reject H_0 if *P* value < α level. Since *P* value is less than 5%, so H_0 can be rejected at a 5% level of significance (Heiberger et al, 2015).

Logistic regression is a classification approach that aids in predicting the likelihood of an event result (Heiberger et al, 2015). When the dependent variable is binary, binary logistic regression is utilized (Amarsingha, 2021). Given a set of predictors, logistic regression can help estimate the likelihood of falling into a specific level of categorical response. The likelihood of RLR violation equation of the binary logistic regression model is shown in Equation 1, when k number of predictors exists (Amarasingha, 2021).

$$\pi(X) = \frac{\exp(\beta 0 + \beta 1\, X1 + \ldots.. + \beta k\, Xk)}{(1+\exp(\beta 0 + \beta 1\, X1 + \cdots. + \beta k\, Xk)} \quad (1)$$

where: π(X) : the probability of RLR violation under the influence of *k* number of predictors,
xi : the influencing predictors for RLR violations, and
βi : regression coefficients (Amarasingha, 2021).

The regression coefficients of this model were estimated using the maximum likelihood method with the help of SPSS software, which uses a numerical analysis involving successive approximations.

4 RESULTS

4.1 Descriptive Data

Table 4 shows the number and percentage of compliance and non-compliance of both male and female pedestrians. The overall RLR violation rate of the pedestrians was 38.83%. The RLR violation rates of males and females are 44.30% and 26.97% respectively.

Table 4: Kandy pedestrians' signal phase compliance versus gender

Variable	Level	Non-Compliance with signal phases (RLR violations)	Non-Compliance Percentage (RLR violations %)	Compliance with signal phases	Compliance Percentage	Total
Gender	Female	48	26.97	130	73.03	178
	Male	171	44.30	215	55.70	386
	Total	219	38.83	345	61.17	564

4.2 Chi-Square Tests

In Chi-square analysis, the dependent variable 'RLR violations (non-compliance with signal phases)' was taken and the way it associated with other variables was analyzed. Table 5 gives the

observed numbers and expected numbers of pedestrians in both compliance and non-compliance with signal phases for each significant variable. Variables such as gender, age, crossing type, carrying an Item, crosswalk utilization, and crossing pattern showed significant differences in RLR violations. Accompanying pedestrians or crossing direction did not show any association with the RLR violations. When investigating the variable 'gender', it showed that females were less likely to violate RLR while males were more likely to violate RLR. Pedestrians whose age is below 20 years were more likely, those aged between 20-60 years less likely, and those aged above 60 years more likely to be RLR violators. Pedestrians who were running across the crosswalk or who crossed out of the marked crosswalk lines were more likely to be RLR violators.

Table 5: Compliance varies with independent variables

Variable	**Level**	**Observed/ Expected**	**Non-Compliance with signal phases**	**Compliance with signal phases**	**Asymptotic Significance (P)**
Gender	Female	Observed	53	134	0.000
		Expected	74	113	
	Male	Observed	169	208	
		Expected	148	229	
Age (years)	< 20	Observed	35	37	0.003
		Expected	28	44	
	20-60	Observed	105	211	
		Expected	124	192	
	60>	Observed	82	94	
		Expected	69	107	
Crossing Type	Walk	Observed	179	318	0.000
		Expected	196	301	
	Run	Observed	43	24	
		Expected	26	41	
Carrying an Item	Baggage	Observed	99	185	0.000
		Expected	112	172	
	Umbrella	Observed	0	11	
		Expected	4	7	
	Heavy Item	Observed	5	0	
		Expected	2	3	
	None	Observed	118	146	
		Expected	104	160	
Crosswalk Utilization	No	Observed	71	53	0.000
		Expected	49	75	
	Yes	Observed	151	289	
		Expected	173	267	
Crossing pattern	Within crosswalk lines	Observed	30	17	0.000
		Expected	19	29	
	Straight outside the marked lines	Observed	44	42	
		Expected	34	52	
	Diagonal outside the marked lines	Observed	148	283	
		Expected	170	261	

4.3 Binary Logistic Regression

Before developing the binary logistics regression model, the six model assumptions were checked (Leung, 2021; Amarasingha, 2021).

Assumption #1: The response variable is binary:

The dependent variable, the "RLR violations", was assigned the value of '1' for pedestrians of non-compliance with signal phases while the value of '0'was assigned for pedestrians' compliance with signal phases. As the dependent variable is RLR violation with 2 responses, the assumption is satisfied.

Assumption #2: The Observations are independent:

As shown in Figure 2, observation order versus standardized Pearson residual graph does not have a clear pattern. Therefore, it can be concluded that observations are independent.

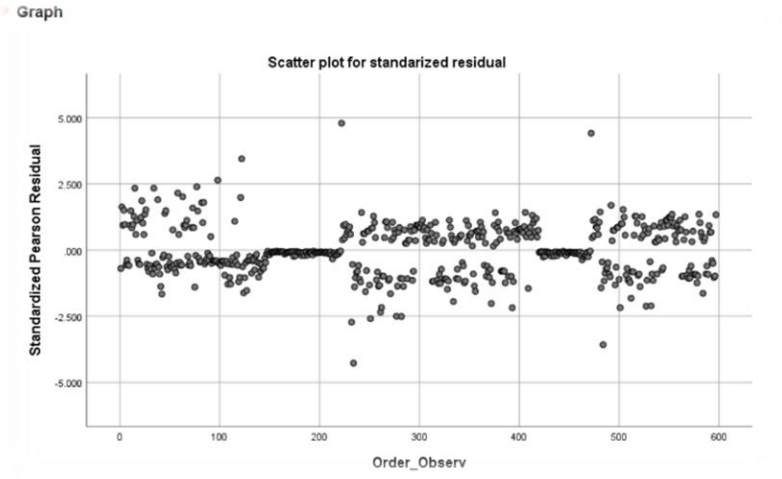

Figure 2: Scatter plot for standardized residual

Assumption #3: There is no multicollinearity among independent variables:

Initially, correlated matrix was prepared with 15 independent variables and highly correlated variables were noted. The highly correlated variable pairs were 'number of traffic lanes', 'pedestrian green time'; 'vehicle flow rate', 'crossing length', 'crossing beyond the line' and 'crosswalk utilization'. Then taking one variable out of the pair of highly correlated variables at a time, the binary logistics regression model was developed, and R-square value was checked. The variable within the lower R-square value was excluded for the rest of the analysis. Accordingly, the 'number of traffic lanes', 'crossing length', and 'crosswalk utilization' were the other three variables that were excluded.

Assumption #4: There are no extreme outliers:

Some outliers were noticed in the dataset as the threshold (= 4/ [sample size - number of parameters including the intercept) is smaller than the Cook distance. Therefore, outliers were removed from observations, and data were refitted to get the best model.

Assumption #5: There is a linear relationship between independent variables and the logit of the dependent variable:

The scatter plot between each independent variable and the logit values was visually observed and the logit linearity was ensured.

Assumption #6: The sample size is sufficiently large:

An adequate number of observations for each independent variable in the data is needed to avoid overfitting the model. The sample size of this study was 564 which could be considered as sufficient.

As all assumptions are satisfied, a binary logistic model was developed of with the Likelihood Ratio Chi-Square statistic of 248.780 with a P-value < 0.001. According to the obtained coefficient estimates in Table 6, five variables out of twelve are statistically significant which is less than 0.05 at a 5% level of significance towards RLR violation of pedestrians.

Table 6: Pedestrian RLR compliance at signalized intersections

Variable (type)	Description	B	Sig (P)
Intercept	-	76.849	0.997
Gender (categorical)	If the pedestrian is female, Gender= 0	-0.658	0.034
	If the pedestrian is male, Gender= 1	0.000	
Age (categorical)	If the pedestrian's age is <20 years, Age= 0	0.309	0.112
	If the pedestrian's age is 20-60 years, Age= 1	-0.385	
	If the pedestrian's age is > 60 years, Age= 2	0.000	
Crossing Type (categorical)	If pedestrians walk, Crossing Type= 0	-3.040	0.000
	If pedestrians run, Crossing Type= 1	0.000	
Accompanying pedestrians (categorical)	If the pedestrian is alone, Accom. ped. =0	0.124	0.872
	If the pedestrian is with one companion, Accom. ped. =1	0.229	
	If it is a group of pedestrians, Accom. ped. =2	0.000	
Crossing with baggage/ Umbrella/ Heavy item (categorical)	If the pedestrian crosses with baggage, Item= 0	-0.036	0.999
	If the pedestrian crosses with an umbrella, Item= 1	-20.092	
	If the pedestrian crosses with a heavy item, Item= 2	22.076	
	If the pedestrian crosses without any item, Item= 3	0.000	
Direction (categorical)	If the pedestrian crosses upstream traffic and then downstream =0	-0.044	0.861
	the pedestrian crosses downstream traffic and then upstream =1	0.000	
Crosswalk Utilization (categorical)	the pedestrian crosses on the marked crosswalk =0	1.406	0.000
	If the pedestrian does not cross on the marked crosswalk =1	0.000	
Mobile Phone Use (categorical)	If the pedestrian uses a mobile phone while crossing =0	21.799	0.999
	If the pedestrian does not use a mobile phone while crossing =1	0.000	
Waiting endurance time (Continuous)	-	-0.003	0.602
Crossing length (Conti...)	-	-11.405	0.997
Number of traffic lane (nominal)	If the number of lanes is two, Lane =2	-1.022	0.000
	If the number of lanes is three, Lane =3	0.000	
Pedestrian Speed (Conti...)	-	-2.556	0.000

The significant variables were gender, crossing type, crosswalk utilization, number of traffic lanes, and pedestrian speed. The variable 'Gender' is significant where the decreasing log of probability -0.658 of compliance for RLR among females was seen compared to that of males. 'Crossing type' is another significant variable which includes walking on the crossing decreases compliance of RLR with the log of probability 3.040 compared to running at the pedestrian crossing. The variable 'Crosswalk Utilization' is also significant when increasing the log of probability 1.406 of compliance with RLR among users of crosswalk compared to that of non- users of crosswalks. Another significant variable is the 'Number of traffic lanes' and log of the probability -1.022 which decreases compliance with RLR. 'Pedestrian speed' is also a significant variable where the log of probability -2.556 which decreases the compliance of the pedestrian's RLR.

5 DISCUSSION

According to the study done by Marisamynathan et al. (2014), pedestrian compliance with traffic signals in India was identified as 44%. But in Sri Lanka, it has gone up to 61.17%. By comparing these two outputs, India's pedestrian compliance is less than Sri Lanka. In other words, pedestrian violation rate at signalized intersections in India is higher than Sri Lanka. In another study, a total of 617 illegal violation samples were chosen at random from a total of 2852 valid pedestrian crossing samples at signalized intersections in Anning District of Lanzhou (Gong et al, 2019). They have identified that the violation rate of pedestrians was 21.6% which is less than Sri Lanka's 38.83%. By comparing these results, Sri Lankan pedestrian violation rate is higher than Lanzhou, China. Besides, Gong et al (2019) compared their result with other cities in China. In comparison to other cities, the violation rate in Lanzhou is higher than in Beijing, China (10%) and lower than in Izmir, Turkey (40%). Even though the violation rate in Lanzhou's Anning District is still quite high, it is not as high as the Sri Lanka's rate of 38.83 %. In addition, Wang et al. (2020) found the pedestrian redlight violations in Beijing, China as 22.1% with 388 cases. It is also lesser than Sri Lanka's RLR violation rate. Guo et al. (2011) found pedestrian violation in Beijing, China at 39.88 % which is nearly equal to the Sri Lankan value of 38.83 %. According to these results, Sri Lankan RLR violation rate is less than India's but not China's.

As a European country, a study was done on pedestrian behavior at signalized crosswalks in France (Dommes et al, 2015). They found that approximately two-thirds of the observed pedestrians (68%) obeyed the pedestrian red light which is greater than 61.17% of Sri Lanka's. Based on this result, Sri Lankan RLR violation rate is higher than France's. The RLR violation of pedestrians' percentages in Sri Lanka shows that male pedestrians are less patient and more likely to crosswalk than female pedestrians, which is consistent with most previous research (Tiwari et al., 2007; Rosenbloom, 2009; and Brosseau et al., 2013). As the obtained result, there are some associations with compliance RLR of pedestrians with age, crossing type, the number of pedestrian crossing, crossing with baggage/umbrella/heavy item, direction, crosswalk utilization, and crossing beyond the line.

According to this study, the variables: gender, crossing type, crosswalk utilization, number of traffic lanes, and pedestrian speed are significant in RLR violations of pedestrian in Sri Lanka. Gender of the pedestrian had a significant impact on pedestrian compliance behavior in India (Marisamynathan et al, 2014). The gender of the pedestrian and their walking speed have been found to have a significant impact on the likelihood of pedestrian jaywalking in Hong Kong (Wang et al, 2017). Dommes et al, (2015) found that, age was not a direct significant predictor of RLR violation which is one result of our model with Sri Lankan data. In addition, Zhu et al. (2020) found age, gender, the presence of a companion, and traffic volume as significant variables in Hong Kong. But only gender was significant in our model. However, according to Ren et al. (2011) gender did not emerge as an important factor in crossing behaviors in results, except for these two: waiting on the roadway (more often observed in women) and running (rarely observed in men). These findings are slightly different from previous research, which found significant gender differences in pedestrian behavior, both as reported by pedestrians and as directly observed in real-world situations (Rosenbloom, 2009; Tom & Granié, 2011; Yagil, 2000). In addition, there are some considerable associations with particular pedestrian crossing behavior and significant variables.

6 CONCLUSIONS

This study finds the RLR violation rates of pedestrian's as 38.83%. Out of 564 pedestrians 219 violated the rules, as found in video observation surveys at the signalized crosswalk in Kandy city, Sri Lanka. It shows that RLR violation rate of males is higher than females. When the pedestrian violation rate in Sri Lanka is compared with India (54%), Sri Lakas' is lower. But not low as in China (21.6%) and France (32%). Usually, the RLR violation rate in developing countries such as Sri Lanka, India etc is higher than in developed countries such as France, China etc. According to the binary logistic regression model, 'gender', 'crossing type', 'crosswalk utilization', 'number of traffic lanes', and 'pedestrian speed' were statistically significant variables for influencing the RLR violations. These findings help improve the effectiveness of pedestrian management and control at

signalized intersections by providing a better understanding of illegal crossings and their impact factors. With a more comprehensive dataset, other environmental factors such as weather, noise, temperature, and land use type would be well worth investigating. Analyzing pedestrian crossing behavior, including pedestrian arrival patterns and influencing parameters, would improve the work's future potential and pedestrian safety. Under this study, some recommendations can be briefly listed as follows: introduce a new fine system for pedestrians who do not obey the traffic rules and regulations, increase existing fines and imprisonment for drivers charged with RLR violations., pedestrians should be informed by government and non-government organization, pedestrians who obey red light would be awarded and appreciated, introduce new subjects to school system such as 'Traffic Safety' and children should be trained to obey traffic rules and regulations. Future researchers will be able to develop a better model by following these suggestions: an automated camera system would be developed rather than manual data collection which takes more time to exact data, sample size should be increased to get very accurate results, and the number of locations should be increased, data only collected during regular days, not holiday and Poya days etc., latest cameras would be placed to capture the large view as well as a video of high quality.

REFERENCES

Amarasingha, N. (2021). Risk factors of crashes involving motorcycles in Sri Lanka. *Journal of South Asian logistics and transport*, *1*(2).

Amarasingha, N., & Ilhaam, M. (2019). Red Light Running Violations of four intersections in Colombo suburban. In Proceedings of the Eastern Asia Society for Transportation Studies (Vol. 12).

Avineri, E., Shinar, D., & Susilo, Y. (2012). Pedestrians' behaviour in cross walks: The effects of fear of falling and age. *Accident Analysis & Prevention*, *44*(1), 30-34. https://doi.org/10.1016/j.aap.2010.11.028

Brosseau, M., Zangenehpour, S., Saunier, N., & Miranda-Moreno, L. (2013). The impact of waiting time and other factors on dangerous pedestrian crossings and violations at signalized intersections: A case study in Montreal. *Transportation Research Part F: Traffic Psychology and Behaviour*, 21, 159-172

Dommes, A., Granié, M., Cloutier, M., Coquelet, C., &Huguenin-Richard, F. (2015). Red light violations by adult pedestrians and other safety-related behaviors at signalized crosswalks. *Accident Analysis & Prevention*, *80*, 67-75. https://doi.org/10.1016/j.aap.2015.04.002

Egodawatta, H. M., & Amarasingha, N. (2019). Mobile Phone Use at Un-signalized Mid-block Pedestrian Crossings in Sri Lanka. In *Proceedings of the Eastern Asia Society for Transportation Studies* (Vol. 12).

Gong, Q., Xiao, L., & Xu, M. (2019). Pedestrian violations crossing behavior at signal intersections: A case study in Anning District of Lanzhou. *IOP Conference Series: Materials Science And Engineering*, *688*(4), 044006. https://doi.org/10.1088/1757-899x/688/4/044006

Guo, H., Gao, Z., Yang, X., & Jiang, X. (2011). Modeling Pedestrian Violation Behavior at Signalized Crosswalks in China: A Hazards-Based Duration Approach. *Traffic Injury Prevention*, *12*(1), 96-103. https://doi.org/10.1080/15389588.2010.518652

Heiberger, R. M., Heiberger, R. M., & Burt Holland, B. H. (2015). *Statistical Analysis and Data Display An Intermediate Course with Examples in R*. Springer.

Insurance Institute for Highway Safety (IIHS), (2020), Highway Loss Data Institute, Fatality Facts 2020Pedestrians, https://www.iihs.org/topics/fatality-statistics/detail/pedestrians

Jayasinghe, J., & Amarasingha, N. (2019). Pedestrian Crossing Behavior at Three Urban Signalized Intersections in Colombo. In *Proceedings of the Eastern Asia Society for Transportation Studies* (Vol. 12).

Johnson, M., Newstead, S., Charlton, J., & Oxley, J. (2011). Riding through red lights: The rate, characteristics and risk factors of non-compliant urban commuter cyclists. *Accident Analysis & Prevention*, *43*(1), 323-328. https://doi.org/10.1016/j.aap.2010.08.030

Leung, K. (2021). Assumptions of logistic regression clearly explained. Towards Data Science, available at https://towardsdatascience.com/assumptions-of-logistic-regression-clearly-explained-44d85a22b290

Marisamynathan, & Perumal, V. (2014). Study on pedestrian crossing behavior at signalized intersections. *Journal Of Traffic And Transportation Engineering (English Edition)*, *1*(2), 103-110. https://doi.org/10.1016/s2095-7564(15)30094-5

Ren, G., Zhou, Z., Wang, W., Zhang, Y., & Wang, W. (2011). Crossing Behaviors of Pedestrians at Signalized Intersections: Observational Study and Survey in China. *Transportation Research Record: Journal Of The Transportation Research Board*, *2264*(1), 65-73. https://doi.org/10.3141/2264-08

Retting, R. (2019). Safety, transportation and trends: pedestrian traffic fatalities by state, Governors Highway Safety Association: Washington, DC, USA.

Rosenbloom, T. (2009). Crossing at a red light: Behaviour of individuals and groups. *Transportation Research Part F: Traffic Psychology and Behaviour*, 12, 389–394.

Sasaki H., Yamamoto Y., Matsumoto A. & Mito K., (2019). Recent high-profile pedestrian fatalities expose Japan's road safety failing. *Mainichi Japan*, City News Department. https://mainichi.jp/english/articles/20190514/p2a/00m/0na/023000c

Sisiopiku, V., & Akin, D. (2003). Pedestrian behaviors at and perceptions towards various pedestrian facilities: an examination based on observation and survey data. *Transportation Research Part F: Traffic Psychology AndBehaviour*, *6*(4), 249-274. https://doi.org/10.1016/j.trf.2003.06.001

Tiwari, G., Bangdiwala, S., Saraswat, A., & Gaurav, S. (2007). Survival analysis: Pedestrian risk exposure at signalized intersections. *Transportation Research Part F: Traffic Psychology and Behaviour*, 10(2), 77-89

Tom, A., &Granié, M. (2011). Gender differences in pedestrian rule compliance and visual search at signalized and unsignalized crossroads. *Accident Analysis & Prevention*, *43*(5), 1794-1801. https://doi.org/10.1016/j.aap.2011.04.012

Wang, W., Yuan, Z., Liu, Y., Yang, X., & Yang, Y. (2019). A random parameter logit model of immediate red-light running behavior of pedestrians and cyclists at major-major intersections. *Journal of Advanced Transportation*, *2019*. https://doi.org/10.1155/2019/2345903

World Health Organization. (2018). *Global status report on road safety 2018*. World Health Organization.

Xie, S., Wong, S., Ng, T., & Lam, W. (2017). Pedestrian Crossing Behavior at Signalized Crosswalks. *Journal Of Transportation Engineering, Part A: Systems*, *143*(8), 04017036. https://doi.org/10.1061/jtepbs.0000055

Yagil, D. (2000). Beliefs, motives and situational factors related to pedestrians' self-reported behavior at signal-controlled crossings. *Transportation Research Part F: Traffic Psychology AndBehaviour*, *3*(1), 1-13. https://doi.org/10.1016/s1369-8478(00)00004-8

Yudhistira, G., Firdaus, M. I., & Agushinta, L. (2015). Transportation System in Japan: A Literature Study. *Jurnal Manajemen Transportasi & Logistik*, *2*(3), 333-352.

Zhu, D., & Sze, N. (2021). Propensities of red light running of pedestrians at the two-stage crossings with split pedestrian signal phases. *Accident Analysis & Prevention*, *151*, 105958. https://doi.org/10.1016/j.aap.2020.105958

Attributes of ADR in the Sri Lankan Construction Industry

Vajira Edirisinghe
Department of Quantity Surveying, Faculty of Engineering,
Sri Lanka Institute of Information Technology, Malabe, Sri Lanka
vajira.e@sliit.lk

Dianne Marsh, Fiona Borthwick, Mohan Siriwardena, Alison Cotgrave
School of Civil Engineering and Built Environment, Faculty of Engineering and Technology, Liverpool John Moores University, Byrom Street, Liverpool L3 3AF, United Kingdom
D.Marsh@ljmu.ac.uk, F.Borthwick@ljmu.ac.uk, M.L.Siriwardena@ljmu.ac.uk, A.J.Cotgrave@ljmu.ac.uk

ABSTRACT

Alternative dispute resolution (ADR) methods were introduced to the construction industry to avoid the negative effects of litigation in relation to the cost, time, and business relationships of a construction project. This study focused on identifying the current ADR practices in the Sri Lankan construction industry and examined the specific attributes of each method to create a more effective process. A qualitative research strategy was carried out with interviews with industry professionals working in the Sri Lankan Construction Industry. Content analysis using NVivo software was used to analyse the data. The key findings revealed that the neutral third party has good knowledge of construction. Despite the differences in each ADR method, disputing parties do not have the confidence in the neutral third party or trust in the process. This study also revealed that the unavailability of these key attributes will finally affect the cost and reputation of the ADR methods. Therefore, the research suggests that to improve the ADR process and its success there should be awareness studies on ADR methods and training for ADR practitioners within the Sri Lankan Construction Industry.

KEYWORDS: *Construction industry, ADR, Attributes*

1 INTRODUCTION

This paper is a part of a current research project to evaluate the attributes of Alternative Dispute Resolution (ADR) to develop a cost-effective framework for ADR in the Sri Lankan construction industry. The paper aims to analyse the current ADR practices in Sri Lanka concerning the defined ADR attributes. The study was conducted in three steps. First, the popular ADR methods in the Sri Lankan construction industry were identified. Secondly, the attributes of ADR practices were defined, and finally, the attributes of ADR practices in the Sri Lankan construction industry were analysed. ADR is an alternative method used to resolve disputes by avoiding costly and time-consuming court procedures, which further leads to damaging relationships among the parties (Niriella, 2016). Further, Polinsky and Shavell, (2012) found that the average litigation cost is about two third of the actual damage. However, unlike other commercial disputes, construction disputes involve complex technical issues, several parties, and a large volume of documents (Fadhlullah Ng et al., 2019), and as a consequence, construction professionals prefer ADR to litigation to resolve construction disputes.

Latham, (1994) warned that a fundamental reason for construction project failure is disputes. Nevertheless, due to the complex nature, challenging environment, and the involvement of different knowledge-based professionals in the industry disagreement is inevitable (Cakmak and Cakmak, 2014). Therefore, having a proper dispute resolution method has become a basic requirement in a project.

2 BACKGROUND

Construction disputes could happen at any point during the design or construction phase of the project (Hall, 2002). According to Ume et al., (2014) construction disputes vary in nature, size, and complexity, but they all are costly both in terms of time and money and can often damage a good working relationship. Furthermore, any delay in construction due to construction disputes will also

impact owners in terms of loss of investment revenue (Marzouk and Moamen, 2009). Several scholars have examined the causes and categories of disputes in the Sri Lankan construction industry such as; Abeynayake and Wedikkara, (2012) identified four dispute categories, Halwathura and Ranasinghe (2013) and Perera et. al., (2021) presented disputes in highway projects, Gunarathna et al., (2018), Illankoon et al., (2019) and Edirisinghe et.al., (2020) identified disputes in the construction industry in general.

2.1 Alternative Dispute Resolution methods in the Sri Lankan construction industry

Alternative dispute resolution (ADR) is a term usually used to refer to an informal dispute resolution process in which the parties meet with a professional third party (Hansen, 2019) who helps them resolve their disputes in a way that is less formal and often more consensual than litigation (Abeynayake and Weddikkara, 2012). The out-of-court conflict management and dispute resolution mechanisms are arbitration, mediation, negotiation, village councils, fact-finding, partnering, dispute resolution boards, and other related dispute resolution processes (Nafees and Ayub, 2016). ADR is a dispute resolution process that encourages or facilitates the disputants to solve their disputes having appointed their judges (Ranasinghe and Korale, 2011). Brooker and Lever (1997) further confirm that the most common reasons to refer to ADR methods are their efficiency in terms of speed and cost compared to litigation. However, the frequently used alternative dispute resolution method in the construction industry are negotiation, conciliation, mediation, adjudication, and arbitration (De Zylva, (2006), Abeynayake and Weddikkara, (2013), Abeynayake and Weddikara (2014)). The following paragraphs briefly discuss those ADR methods.

Negotiation - Early settlement in construction disputes will prevent aggravation of negative impact on project performance (Chan and Suen, 2005). Although there are several possible resolution methods, disputes are always negotiated first before other methods are considered (Cheung et al., 2006). Even in the Sri Lankan construction industry negotiation is the initial attempt to resolve construction disputes (Jayasena and Yakupitiyage, 2012; Gunasena, 2010). Moreover, negotiation provides an opportunity for the parties to exchange promises and commitments to aid the resolution of differences (Tucker, 1996). The success of a negotiation is determined by the extent to which the parties are willing to compromise their needs (Hoogenboom and Dale, 2005) without the involvement of a third party (Gulliver, 1979).

Mediation - Mediation is a voluntary nonbinding process in which a neutral third party assists two or more disputing parties to reach an agreement as to how that dispute is to be settled (Morgerman, 2000). The third-party facilitator, who is a mediator does not possess any power to make decisions as to the agreement or to issue decrees but only assists the productive communication between the parties to the dispute (Saranee and Gunathilaka, 2017). Further, mediators have no authority to resolve disputes or to make decisions that are binding on the parties (Silberman, 1997). Today, in Sri Lanka, mediation has become a preferred choice for parties to a dispute (Alexander, 2002). The Construction Industry Development Authority encourages mediation activities by instructing the construction contracting parties to forward their disputes to mediation (Abeynayake and Wedikkara, 2013).

Conciliation - Similarly, in mediation, conciliation involves third-party intervention but requires more active participation of the conciliator rather than in mediation in generating solutions (Ifeanyi, 2000). In mediation, a neutral and independent person assists the disputing parties to reach a mutually acceptable solution, where the conciliator makes his formal recommendations for a settlement which may be either accepted or used as a basis for the parties to further negotiate and reach a settlement (Ranasinghe, 2012). The conciliation process is confidential, and the documents prepared during the process are without prejudice and cannot be referred to or used in any subsequent proceedings (Ramsbotham et.al, 2011). In particular, the content of any recommendation made by a conciliator must not be made known to any arbitrator or judge (Hill and Wall, 2008).

Adjudication - Adjudication is a system by which disputes are referred to the neutral third party, for a decision that is binding on the parties until the dispute is finally resolved by agreement, arbitration, or litigation (Joint contracts tribunal). In Sri Lanka, adjudication is conducted according to the Construction Industry Development Authority (CIDA) and FIDIC conditions of the contract. CIDA introduced the adjudication process to the Sri Lankan construction industry as an immediate step of

construction dispute resolution in their first revised edition of the Standard Bidding Document (SBD) in 2007. According to CIDA conditions, the adjudicator shall give his/her determination on the dispute within 28days, or such other period agreed by the parties of the receipt of such notification of a dispute. However, the adjudication procedure according to FIDIC is when a dispute refers to an adjudication decision, which is to be given within 84 days or such other time as is proposed by the DAB and approved by the parties.

Arbitration- The main difference between arbitration and litigation is that arbitration is consensual and final where the award may treat only those matters that are referred to arbitration by the parties (Fadhlullah Ng et al., 2019). Deffains et al., (2017) claimed several other differences between arbitration and litigation such as; the litigation process follows court procedures based on the Code of Civil Procedures of the jurisdiction, proceedings are open to the general public, councilors do not have expert knowledge in construction or construction disputes. Britain formally introduced Arbitration to Sri Lankan legal system in the 19th Century by enacting two statutes; The Arbitration Ordinance no:15 of 1866 and the civil procedure code of 1889 (Abeynayake and Wedikkara, 2012a). However, both statutes were replaced by the Arbitration Act of Sri Lanka No.11 of 1995, which was inspired by the Swedish Arbitration Act and UNCITRAL model law ((Asouzu and Raghavan, 2000). By enacting the Arbitration Act of Sri Lanka No.11 of 1995 on 30th June 1995 in the Sri Lankan parliament, Sri Lanka became the first country in South Asia to enact an Arbitration Law (Abeynayake and Wedikkara, 2012b).

2.2 Attributes of ADR in the Sri Lankan construction industry

Each ADR process has its attributes that influence the adoption of a specific process in specific circumstances (Cheung, 1999). York(1996)listed ADR attributes such as; confidentiality, degree of control by parties, choice over the identity of a judge or neutral, flexibility in issues and strategy, delay risk, forensic tactics, witness control, consolidation of claims by order, available remedies, binding decision and enforcement, appeals, liability for costs, cost of the tribunal, relative cost, time required of parties, preservation of relationships, overall duration, neutrality, professional behavior, experience in construction and credibility. In contrast, Ilter and Dikbas, (2008) identified attributes of ADR in terms of control by a neutral, wide range of issues, transparency of judgment, enforceability, liabilities to the opponent's cost, voluntariness, and width of remedy. Jayasena and Yakupitiyage, (2012) further categorized the attributes into main and sub-attributes for the Sri Lankan construction industry. By reviewing the scholars' work this study has listed ADR attributes as the main and sub-attributes as demonstrated in Figure 1.

Even though the construction industry professionals have shown a marked preference towards ADR instead of litigation, recently the popularity of ADR practice is diminishing due to several reasons, as an example, current arbitration practice shows adversarial characteristics (Brooker and Lavers, 1997), adjudication decisions are unsuccessful and neither party was satisfied with the outcome (Jayasinghe and Ramachandra, 2016). Similarly, other voluntary processes such as negotiation, mediation, and conciliation have failed and ultimately arbitration had become a costly and a time-consuming process. (Cheung et al., 2002). Therefore, the study aims to revisit the current ADR practices in the Sri Lankan construction industry.

3 METHOD

Semi-structured interview questions developed through an extensive literature survey on the attributes of ADR were used to collect qualitative data. The purpose of the interview was to strengthen and verify the research areas in the Sri Lankan context. The experts were CIDA registered 8 Arbitrators/ Adjudicators (AA), and 12 industry practitioners, representing consultant engineers (CE), consultant quantity surveyors (CQS), consultant architects (CA), and senior engineers (SE). All the participants have 13-56 range of years' experience and work in high-level positions in their construction organizations, in Sri Lanka. The selected arbitrators/adjudicators were popular in resolving disputes in mostly local construction and international construction contracts. Other participants are in very senior positions in construction organizations with more than 5-8 Million Rupees annual turnover.

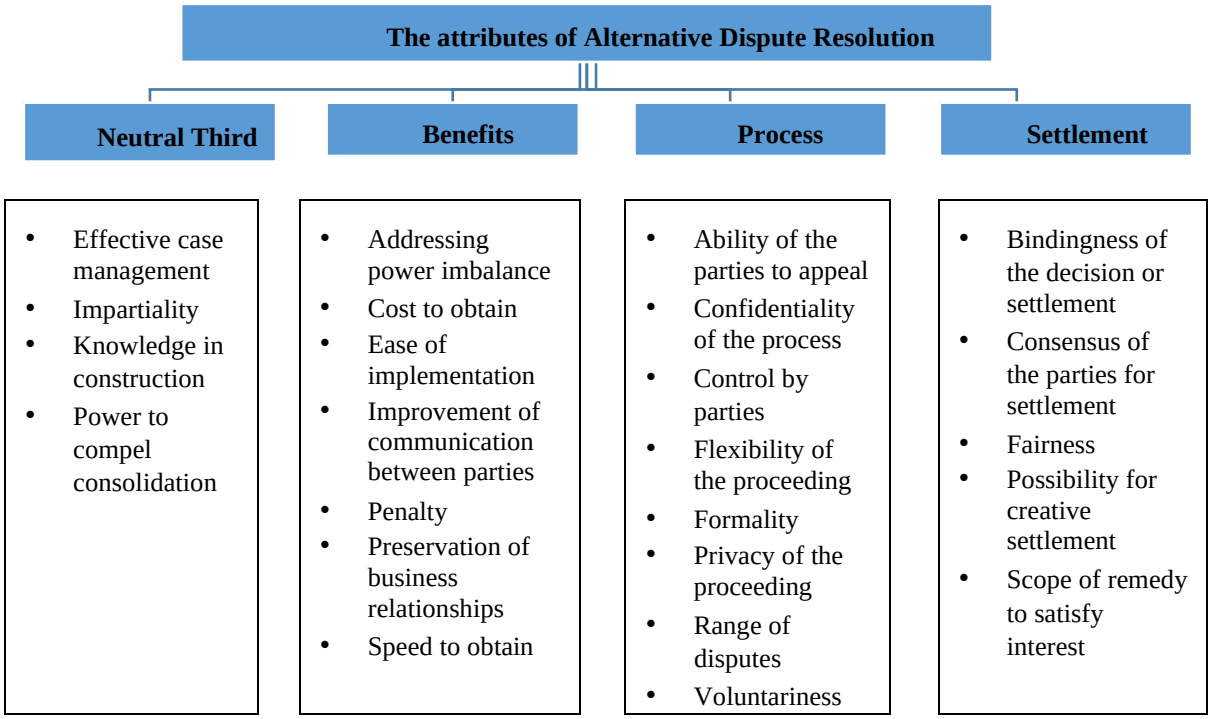

Figure 1 Hierarchy model of ADR attributes (Developed from Literature).

The duration of the interview was nearly 45-60 minutes, and the recordings were transcribed and entered in NVivo for data analysis.

4 RESULTS AND ANALYSIS

This section focuses on how current industry professionals evaluate the attributes of current ADR practices in the Sri Lankan construction industry. The study involved a qualitative research strategy where the results obtained through the literature review were compared with the current practices and the ideas of the construction industry professionals.

The four main attributes and twenty-four sub-attributes of ADR were presented to 20 construction industry professionals during the semi-structured interviews. The interviewees were requested to explain and comment on each attribute with reference to the current ADR practices in Sri Lanka. This qualitative data was analyzed through NVivo 12 using thematic analysis. Coding in NVivo 12 was conducted in three separate themes such as; ADR methods (high-level themes), main attributes (mid-level themes), and sub-attributes (low-level themes). Then a thematic framework for five different types of interviewees (cases) namely, adjudicator/arbitrator (AA), senior engineer (SE), consultant engineer (CE), consultant quantity surveyor (CQS), and consultant architect (CA) was developed. Additionally, when analyzing the predefined themes, the focus was predominantly on a case rather than the individuals within them. When analyzing the interaction, particular attention was paid to how, and whether, the groups established common grounds. Thus, the analysis focused on the content of the discussions and the dynamics of interactions within the groups. In that sense, the detailed analysis of five common ADR practices against attributes was discussed in four sections.

4.1 Evaluating Attributes of ADR

By considering the pattern of the results, the interviewees were further categorized into two groups namely Group 1 and Group 2. Group 1 include adjudicators/arbitrators whereas group 2 included CQS, CE, SE, and CA.

In relation to the negotiation, both groups expressed similar thoughts. Negotiation is a nonbinding dispute resolution method conducted without the involvement of an external party (Gulliver,

1979). Therefore, sub-attributes relevant to a neutral third party were not discussed under negotiation. As shown in table 1negotiation provides many benefits compared to other ADRs as per groups 1 and 2. Nevertheless, those benefits can be achieved if parties positively corporate within the process.

Table 1 Evaluating Attributes – Negotiation and Mediation

		Negotiation		**Mediation**	
Mid-level themes	**Low-level themes**	**Group 1**	**Group 2**	**Group 1**	**Group 2**
Neutral third	Effective case management	Negotiation happens among the disputing parties. There is no external party intervention.		Available	Available
	Impartiality			Available	Available
	Knowledge in construction			Available	Available
	Power to compel consolidation			Not relevant	Not relevant
Benefits	Addressing power imbalance	Available	Available	Not sure	Not sure
	Cost to obtain	Can be considered as zero cost		Low cost	Low cost
	Ease of implementation	Party autonomy	Party autonomy	Party autonomy	Party autonomy
	Improvement of communication between parties	Available	Available	Available	Available
	Penalty	No	No	No	No
	Preservation of business relationships	Yes	Yes	Yes	Yes
	Speed to obtain	Speedy	Speedy	Comparatively high	Comparatively high
Process	Ability of the parties to appeal	No	No	No	No
	Confidentiality of the process	Available	available	available	available
	Control by parties	yes	yes	95% control is there	yes
	Flexibility of the proceeding	available	available	available	available
	Formality	no	no	Few formalities are available	
	Privacy of the proceeding	available	available	available	available
	Range of Disputes	Can resolve any range of dispute		Available but some government policies cannot resolve	
	Voluntariness	yes	yes	Yes, in many instances	
Settlement	Bindingness of the decision/award	Party autonomy	Party autonomy	Party autonomy	Party autonomy
	Consensus of the parties for settlement	Yes	Yes	Yes	Yes
	Fairness	Depends on the parties		Depends on persons	
	Possibility for creative settlement	Depends on the parties		Depends on the mediator	
	Scope of remedy to satisfy interest	Depends on the parties		Yes	Yes

The mediator who is acting as the neutral third party possesses almost all the attributes according to both groups. Not only that, but it is also a speedy and cost-effective method. However, like in negotiation, parties need to act positively to get the benefits of the method.

Half of the group 1 interviewees claimed that the conciliator is impartial whilst group 2 believed it depends on the personality and integrity of the person (Table 2). The availability of benefits in conciliation is most similar to negotiation and mediation. The speed to obtain the decision is agreed to be faster than adjudication and arbitration.

Table 2 Evaluating Attributes – Conciliation and Adjudication

		Conciliation		**Adjudication**	
Mid-level themes	**Low-level themes**	**Group 1**	**Group 2**	**Group 1**	**Group 2**
Neutral third	Effective case management	Available	Doubtful	Available	-
	Impartiality	50% agreed	This depends on the person	Somewhat available	No
	Knowledge in construction	Available	Available	Available	Available
	Power to compel consolidation	Not relevant	Not relevant	Available	Available
Benefits	Addressing power imbalance	Available	Available	Depends on the adjudicator	
	Cost to obtain	Low cost	Low cost	High cost	High cost
	Ease of implementation	Party autonomy	Party autonomy	Party autonomy	Party autonomy
	Improvement of communication between parties	Available	Available	Did not consider as important	Not sure, but better to have
	Penalty	No	No	No	No
	Preservation of business relationships	Yes	Yes	Not sure	Not sure
	Speed to obtain	Compared to adj/arb high	Compared to adj/arb high	More time	More time
Process	Ability of the parties to appeal	No	No	No	No
	Confidentiality of the process	Available	available	available	available
	Control by parties	90% control is there	yes	Until the adjudicator is appointed	
	Flexibility of the proceeding	available	available	available	available
	Formality	Formal	formal	formal	formal
	Privacy of the proceeding	available	available	available	available
	Range of Disputes	Available but prefer less		Available but prefer less	
	Voluntariness	Yes, in many instances		No	No
Settlement	Bindingness of the decision/award	Party autonomy	Party autonomy	Party autonomy	Party autonomy
	Consensus of the parties for settlement	Yes	Yes	No	No
	Fairness	Depends on the person		Yes	doubtful
	Possibility for creative settlement	Depends on the conciliator		Depends on the adjudicator	
	Scope of remedy to satisfy interest	yes	yes	yes	yes

In conciliation, according to group 1, party to the dispute is having 90% control over the process. Furthermore, group 1 further agrees on the conciliator while creating communication between the disputing parties decides with his expert knowledge. However, all three methods are voluntary, non-binding processes with the majority of benefits compared to adjudication and arbitration.

In adjudication, both groups agreed that the adjudicator possesses the required knowledge in construction but disagreed on the ability to effectively manage the referred cases. Interestingly, CQS agrees on group 1 in power to compel consolidation of the adjudicator. Both groups agree that the cost and time spend on the process are higher than the above non-binding methods. But the similarity is in the implementation of the decision where it depends on the parties. Regarding the adjudication process, parties are not allowed to appeal and both groups agreed on that. In addition, the process is formal, flexible, and private as explained in the literature. However, both groups agree that it is not a voluntary process. Group 1 further explained the contract agreement instructs the parties to refer their dispute to adjudication for resolution.

Group 1 is confident in the ability to manage cases effectively by the arbitrator whereas group 2 doubted this (Table 3).

Table 3 Evaluating Attributes - Arbitration

		Arbitration	
Mid-level themes	**Low-level themes**	**Group 1**	**Group 2**
Neutral third	Effective case management	Available	Doubtful
	Impartiality	Somewhat available	No
	Knowledge in construction	Available	Available
	Power to compel consolidation	Available	Not sure
Benefits	Addressing power imbalance	Not considered	Not considered
	Cost to obtain	High cost	High cost
	Ease of implementation	Since it has statutory powers, a court can enforce	
	Improvement of communication between parties	Did not consider as important	Did not consider as important
	Penalty	Winning party can claim	Even though the winning party can claim the cost for arbitration parties should take only what they are entitled rather than making it a penalty
	Preservation of business relationships	Not sure	Not sure
	Speed to obtain	more time	More time
Process	Ability of the parties to appeal	Disagreeing party can go to court and appeal	
	Confidentiality of the process	Available	available
	Control by parties	Until the arbitrator appointing	
	Flexibility of the proceeding	available	available
	Formality	Formal	formal
	Privacy of the proceeding	available	available
	Range of Disputes	Prefer to have a smaller number of disputes	
	Voluntariness	No	No
Settlement	Bindingness of the decision/award	yes	yes
	Consensus of the parties for settlement	important	No
	Fairness	Yes	doubtful
	Possibility for creative settlement	Depends on the arbitrator	
	Scope of remedy to satisfy interest	yes	yes

Similarly, group 1 believed that impartiality was demonstrated by some arbitrators, however, group 2 did not believe in the impartiality of the arbitrator. Nevertheless, both groups agreed that arbitration is a costly, time-consuming process and is not supported by the human relationships between the parties. Whilst it was agreed that the arbitration award had statutory powers and could be enforced in the courts, group 2 questioned the fairness of the settlement whilst group 1 believed the award given by the arbitrator is fair and creative.

5 CONCLUSIONS

There were both negative and positive comments given for the attributes of ADR discussed above. The neutral third party for ADR resulted in the greatest variance of response (except negotiation) as some of the interviewees were not convinced of the impartiality of the arbitrators and adjudicators. Even though half of AA claimed the conciliator to be impartial, CA explained it is dependent on the person.

The benefits of adjudication and arbitration were similar in addressing power imbalance, the cost to obtain, improvement of communication between parties, preservation of business relationships, and the speed to obtain a decision. Both methods were acknowledged as costly and time-consuming. The decision will depend solely on submitted documents and witness evidence. Even though there is no penalty granted in adjudication, in arbitration the winning party can claim the money for arbitration during the submission of the arbitration claim.

The desirable benefit of arbitration is the ability to implement arbitral awards through the courts. Any other ADR does not have that facility. Concerning conciliation and mediation, the cost and time will be much less. Further, both methods will help to improve the communication between the parties and preserve their business relationship. With regard to benefits, negotiation was identified as the best option. The main reasons behind that are its cost effective and time effective features. The arbitration process is highly adversarial compared to adjudication. Therefore, the parties who do not wish to go ahead with the decision/award in arbitration can go to courts to appeal whereas no other method is allowed. Not only is that in addition, but arbitration is also formal and not voluntary. It is similar to adjudication but different from the other three ADRs. Both groups prefer to have less number of disputes at a time. Flexibility and party autonomy can be more visible in negotiation, and conciliation other than in arbitration and adjudication.

Whilst an arbitral award is binding all other, ADR decisions are binding until the disagreeing party refers the dispute to the next level of ADR. The fairness of the settlement is a major issue as the majority of those interviewed agreed that the outcome of arbitration and adjudication is often not fair. If the disputing parties are willing to come to a fair, creative settlement with the scope of remedy to satisfy interest, negotiation as an ADR appears to be the best option.

Informed by the above findings, the next step of this research will proceed to develop a cost-effective framework for ADR in the Sri Lankan construction industry.

REFERENCES

Abenayake, M. and Weddikara, C. (2013). Special features and experiences of the full-term dispute adjudication board as an alternative dispute resolution method in the construction industry of Sri Lanka. Sri Lanka: University of Moratuwa.

Abeynayake, M. and Wedikkara, C. (2012a). Arbitration as an Alternative Dispute Resolution Method in the Construction Industry of Sri Lanka. *World Construction Conference 2012 – Global Challenges in Construction Industry*, Colombo.

Abeynayake, M. D. T. E., &Weddikkara, C. (2012b). Critical analysis on success factors of adjudication and arbitration practices in the construction industry of Sri Lanka. In *proceedings of 9th International Conference on Business Management 2012, 28 February-1March 2013* (pp. 209-222).

Abeynayake, M., &Weddikkara, C. (2014). Critical analysis of alternative dispute resolution methods used in srilankan construction industry. In *The 3rd World Construction Symposium 2014:*

Sustainability and Development in Built Environment (pp. 127-137). Colombo: Ceylon Institute of Builders - Sri Lanka.

Alexander, N. (2002). From Communities To Corporations: The Growth of Mediation In Sri Lanka [online] Available at: https://www.mediate.com/articles/alexander.cfm [Accessed 21st May 2020].

Brooker, P., and Lavers, A. (1997). Perceptions of alternative dispute resolution as constraints upon its use in the U.K. construction industry. *Construction Management And Economics*, 15(6), 519– 526.

Cakmak, E. and Cakmak, P. (2014) An Analysis of Causes of Disputes in the Construction Industry Using Analytical Network Process. *Procedia - Social and Behavioral Sciences*, 109 pp.183-187 DOI: 10.1016/j.sbspro.2013.12.441.

Chan, E. and Suen, H. (2005) Dispute resolution management for international construction projects in China. *Management Decision*, 43 (4), pp.589-602 DOI: 10.1108/00251740510593576.

Cheung, S., Suen, H. and Lam, T. (2002) Fundamentals of Alternative Dispute Resolution Processes in Construction. *Journal of Construction Engineering and Management*, 128 (5), pp.409-417 DOI: 10.1061/(asce)0733-9364(2002)128:5(409).

Cheung, S., Yiu, T. and Yeung, S. (2006) A Study of Styles and Outcomes in Construction Dispute Negotiation. *Journal of Construction Engineering and Management*, 132 (8), pp.805-814 DOI: 10.1061/(asce)0733-9364(2006)132:8(805).

De Zylva, E. (2006). Alternative dispute resolution systems for construction contracts. Arbitration law in Sri Lanka, K. Kanagawasam and S. S. Wijeratne, eds., *Institute for the Development of Commercial Law and Practice*, Colombo, Sri Lanka.

Edirisinghe, V., Marsh, D., Borthwick, F. and Cotgrave, A., (2020). An Investigation into the Significant Causes of Disputes in the Sri Lankan Construction Industry. *EPiC Series in Built Environment*, 1, pp.347-355.

Fadhlullah Ng, N., Ismail, Z. and Hashim, F. (2019). Towards Sustainable Dispute Resolution: A Framework to Enhance the Application of Fast Track Arbitration in the Malaysian Construction Industry. *International Journal of Sustainable Construction Engineering and Technology*, 10 (2), DOI: 10.30880/ijscet.2019.10.02.009.

Gulliver, P. H. (1979). Disputes and negotiations: A cross-cultural perspective. *New York: Academic Press*.

Gunarathna, C., Yang, R. and Fernando, N. (2018). Conflicts and management styles in the Sri Lankan commercial building sector. *Engineering, Construction and Architectural Management*, 25 (2), pp.178-201 DOI: 10.1108/ecam-10-2016-0233.

Gunasena, K. B. D. (2010). Performance of critical attributes in alternative dispute resolution (ADR): A study in Sri Lankan construction industry. ⟨http://www.slqs-uae.org/SLQS-Journal/SLQSJournal-4/Page%2042 -48.pdf⟩ (Mar. 22, 2014).

Hall, J. M. (2002). Ineffective communication: Common Causes of Construction Disputes Alliance‟s Advisory Council Legal Notes. Vol. 13, No.2

Halwatura, R. and Ranasinghe, N. (2013). Causes of Variation Orders in Road Construction Projects in Sri Lanka. *ISRN Construction Engineering*, 2013 pp.1-7 DOI: 10.1155/2013/381670.

Hansen, S. (2019). Challenging Arbitral Awards in the Construction Industry: Case Study of Infrastructure Disputes. *Journal of Legal Affairs and Dispute Resolution in Engineering and Construction*, 11 (1), p.06518004 DOI: 10.1061/(asce)la.1943-4170.0000281.

Hoogenboom, J. and Dale, W.S. (2005). Dispute resolution strategy and decision analysis. AACE International Transactions, p.CD151.

Illankoon, I., Tam, V., Le, K. and Ranadewa, K. (2019). Causes of disputes, factors affecting dispute resolution and effective alternative dispute resolution for Sri Lankan construction industry. *International Journal of Construction Management*, pp.1-11 DOI: 10.1080/15623599.2019.1616415.

Ifeanyi, T. A. (2000). Mediative conciliation. AACE International Transactions, R12A.

Jayasena, H.S. and Kavinda, Y.H. (2012). Most appropriate dispute resolution strategy for Sri Lankan construction industry. In World Construction Conference 2012–Global challenges in construction industry (pp. 180-187).

Jayasinghe, H. and Ramachandra, T. (2016). Adjudication Practice and Its Enforceability in the Sri Lankan

Construction Industry. *Journal of Legal Affairs and Dispute Resolution in Engineering and Construction*, 8 (1), DOI: 10.1061/(asce)la.1943-4170.0000178.

Latham, M. (1994). Latham Report, Constructing the Team. Joint Review of Procurement and Contractual Arrangements in the United Kingdom Construction Industry.

Marzouk, M. and Moamen, M. (2009). A framework for estimating negotiation amounts in construction projects. *Construction Innovation*, 9(2), pp.133-148.

Morgerman, G. (2000). Mediation will be the prime forum for resolving construction disputes. New York Construct. News, July, 51–52.

Nafees, S. and Ayub, Z. (2016). Resolution of Islamic Banking Disputes by Way of Arbitration in Sri Lanka. Arab Law Quarterly, 30 (4), pp.305-335 DOI: 10.1163/15730255-12341329.

Niriella, M. (2016). Amicable settlement between the disputed parties in a criminal matter: an appraisal of mediation as a method of alternative dispute resolution with special reference to Sri Lanka. *Sri Lanka Journal of Social Sciences*, 39 (1), p.15 DOI: 10.4038/sljss.v39i1.7399.

Perera, B., Ekanayake, B., Jayalath, C. and Jayathilaka, G. (2019). A study on variation-specific disputes that arise in road projects in Sri Lanka: a qualitative approach. *International Journal of Construction Management*, 21 (6), pp.571-581 DOI: 10.1080/15623599.2019.1573478.

Polinsky, A. and Shavell, S. (2012). Costly Litigation and Optimal Damages. *SSRN Electronic Journal*, DOI: 10.2139/ssrn.2173597.

Ranasinghe, A. and Korale, J. (2011). Adjudication in Construction Contracts. Engineer: *Journal of the* Institution *of Engineers*, Sri Lanka, 44 (2), p.73 DOI: 10.4038/engineer.v44i2.7025.

Ranasinghe, A. (2012). Construction arbitration in Sri Lanka. Proceedings of the Institution of Civil Engineers- Management, Procurement and Law, 165(2), 91-94.

Saranee, W., & Gunathilaka, W. (2017). Mediation in Sri Lanka: its efficacy in dispute resolution. In *Proceedings of APIIT Business, Law & Technology Conference*. Colombo: ISBN978-9557678-02-3.

Silberman, A. (1997). COMMENTARY: Mediation is Not Arbitration. *Journal Of Management In Engineering*, *13*(4), 19-20. doi: 10.1061/(asce)0742-597x(1997)13:4(19)

Tucker, J.B., 1996. Interagency bargaining and international negotiation: Lessons from the Open Skies treaty talks. *Negotiation Journal*, 12(3), pp.275-288.

Ume, M., Farooqui, R. and Azhar, S. (2014). Key Causes of Disputes in the Pakistani Construction Industry– Assessment of Trends from the Viewpoint of Contractors. Available at: http://ascpro0.ascweb.org/archives/cd/2014/paper/CPRT262002014.pdf [Accessed 7th October 2018].

Vertical Axis Wind Turbine for Sri Lankan Southern Highway

Samidu Perera, Dilumi Nandasena, Dilini Wijayakumara and Kasuni Guruvita
Department of Electrical and Electronic Engineering,
Sri Lanka Institute of Information Technology
Malabe, Sri Lanka
{samidu72, diluminandasena, dwijayakumara}@gmail.com, Kasuni.g@sliit.lk

ABSTRACT

Based on studies, most of the areas in Sri Lanka have an average amount of wind that could be resourceful in generating wind power. The area from Colombo along the coastal line to Matara is considered to have less wind potential. It's a major disadvantage to the country's energy generation plan as wind is one of the best renewable energy sources available in Sri Lanka. Concerning the energy crisis in the country, the necessity for a renewable energy source has arisen. Since renewable resources are used as standalone systems, the level of advancement increases while reducing the amount of stress on the main electrical grid when balancing the frequency. Highways can be followed as one of the country's leading divisions that could be used for the use of renewable energy. The southern expressway in Sri Lanka requires an average of 375 kW of electricity only for lighting purposes. If the lights are turned on for 12 hours, then the amount of energy requirement is 4,500 KWh. It would save a considerable amount of energy from the national grid if that energy could be provided using renewable sources. This reduction of energy consumption from the main grid would benefit both the authorities of the Sri Lankan power system and the public. To address the aforementioned issue, a vertical axis wind turbine is proposed in this project to be installed on highways. The main requirements of the project are highlighted in the introduction and problem statement. All the details of the outcomes such as optimized rotor, gear system, generator and the PIC-based power management system are explained in detail with the steps taken to optimize the system at every possible step. There are plans which may facilitate the future development of the product included in the latter part of the document.

KEYWORDS: *Highway and Wind Power, Power Systems, Renewable Energy, Vertical Axis Wind Turbine, Wind Power Generation, Wind Power Plant, Wind Turbine Model*

1 INTRODUCTION

The requirement for power has increased drastically in the previous decades in Sri Lanka. The growth factor of the power requirement is increasing while leading the country into an energy crisis. According to the power control authorities, the requirement of higher demand is fulfilled by maximizing the power generation in diesel and coal power plants. This will result in a polluted environment. The use of renewable energy sources such as wind and solar are alternative methods of generating power, which will address the energy crisis. According to experts, wind power is the most reliable and widely available renewable source of energy. Subsequently, the urban areas in Sri Lanka utilize less wind power due to the unavailability of spaces to install wind turbines. Thus, the requirement of a small-scale wind turbine arises in the domain of renewable energy. Highways in the country have a wider potential for wind coverage due to the unavailability of skyscrapers compared to coastal areas, where the available wind farms are located. One such sector of the country can be focused on developing a vertical axis wind turbine as in many other developed countries. These turbines are suitable for small wind scales and can be used to illuminate the highways during night time. Therefore, developing such a wind turbine would be a major advancement for this country.

2 LITERATURE REVIEW

2.1 Advantages of Wind Power

Sustainability of energy is closely correlated to the world's well-being and prosperity. In modern society, the need for affordable and steadfast energy sources has become a basic necessity. Hydrocarbons, such as heavy oils are the main sources of fuel for energy requirements in the world (Imperial, n.d.). The consumption of these fossil fuels has a significant effect on the atmosphere in the form of emitting toxic atmospheric pollution, causing numerous environmental problems, such as global warming and climate change (Union of Concerned Scientists, 2014). Therefore, decreasing the consumption of such non-renewable energy sources has become a major global initiative. As a result, several green energy harnessing strategies have been developed that have a much lower effect on the atmosphere relative to fossil fuels, such as wind power. Due to its benefits in the field of energy development, wind energy is one of the world's fastest-growing sources of energy. Effectively, the use of wind power also reduces hazardous waste emissions. Wind energy will therefore have the right solutions in place to address the energy crisis and its consequences (El. maksod, 2018). As the cost of wind power per kWh is much lower than that of other energy resources, wind power is remarkable for its cost-effectiveness (El. maksod, 2018). Also, the power generated by wind turbines is sold at a fixed price for a long period and rapid changes in bills are not accounted for, in these cases (Inspire, n.d.). The large space required by the wind turbines can be utilized with cultivation, making them efficient in every aspect. Referring to the factors discussed, wind energy can be identified as one of the best renewable energy sources that can be used in the Sri Lankan context.

2.2 Requirements in Generating Wind Power

In order to develop wind power in any region, a set of parameters should be considered. These must be the vital necessities that need to be identified before designing a wind turbine. One of the parameters is the availability of room for mounting wind turbines. Open spaces are generally regarded as potential locations for wind farms. Besides, prior to the development of a design, sensitive areas and other locations are also considered. For wind turbines, this is commonly referred to as the Setback (American Wind Energy Association, n.d.). The availability of suitable wind speeds in the selected area is another requirement. If the wind speeds are very low, there will be less power generation. Environmental constraints are also one of the most important considerations in wind turbine design. Despite the turbine type, either a vertical axis or a horizontal axis, some of the factors mentioned above were treated mutually in the design stage. The space requirement of a vertical axis wind turbine (VAWT) is comparatively smaller than that of a horizontal axis wind turbine (HAWT). To apply these turbines in highly dense areas, the noise level generated must be relatively low.

2.3 Highways and Wind Power

The space of the median between the lanes on the highway should be wide enough to install a VAWT. Highways consist of both natural and uncontrolled turbulent flow of the wind. The demand for designing vertical axis wind turbines remains higher compared to other wind turbines. The application area would be highways that have a sufficient amount of wind potential to run a VAWT. The designs are required to support the boundary limits between the motorways and edges. It is important to obtain accurate wind speed data for the site in mind before any decision can be made as to its suitability (ROYMECH, 2019). Wind turbines provide high power levels in open space because of their higher capacity factors. This is beneficial when the wide spaces between the motorways are not covered with obstacles.

3 METHODOLOGY

3.1 Acquisition of Wind Data in Highways

Data acquisition was conducted at the peak and off-peak hours of the day to assess the intensity

of wind velocity on the highway. In deciding the average wind speed needed to operate the VAWT in a rated environment, the detection of wind patterns is important. Also, to model the turbine limits, the maximum or peak velocity was obtained. The data acquisition was performed in the outer circular expressway (E02) near the Kothalawala interchange covering the peak and off-peak time from 8.00 AM to 10.00 AM and 4.00 PM to 6.00 PM.

The device configuration for the measurement of wind data consisted of a digital anemometer, an Arduino Nano and a data recording and a storage SD card module. Once the relevant data sets were collected, the peak and average wind speeds were determined by manipulating those values. The average wind velocity was estimated as 6.3 m/s during the peak time, while the off-peak wind velocity was measured as 6.19 m/s. Those values were used for calculations and simulations in the following sections.

3.2 VAWT Rotor Design

The design process of the rotor to obtain the optimum output with regards to the project objectives was conducted under three main steps such as determination of initial turbine parameters, mathematical representation and calculations of the rotor and simulation-based modelling of the blade.

3.2.1 Determination of Initial Turbine Parameters

Estimation of initial parameters is required to be specified to provide proper guidance to the design procedure. There are several approaches to estimate these values by referring to research papers, analysing data extractions from turbines of similar markets, and using logical explanations. Rotor radius is one of the most crucial parameters that is required in the turbine design. If the rotor is too large, there is a possibility of hindering vehicle movements on the highway. Therefore, by considering factors such as the width of the median strip, an average value of 0.75m was obtained as the rotor radius. Blade length is also essential for the calculations of swept area and aspect ratio. Even though the power production increases with the blade length, the cost of implementation is also increased. Therefore, the blade length was selected to be an optimum value. After fine considerations of the installation region and the cost of design, a length of 1m was selected as the blade length value. Furthermore, the turbine height was decided to be taken as 2m (Ahmad Sedaghat, 2018). The maximum amount of wind was required to obtain the maximum power output. Hence, by using the data acquisition and analysis that were done on the highway, the wind velocity value was defined as 6.3 m/s. The tip speed ratio was taken according to research data. For Darius rotors, it has been found that the maximum efficiency of 30% to 35% can be obtained with a tip speed ratio ranging from 5-6 (Hassan, 2014/2015). Therefore, the tip speed ratio was selected as 5 for our design. The number of blades for the design was selected as three since the optimum performance can be obtained using 3 blades. Moreover, the chord length was selected as 0.2m to maintain the chord/radius ratio within the range of 0.1 to 0.4 as specified in research findings.

Additionally, the blade material was decided to be aluminium since they are durable, available as well as cost-effective. Airfoil or the blade profile is one of the crucial parameters in designing the turbine blade. A set of steps was followed to adapt the best existing airfoil for our project. First, the Reynolds number for the design was roughly calculated. Then by analysing the research papers for similar designs, the most suitable types of airfoils were selected. Accordingly, traditional small vertical axis wind turbine airfoils such as NACA 0015, NACA 0018, and NACA 0021 were compared to select the optimum choice. A thicker airfoil design was needed to be selected for efficiency at low wind speeds. Therefore, NACA 0021 was selected as the airfoil for our design (Airfoil Tools, n.d.).

The initial angle of attack (α) was selected as 0° because higher values of the angle of attack are only beneficial for higher values of tip speed ratios. The pitch angle (β) was also selected as 0° because it was decided to have a fixed pitch (stall control) in the design.

3.2.2 Mathematical Representation and Calculations of the Rotor

The subsequent step in the design process of the rotor is the mathematical representation of the rotor parameters. Calculations of swept area, wind power, power coefficient, mechanical power, angular speed, mechanical torque, the Reynolds number, solidity and aspect ratio are required for this procedure.

Swept area is known as the region of air that encompasses the turbine in its rotation. The swept area of an H-rotor VAWT takes a rectangular shape (El. maksod, 2018). It was calculated using the following equation where S is the swept area (m2), R is the rotor radius (m), and L is the length of the blade (m).

$$S = 2 \times R \times L \tag{2}$$

The power harvested from the wind (P_W) is an important parameter to determine the performance of the turbine. It was calculated using the following equation where ρ is the air density (1.225 kg/m3), V_0 is the velocity of the wind (m/s), and S is the swept area (m^2).

$$P_W = \frac{1}{2} \times \rho \times S \times (V_O)^3 \tag{3}$$

Power coefficient (C_P) is used to calculate the captured mechanical power by the blades. It can be also derived from the efficiency of the wind turbine. Based on the tip speed ratio and pitch angle, the following equation was adapted to calculate the C_P value.

$$C_P(\lambda, \beta) = C_1(C_2\lambda_1 - C_3\beta - C_4)E^{\frac{-C_5}{\lambda_1}} + C_6\lambda \tag{4}$$

Where, C_1=0.5176, C_2 = 116, C_3 = 0.4, C_4 =5, C_5 = 21 and C_6 = 0.0068 are constant coefficients. λ is the tip speed ratio and β is the pitch angle. λ_1 is defined as follows.

$$\frac{1}{\lambda} = \frac{1}{\lambda + 0.08\beta} - \frac{0.035}{\beta^3 + 1} \tag{5}$$

The mechanical power (P_m) was derived in Watts using the available wind power and power coefficient as given below.

$$P_m = \frac{1}{2} \times \rho \times S \times (V_O)^3 \times C_P(\lambda, \beta) \tag{6}$$

The angular speed (ω) was calculated in rad/s using the equation defined for the tip speed ratio is given below.

$$TSR(\lambda) = \frac{R \times \omega}{V_O} \tag{7}$$

The mechanical torque (T_m) was calculated in Nm using the captured mechanical power by the blades and the angular speed of the rotor as follows.

$$T_m = \frac{P_m}{\omega} \tag{8}$$

The Reynolds number is a significant parameter that is used in selecting the proper airfoil design for the turbine. Better performance can be achieved with a higher Reynolds number. This is because when the Reynolds number increases, the lift coefficient increases while decreasing the drag coefficient (S. Brusca, 2014). Hence, the Reynolds number was calculated by adapting the following equation where, V_0 is the free-stream wind speed (m/s), $\lambda_{CP\,(max)}$ is the tip speed ratio that maximizes C_P, c is the chord length (m), and v is the kinematic viscosity of the fluid (m^2/s).

$$Re = \frac{V_O \times \lambda_{CP(\max)} \times c}{v} \quad (9)$$

The solidity of the turbine is known as the total cross-sectional area of the side of the blades to the frontal swept area. If the solidity is higher, the self-starting torque is increased. Therefore, the drag component is increased. Hence, solidity must be kept at a lower value to get the turbine to start rotating (Ibrahim Ara). The solidity (σ) was calculated using the equation given below where, *N* is the number of blades, *c* is the blade chord (m), and *R* is the rotor radius (m).

$$\sigma = \frac{N \times c}{R} \quad (10)$$

Aspect ratio (*AR*) is defined as the ratio between the blade height and the rotor radius. To maximize the power coefficient value, the rotor's aspect ratio must be kept as small as possible. Hence, the turbine performance can be derived using this parameter (S. Brusca, 2014). The following equation was used to calculate the aspect ratio.

$$Aspect\ Ratio\ (AR) = \frac{Height\ of\ the\ blade(length)}{Rotor\ radius} \quad (11)$$

3.2.3 Simulation-Based Modelling of the Blade

Simulation-based modelling was performed as the next step of the design process to obtain verification of the turbine performance. For this purpose, it was decided to use programs such as MATLAB Simulink and QBlade because of their reliability, simplicity, and less consumption of time. MATLAB was used to develop the mathematical model of the design while QBlade software was used to simulate the rotor blade and obtain graphical interpretations of the blades.

3.3 Gear System and Generator Design

Based on literature and background analysis, the design process of the generator and the gear system to obtain the optimum output with regards to the project objectives was conducted by mathematical representation and calculation of the gear system and generator, simulation-based modelling of the gear system and the generator. A set of equations and mathematical parameters were used in determining the parameters. Once the calculations were performed, those outcomes were verified using the simulation models while differentiating errors.

3.3.1 Mathematical Representation of the Gear System and the Generator

Based on literature and background analysis, a set of equations and mathematical parameters were used in determining the generator and gear parameters. The following section describes out the continuation of the design based on mathematical equations.

According to the breakdown of gear systems, a spur gearbox with a lower gear ratio was selected for the design considering the reliability, simplicity, low cost of building and designing, non-complex gear analysis and easy simulations. Before continuing the design details and calculations, a set of parameters and equations were referred to identify the vital design procedures and techniques in gearing.

Gear tooth systems known as the diametral pitch system and the module system, specify the connection between addendum, dedendum, working depth, tooth thickness and pressure angle. In the gear system, increasing the gear module results in larger teeth designs, while increasing the pressure angle results in smaller teeth designs. These elements and theories were studied in calculating gear system parameters during the designing phase. The gear efficiency and the torque conversion are some of the vital aspects in determining the gear type. The efficiency of the gear system was calculated using the equation mentioned below.

$$\eta = \frac{Output\ shaft\ power}{Input\ shaft\ power} \times 100\% \quad (12)$$

Power losses were mainly concerned with tooth friction and lubrication losses in the gear systems. According to studies, the losses were mostly related to the peripheral velocity of the fluid rotating through the gears. Frictional losses in the gears are related to the configuration of the gear, the reduction ratio, the angle of pressure, the height of the gear and the friction coefficient (Bin Wu, 2011). Since losses are hard to quantify, during the initial gear design, calculations based on practices were often used.

The following remarks were mostly referred to estimate the percentage of the gear train efficiency correlated with tooth friction. A basic table is given below showing the efficiencies of various types of gears. The efficiencies for each mesh in the line are multiplied together to calculate the efficiency for the entire drive train.

Table 3 Gear efficiencies related to different gear types (Bin Wu, 2011)

Type	**Gear Ratio**	**Efficiency**
Spur	1:1 to 6:1	98-99%
Helical	1:1 to 10:1	98-99%
Double Helical	1:1 to 15:1	98-99%
Bevel	1:1 to 4:1	98-99%
Worm	5:1 to 75:1	20-98%
Crossed Helical	1:1 to 6:1	70-98%

When designing the gear system, a proper efficiency calculation along with the percentage power loss was carried out without using the approximated gear efficiencies. Particularly, a spur gear was selected considering the ease of calculations and efficiency. Hence, a gear ratio of 4:1 was selected. Since the design is a single mesh gear system having a pinion gear and a spur gear, the following mathematical equations were used to calculate the percentage power loss (P). where R_g is the Gear ratio, Ro is the Gear outside diameter (m), r_o is the Pinion outside diameter (m), d_G is the Gear pitch diameter (m), d_P is the Pinion pitch diameter (m), α is the Pressure angle and μ is the Friction coefficient.

$$P = \frac{50\mu}{Cos\alpha}\left[\frac{{H_S}^2+{H_t}^2}{H_S+H_t}\right] \tag{13}$$

$$H_S = (R_g + g)\left[\sqrt{\left(\left(\frac{R_O}{d_G}\right)^2 - cos^2 \propto\right)} - sin \propto\right] \tag{14}$$

$$H_t = \left(\frac{R_g+g}{R_g}\right)\left[\sqrt{\left(\left(\frac{R_O}{d_G}\right)^2 - cos^2 \propto\right)} - sin \propto\right] \tag{15}$$

The generated torque from the turbine was transferred into the generator by using a gear train. When using a pinion gear system connected to the main gear, the torque can be either higher or lower than the torque of the gear connected to the turbine. It is proportional to the gear ratio and inversely proportional to the angular speed of the gears, which was calculated using the following expression where ω_p is the Angular velocity of the pinion, ω_G is the Angular velocity of the gear, d_P is the Diameter of the pinion, d_G is the Diameter of the gear, T_P is the Torque of the pinion and T_G is the Torque of the gear.

$$\frac{\omega_G}{\omega_P} = \frac{d_P}{d_G} = \frac{N_P}{N_G} = \frac{T_P}{T_G} \tag{16}$$

Therefore, the torque delivered to the generator was calculated from the following expression, where T_G is equal to the mechanical power delivered from the wind turbine.

$$T_P = T_G \times \frac{N_P}{N_G} \tag{17}$$

A permanent magnet synchronous generator was selected as the generator for the vertical axis wind turbine considering the factors discussed in previous sections. PMSG has a different set of configurations and power control techniques, which were considered during the design phase. However, some were highly cost-effective when it came to the selection of permanent magnets. Therefore, a simpler and more accurate mathematical model was used in the design stage of the generator.

The mathematical model of the generator was formulated using a set of equations required to calculate the generator parameters. According to (Y. Erramia, 2013), the following set of equations was used. First, the electromagnetic torque generated in the system was found. Using the expression given below. Where, L_d, L_q is the d and q axis self-inductance, P is the number of pole pairs and λ_r is the rotor flux linkage.

$$T_e = \frac{3P}{2}\left(\lambda_r i_{qs} - (L_d - L_q)i_{ds}\right. \tag{18}$$

i_{qs} and i_{ds} are dq axis current components, which were found using the following two equations. Where, R_s is the resistance of the stator winding and v_{ds} and v_{qs} are the voltages of the dq axis in the stator.

$$\frac{di_{ds}}{dt} = -\frac{Rs}{Ld} i_{ds} + \frac{L_q}{L_d}\omega i_{qs} - \frac{1}{L_d} v_{ds} \tag{19}$$

$$v_{ds} = -R_s i_{ds} + \omega_e L_q i_{qs} - L_d \frac{di_{ds}}{dt} \tag{20}$$

The voltages of the stator windings were found using the following equation, concerning the generator electrical speed (ω_e), stator inductance, stator resistance and dq axis currents.

$$v_{ds} = -R_s i_{ds} + \omega_e L_q i_{qs} - L_d \frac{di_{ds}}{dt} \tag{21}$$

$$v_{qs} = -R_s i_{ds} - \omega_e L_q i_{qs} + \omega_e \lambda_r - L_d \frac{di_{ds}}{dt} \tag{22}$$

ω_e in the equations given above are known as the electrical angular speed of the generator, which was calculated using the following formula.

$$\omega_e = \omega_g \times P \tag{23}$$

Most of the synchronous generator types consist of different power control strategies. These are used to significantly increase the amount of power generated. Among the control strategies of maximum power point tracking, pitch control, excitation current vector control and grid side control strategies, vector control provides a more efficient conversion of energy during variable wind speeds (Hassan, 2014/2015). Thus, this technique was used in determining the power and torque.

Excitation of the current vector control of the generator provides better control over the linear relationship between the stator current and the electromagnetic torque while delivering the maximum torque with a minimum stator current (Rim Ben Ali, 2017). Therefore, when calculating the generator parameters, i_{ds} was kept at zero. In that case, the electromagnetic torque and the stator currents were calculated using the following expressions.

$$T_e = \frac{3P}{2}\lambda_r i_{qs} = \frac{3P}{2}\lambda_r i_s \tag{24}$$

$$i_s = \sqrt{{i_{ds}}^2 + {i_{qs}}^2} = i_{qs} \tag{25}$$

Then the mechanical power at the generator shaft was calculated using the equation given below, acknowledging T_g and ω_g as the torque and the rotational speed of the gear system.

$$P_m = T_g \omega_g \tag{26}$$

The active power (P_L) delivered to the system was less than the mechanical power because of the stator copper losses ($P_{cu,s}$). Thus, the stator copper loss was calculated as follows.

$$P_{cu,s} = 3{I_s}^2 R_s = 3 I_s V_s \tag{27}$$

$$P_L = P_m - P_{cu,s} \tag{28}$$

Since i_{ds} was considered as zero, the stator current and voltage were found using the following equations. Also, the 3-phase voltage and current values of the generator were calculated once the following parameters were obtained.

$$I_s = \frac{i_{qs}}{\sqrt{2}} \tag{29}$$

$$V_s = \frac{V_{qs}}{\sqrt{2}} \tag{30}$$

3.3.2 Simulation of the Gear System and the Generator

The gear system parameters were assumed based on the background analysis when using the mathematical equations for gear design. For the MATLAB simulation, some of the assumed parameters such as the gearing ratio and the centre distance between the gears were moderated depending on the standards from gear manufacturers. Then the SIMULINK software was used to determine the number of teeth in the spur gear and pinion gear.

Thereafter, determination of the torque was generated, and power conversion efficiency was performed using the results obtained by the previous simulation. The simulation required a set of other parameters such as pressure angle, pitch diameters and the friction coefficient. These are preferred to retain the requirements as the mentioned in the literature review. Eventually, another simulation block was used to connect the turbine and the generator simulation blocks.

When specifying parameters for the generator simulations, some of the parameters were determined using the available designs as mentioned in the previous section. When the simulations were performed, some of the software programs delivered opposing results. Therefore, the existing generator parameters were compared when validating the simulations. The main objective of the simulation was to test the proposed generator's performance under various conditions. MATLAB Simulink outperformed most of the power analysis software packages. Thus, it was used for the evaluation of the generator. The torque transferred from the gear model was transmitted into the PMSG subsystem to generate the power, based on the given stator parameters and machine characteristics. Then the generated alternating voltage and current components were measured using the V-I measurement block. These values were compared with the existing power quantities. A load was added to represent the direct use of dc voltage and the current components deduced from the Universal Bridge, which consists of six power diodes. The representation of the generator system can be given in the following simulation model.

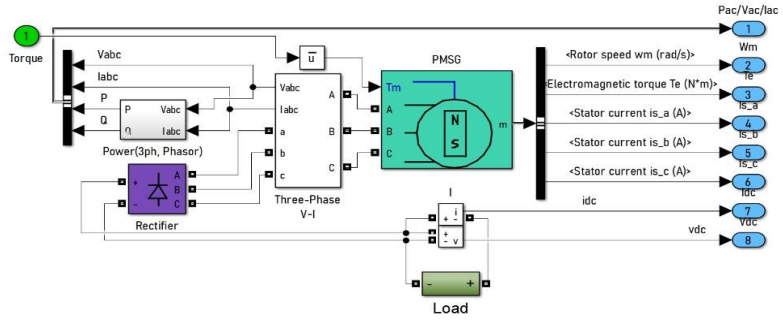

Figure 3 Simulink block diagram of a modelled PMSG system

However, controlling the fluctuation of frequency and the output voltage relevant to a variable wind speed was not accounted for in this model. Therefore, the generated voltage and the frequency were fluctuating according to the average wind speed. The machine was modelled using a dual-phase magnetic flux frame with equal d and q axis inductance and phase-shifted by 90 degrees. This was implemented in the system by the PMSG system block diagram in the above model. Once the simulation was performed, the output scopes displayed the amount of active and reactive power, electromagnetic torque, and dc quantities of the model.

3.4 Charge Controller Design

The wind charge controller of the system is designed and simulated using the Proteus software. The micro-controller PIC12F675 is used as the controlling component of the circuit as it is cost effective and more reliable for small scale applications.

3.4.1 Battery

Lead-acid batteries are deep-cycle batteries, which are ideal for small-cycle renewable energy integration applications. Due to their construction, it is suitable for small scale wind energy projects and requires low maintenance. They are widely used in off-grid power systems and similar roles. The voltage of the selected battery was in the range of 12 Volts and the current was in the range of 20Ah.

3.4.2 Charge Controller

The voltage generated by the wind turbine was considered as 200VAC. Thereafter that voltage was stepped down for about 20VAC. After that, the voltage was regulated to 13.8 VDC. The charging and discharging of the battery are controlled by a PIC12F675 micro-controller as it can read a range of analog signals, unlike PIC16f877A which can only read a referenced analog signal (MICROCHIP, n.d.). During the design stage, the 12V output of the battery was stepped up to 220V before passing the voltage to the load. The load was a 250/220V High-Pressure Sodium (HPS) bulb.

3.4.3 Circuit Implementation

There was no similar component to a wind turbine in the Proteus software. Therefore, an AC voltage source was used as the input to the circuit. The source had a constant current of 20A. The voltage regulator LM7805 was used to feed the 5V to the micro-controller. The voltage received from the turbine was regulated to 13V by a Zener diode and then it was sent to the battery by using the PWM technique to charge the battery (EL-PRO-CUS, 2013). The PIC12F675 was used to control overcharging, discharging, and cut-off of the battery. There is an inbuilt oscillator in this micro-controller which was used to obtain a periodic signal to control the voltage. In this micro-controller, a soft PWM was used to activate the PWM module. When the battery was charged using the PWM technique, an LED was used to detect whether the battery was charging. When the battery was fully charged, PWM emitted a small pulse with less pulse width into the battery to eliminate charging the battery.

Furthermore, the drain cut-off was done using a 5V relay. When the battery was charging the relay was in the normally open position and when the battery was discharging up to about 11V, the relay was shifted to the normally closed position. Then the LED indicator was turned off. As the relay was a 5V relay, the battery voltage could be used to function it. The 555 timers were used to generate and divide pulses in the inverter circuit (Electronic-Tutorials, n.d.). Then the 12VAC was obtained and it was stepped up to 240VAC by using a centre-tapped transformer with a 1:20 winding ratio (COMPONENTS101, 2018). After that, this voltage was sent to the load, which was a 230V,250W HPS bulb. The voltage of 240VAC was obtained to compensate for the losses in the circuit. The image given below shows the arrangement of the components in the circuit.

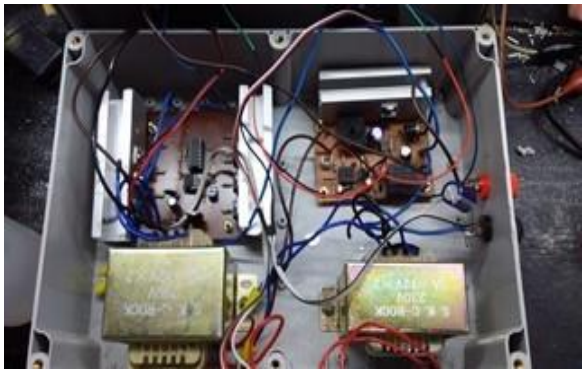

Figure 4 Charge Controller

4 DISCUSSION

The amount of power that can be efficiently generated from a particular turbine depends on the area enclosed by the rotor blade. According to this theory, the designing of VAWT for Sri Lankan highways was carried out followed by a data analysis. This provided a clear overview of the amount of power that can be generated. The analysis of wind speeds obtained from a digital anemometer concluded the average wind velocity as 6.3 ms^{-1}.

The turbine rotor design was performed with the aid of manual calculations as well as simulation-based modelling using QBlade and MATLAB Simulink software programs. The results obtained using the QBlade software includes airfoil design, rotor blade design, rotor DMS simulation, multiparameter DMS simulation, turbine DMS simulation, and turbulent Windfield generation. Given below is a representation of the simulation.

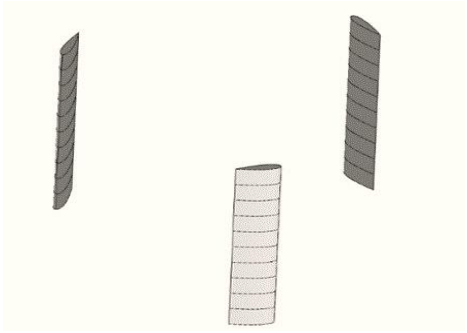

Figure 5 Rotor blade design

When comparing the results of manual calculations and simulation-based modelling, some slight deviations in wind power, power coefficient, mechanical power, rotational speed, and mechanical torque were observed. The main reason for this difference in values is the computational changes when calculating the power coefficient. A slight change in constants used in the manual calculation and simulation can cause a significant difference in the outcome. Nevertheless, the deviation can be overlooked as because the range of error is considerably low. The table given below illustrates the comparison between the results and the parameters used.

It is beneficial to comprehend how particular changes in parameters can influence turbine efficiency. One such parameter which directly affects the turbine performance is the tip speed ratio. When observing the relationship between TSR and power coefficient, initially the power coefficient increased with the TSR, after reaching a threshold value, the power coefficient gradually decreased. Hence, to maximize the performance of the turbine, an optimum value of TSR must be selected. Furthermore, it was noticed that higher power outputs can be gained with higher wind velocities. But the output of the turbine is at its highest when the torque entering the generator corresponds to the angular velocity of the turbine. Moreover, it is clear that by increasing the blade chord, rotor radius and blade length, the rotor performance increases as well.

Table 4 Comparison between the results and parameters

Parameters	**Calculation**	**Simulation**
Rotor radius	0.75 m	0.75 m
Blade length	1 m	1 m
Turbine height	2 m	2 m
Wind velocity	6.3 m/s	6.5 m/s
Tip speed ratio	5	5
Number of blades	3	3
Airfoil	NACA 0021	NACA 0021
Blade chord	0.2 m	0.2 m
Angle of attack	0◦	0° and 9.5°
Pitch angle	0◦	0◦
Swept area	1.5 m^2	1.5 m^2
Power in wind	229.73 W	252.31 W
Power coefficient	0.2628	0.354
Mechanical power	60.373 W	93.89 W
Rotational speed	401.07 rpm	400 rpm
Mechanical torque	1.437 Nm	2.24 Nm

The calculation carried out for the gear train design was used to determine the feasibility of using the gear train design on the vertical axis wind turbine project. When considering the results of the gear system, the torque and the velocity of the connected gears were clarified. In the gear design, the pinion and the main gear were designed to prevent losses due to friction. Thereafter, a set of new gear diameters and tooth sizes were selected because the mathematically modelled gears had a larger diameter compared to the overall design dimensions and the power loss was relatively higher. The pitch angle of the simulation was changed to 25° based on the performance. Once the space between the gears was selected, it was utilized to find the diameters of the gear and the pinion. Pitch diameter was also altered depending on the losses in the system.

The output AC power, current and voltage from the generator were compared with the variation of generator models. Parameters such as stator resistance, dq axis inductance, flux linkage and the number of poles were changed accordingly to obtain the most reliable outcomes using the simulation. The purpose of the simulation was to validate the variation between the electrical power and the attributes of the generator.

The amount of peak power from the model was simulated as 42W at 90VAC. Since the available wind velocity average was 6.3ms^{-1}, the amount of power generated was also reduced. The design was capable of providing an annual power rating of 0.368 MWh, which is a sizable amount of power compared to non-renewable energy sources. The amount of DC power generated was measured using a load connected at the generator terminal. The load was rated with a value of 150 ohms. The peak value of the DC voltage was around 93V while the peak current was at 0.55A.

In the charge controlling system, the PIC12F675 microcontroller is the controlling element of the system. The main application of the algorithm built into the PIC12F675 microcontroller is designed and optimized to perform the charging and discharging of the battery and to control relay on/off control for drain cut-off. Further, when creating the code, the upper limit of the battery is assumed as 13V, and the lower limit is assumed as 11V. The algorithm does not allow the draining of the battery voltage below the lower limit, and it performs fast-charging up to 70% of the battery capacity (GLOBAL-CIRCUIT, n.d.). After that, it sends PWM pulses with a delay which is about 5 seconds when the battery is charging from 70% to 100%. This is done to reduce the rate of charging. To indicate the charging of the battery, a blinking green LED bulb is used.

The completed project consisted of other system models that performed well in the simulations and the variation of wind power affected the overall efficiency of the system. Higher wind velocities were capable of producing higher electrical power. But the simulated model had its limitations in many cases, which affected the overall performance of the wind turbine.

5 CONCLUSIONS

An H-rotor Darrieus turbine was selected as the rotor type for this application considering its simplicity and cost-effectiveness. Initially, 6.3 m/s was derived as the average wind speed from the data analysis. Next, focusing on the available low wind speeds a thicker airfoil design (NACA 0021) was selected as the blade profile. Furthermore, a rotor radius of 0.75 m, blade length of 1 m, turbine height of 2 m, blade chord of 0.2 m and a tip speed ratio of 5 were selected as parameters in the design procedure. To model the performance of the turbine, two simulation software programs were used. Accordingly, the mechanical power was estimated as 60.373 W with a mechanical torque of 1.437 Nm.

The amount of turbulent wind was inadequate to produce a constant rotation in the generator. Therefore, a linear gear system was included in the design. A PMSG was used in the wind turbine model to eliminate the use of electricity to excite the generator, making the design more renewable. Based on the determined wind data, the turbine height was selected as 2m. The average wind speed of 6.3 ms^{-1} produced an electrical power of 42 W continuously in the simulation, using a rotor blade consisting of a height of 1m and a radius of 0.75 m. This amount of power is sufficient for small applications such as lighting.

The charge controller system was focused to manage and optimize the power harvested from the wind. Besides that, the charge controller has successfully managed the battery discharging and charging processes during the peak and off-peak periods of wind sources. The generated voltage of 220VAC was stepped-down to 20VAC and was regulated to 13VDC. Then the regulated voltage was used to charge the 12V battery and to power the load when necessary. The charge controller system increased the utilization of the available energy sources or stored energy with the least dependency on the grid network for the power source supply.

REFERENCES

Ahmad Sedaghat, E. B. (2018). Feasibility of highway energy harvesting using a vertical axis wind turbine. *Energy Engineering: Journal of the Association of Energy Engineers*.

Airfoil Tools. (n.d.). Retrieved 10 01, 2020, from http://airfoiltools.com/airfoil/details?airfoil=naca0021-il

American Wind Energy Association. (n.d.). Retrieved 10 28, 2020, from https://www.awea.org

Bin Wu, Y. L. (2011). *Power Conversion and Control of Wind Energy Systems.* Wiley-IEEE Press.

COMPONENTS101. (2018). Retrieved 2020, from https://components101.com/transformers/12-0-12-center-tapped-transformer

El. maksod, I. G. (2018). *Performance Analysis - Design and Manufacturing of Vertical Axis Wind Turbine.*

Electronic-Tutorials. (n.d.). Retrieved 2020, from https://www.electronics-tutorials.ws/waveforms/555_timer.html

EL-PRO-CUS. (2013). Retrieved 2020, from https://www.elprocus.com/full-wave-bridge-rectifier-versus-center-tapped-full-wave-rectifier/

GLOBAL-CIRCUIT. (n.d.). Retrieved 2020, from https://circuitglobe.com/lead-acid-battery.html

Hassan, A. (2014/2015). *Based Design and Development of a Vertical Axis Wind Turbine Computational Model.* Leicester.

Ibrahim Ara, F. A. (n.d.). Highway Vertical Axis Wind Turbine with Vortex Generators.

Imperial. (n.d.). Retrieved 10 27, 2020, from https://www.imperialoil.ca/en-CA/Company/About/The-importance-of-energy

Inspire. (n.d.). Retrieved 10 27, 2020, from https://www.inspirecleanenergy.com/blog/clean-energy-101/advantages-of-wind-energy

MICROCHIP. (n.d.). (MICROCHIP) Retrieved 2020, from https://www.microchip.com/wwwproducts/en/PIC12F675

Rim Ben Ali, H. S. (2017). *Modeling and Simulation of a small Wind Turbine system based on PMSG generator.* Slovenia.

ROYMECH. (2019). Retrieved 10 10, 2020, from https://roymech.co/Useful_Tables/Drive/Gear_Efficiency.html

S. Brusca, R. L. (2014). Design of a vertical-axis wind turbine and how the aspect ratio affects the turbine's performance.

Union of Concerned Scientists. (2014, 06 19). Retrieved 10 27, 2020, from https://ucsusa.org/resources/environmental-impacts-natural-gas

Y. Erramia, M. O. (2013). Control of a PMSG based wind energy generation system for power maximization and grid fault conditions. *Mediterranean Green Energy Forum MGEF-13*(42), 220-229.

Developing a Rubber based Nanocomposite

Muhamed Ismaeel Faisal Sadique[1]
[1]School of Civil and Mechanical Engineering, Faculty of Science and Engineering,
Curtin University, Kent St, Bentley WA 6102, Australia
Migara Liyanage[2]
[2] Faculty of Engineering, Sri Lanka Institute of Information Technology
New Kandy Rd, Malabe, 10115, Sri Lanka
Chitral Angammana[3]
[3]University of Waterloo, 200 University Ave W, Waterloo, ON N2L 3G1, Canada
migara.l@sliit.lk, cangammana@gmail.com Corresponding author: m.faisalsadique@graduate.curtin.edu.au

ABSTRACT

Polymer compounds such as Natural Rubber (NR), which consists of compounds such as isoprene, are capable of being processed for the manufacture of a range of rubber based products for a large variety of applications. The properties of a natural rubber compound are susceptible to enhancements in their properties through the incorporation of nanofillers into its matrix. This study addresses the preparation of a natural rubber based nanocomposite that utilizes graphene as a nanofiller for the facilitation of the required enhancement in the rubber compounds properties. The nanocomposite specimens used in the study were prepared by means of acid-coagulation. The acid-coagulation formulation utilized was adapted from methodologies employed in commercial applications. The enhancement in the rubber properties due to the incorporation of the nanofiller was validated by means of mechanical testing. Prior to the testing, the applicable standard for tensile property testing was identified to be ASTM D412. Through the acclaimed standard, a mould to facilitate the preparation of the required specimens was 3D printed from PETG. The primary aim of the study was to determine the effect of large concentrations of graphene (beyond 2.5wt %).The results from the mechanical testing of the acid-coagulated samples exhibited enhancements in the elongation at break and tensile strength between unfilled NR and the graphene filled NR nanocomposite. With the incorporation of 5wt% of graphene, the elongation at break of the rubber increased to 687%, showing a 25% increase. The tensile strength of the rubber increased to 4.07 MPa, showing an enhancement of 102% in comparison to the pristine rubber compound.

KEYWORDS: *Natural Rubber, Graphene, Acid-Coagulation, Tensile strength, Elongation at break.*

1 INTRODUCTION

Natural rubber (cis-1, 4-poly (Isoprene)) is a polymer that is procured from the latex of the Hevea Brasiliensis tree along with other non-polymer by products. The NR can be isolated and made into sheet through the process of coagulation. Coagulation is primarily influenced by the type of coagulating agent utilized. The most commonly used category of coagulating agent is an acid, primarily, Formic acid. Formic acid is a caustic Carboxylic acid that is colorless, pungent and is highly advocated for use as a coagulant due to its generation of a favorable level of dry rubber in the coagulated compound (Oktriyedi, Dahlan, Irfannuddin, & Ngudiantoro, 2021). In the process of acid-coagulation, the addition of the easily ionized Formic acid into the latex allows for the latex to coagulate into a solid. When the Formic acid ionizes, the produced hydrogen ions react with the negative charges on the surface of the polymer membrane, allowing for the formation of neutrally charged rubber particles. Thereafter, on the collision between the neutrally charged particles, the outer membrane of the polymer particles fragment apart allowing the polymer molecules to agglomerate and coagulate to form a solid compound (Veerendra, 2020). The generated natural rubber presents a large range of applications, in the manufacture of tires, gloves and other engineering products (Erman, Mark, & Roland, 2013). However, owing to its deficient strength and low modulus, the applications of natural rubber have been restricted. In order to overcome the barriers presented, studies focused on the preparation of natural rubber-based nanocomposites through the assimilation of a suitable nanofiller phase into the matrix of the natural rubber to obtain

improvements in the mechanical properties of the rubber beyond those offered by the unfilled rubber (Wang, Liu, Wu, Wang, & Zhang, 2010). Studies carried out on graphene nanoparticles have shown that the incorporation of a miniscule amount of graphene can result in great enhancements to the properties of the rubber compound. This is a result of the greater aspect ratio of graphene (Sur, 2012) along with its inherently high mechanical properties (Liu, et al., 2021). Additionally, graphene can be functionalized to further elevate the properties and reactivity of the nanofiller. This is demonstrated in a study by Jose and Susamma (Jose & Susamma, 2021), where the incorporation of 0.5phr of graphene modified with dodecyl amine led to the tensile strength of the rubber compound increasing by 74%.

Although numerous methods of nanocomposite preparation exist, the most widespread method for nanocomposite preparation is the method of latex mixing (Bu, Wang, Zhang, Lavorgna, & Xia, 2017). The principal behind latex mixing comprises of blending the rubber latex with a suspension of the graphene nanofiller for the generation of a homogeneous dispersion. The dispersion can subsequently be coagulated or vulcanized for the generation of the final nanocomposite sample. The method of latex mixing provides advantages such as allowing a greater attainable degree of nanofiller dispersion and being environmentally friendly due to the requirement for an organic solvent (Bu, Wang, Zhang, Lavorgna, & Xia, 2017). However, due to the requirement of high-speed equipment for the dispersion of graphene within the latex, costs may escalate in the case of mass production of the dispersion (Bu, Wang, Zhang, Lavorgna, & Xia, 2017).

This paper utilizes a standard rubber curing method for the preparation of the rubber compounds with and without the incorporation of a nanofiller. This is done in order to observe the improvements in the mechanical properties of the natural rubber as a result of the graphene nanofiller assimilation. Additionally, the paper attempts the determination of the optimum concentration of graphene that leads to a maximum yield in the attained mechanical properties. This was accomplished through the testing of a large range of incorporated graphene concentrations (an expanded range was used, mainly beyond 2.5wt %, since a small range would be insufficient to provide clarity on the point of percolation). The range tested enabled the identification of the graphene loading beyond which the tested mechanical properties showed no further improvement. The range utilized for the testing was established through a literature survey that was carried out to determine the standard testing loadings. In addition, paper also addresses the use of standards such as ASTM D412 and ASTM D1415 for the manufacture of a mould to facilitate the specimen preparation. Since the subject of using nanoparticles for the reinforcement of rubber is a relatively new field of study, this paper aims to contribute to advancements in the field.

2 EXPERIMENTAL PROCEDURE

2.1 Materials

Natural Rubber latex used for the study was centrifuged NR latex that was purchased from Almar Trading Co., (PTE) LTD. The composition and properties of the NR latex used are shown in Table 1.

Table 1. Composition and properties of NR latex

Quality Parameter	**Unit**	**Value**
Total solid content	%wt	61.50
Dry rubber content	%wt	60.00
Non-rubber content	%wt	1.5
Ammonia content	%wt	0.8 (max)
Mechanical stability time	sec	800-1000
Volatile fatty acid number		0.025
KOH number		0.53
pH value		10.20

The graphene suspension used as the nanofiller was obtained from CeyGrene (Pvt) Ltd. The graphene was obtained as a suspension through the liquid phase exfoliation of vein graphite. The composition of the graphene suspension is given in Table 2.

Table 2. Composition of Graphene suspension

Chemical	**%Weight**
Distilled water	<80
Graphitic carbon	>15
Proprietary additive (PVP)	<5

For the facilitation of the acid-coagulation methodology, Formic acid was used as the main coagulant. The required formic acid was purchased from Glorchem Enterprise.

2.2 Mould design for specimen preparation

Design of the mould to be used for the preparation of the nanocomposite specimens was carried out by initially identifying the associated standards. The standards required to be utilized for the specimen dimensions were identified through a study that was carried out.

Through the study, it was identified that for the tensile testing of rubber, the ASTM D412 standards was used. This allowed for the determination of the elongation at break and the tensile strength of the rubber specimens. The standard specimen shape stipulated by ASTM D412 was a dog-bone/ dumbbell shape as shown in Figure 1.

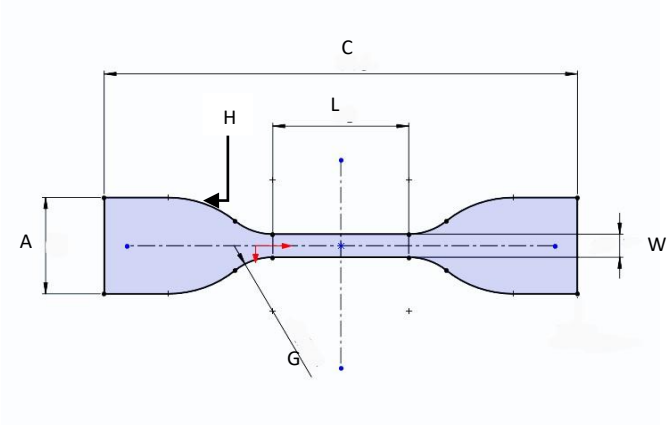

Figure 1. Design schematic for tensile specimen

ASTM D412 reports of six alternate dimension combinations for the specimen. The most generally preferred and used combination was that of "Die C". Based on the specification for "Die C", the dimensions of A, C, G, H, L and W are shown in Table 3.

Table 3. Die C specification for tensile specimen (ASTM International, 2009)

A	25 mm
C	115 mm
G	14 mm
H	25 mm
L	33 mm
W	6 mm

The specimen thickness was designated to be 2 mm according to the ASTM D412 standard.

Additionally, it was determined that the dimensions for a hardness testing specimen was dictated by the ASTM D1415 standard. According to this standard, the hardness specimen required its lateral dimensions to be greater than 20 mm. The specimen thickness was to be sustained between 8 – 10 mm

(minimum value for thickness was 2 mm). The specimen was designed with lateral dimensions as shown in Figure 2, while the specimen thickness was set to be 10 mm.

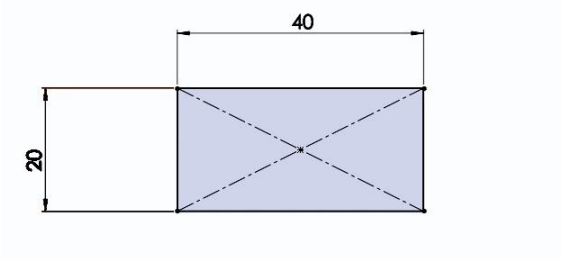

Figure 2. Design schematic for hardness specimen

The final mould was designed to hold five cavities for the tensile specimens (for the determination of average tensile strength) and a single cavity for the hardness specimen. The material used for the mould was Polyethylene terephthalate glycol (PETG) owing to its good chemical resistance against the coagulating agent (formic acid).

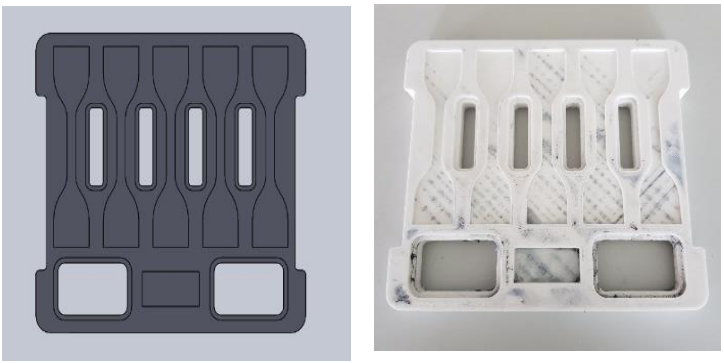

Figure 3. (a) SolidWorks mould design; (b) PETG printed mould

2.3 Coagulation methodology for specimen preparation

The applied coagulation methodology was derived from the methodology utilized in the rubber processing plant of Agalwatte Plantations PLC. For the study, 0.18g of formic acid was diluted with 14.4g of water. Prior to the addition of the diluted acid into the latex, the graphene suspension was incorporated and dispersed within the NR latex to obtain an NR-graphene mixture. The concentrations of graphene tested ranged from 0 to 20 wt% in NR. The dispersion of the graphene was facilitated by stirring for five minutes with a mixer. The diluted Formic acid was thereafter mechanically stirred into 40g of the NR-graphene mixture. Mixing was carried out in a glass beaker until the Formic acid was homogenized within the latex. The mixture was thereafter poured into the prepared mould and was left to coagulate for a period of 24 hours. A summary of the formulations tested are shown in Table 4.

Table 4. Summary of formulations tested

Test No.	Graphene (%wt)	Latex used (g)	Formic acid (g)	Water (g)
1	0	40	0.18	14.4
2	2.5			
3	5			
4	10			
5	20			

2.4 Mechanical property testing

The initially determined mechanical test to be carried out were:

- Tensile testing
- Hardness testing

However, due to issues with the hardness of the specimen prepared (as seen in results), only the tensile properties were tested for. The tensile properties tested were: the tensile strength and elongation at break. The prepared coagulation specimens were sent to the Industrial Technology Institute (ITI) for the tensile property testing.

3 RESULTS AND DISCUSSION

3.1 Coagulated samples

The samples prepared through the coagulation methodology are illustrated below.

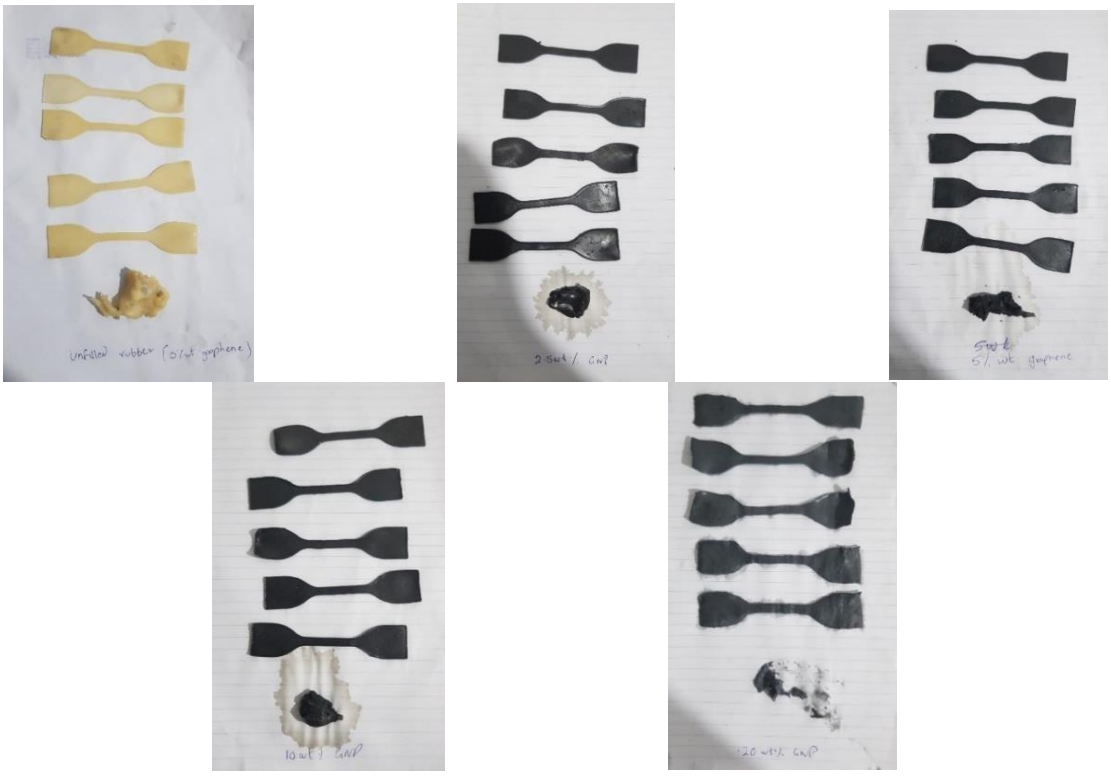

Figure 4. (a) unfilled sample; (b) 2.5wt% graphene; (c) 5wt% graphene; (d) 10wt% graphene; (e) 20wt% graphene

From the prepared samples, it can be identified that the hardness of the specimen for each sample shows a degree of disfigurement. This prevented the hardness of specimens from being used for mechanical testing. The observed disfigurement was attributed to a slight amount of pre-coagulation that took place on the addition of the Formic acid. This likely reduced the total rubber content in the latex, thereby leading to the hardness specimen being less structurally sound in comparison to the tensile samples. The pre-coagulation an issue for the tensile specimens owing to the lower thickness of tensile specimens.

3.2 Mechanical properties of NR-graphene nanocomposites

Through the test carried out by ITI, it was observed that for certain specimen fractures eventuated from the grips instead of the specimen gauge length. The data from these particulars, specimens were excluded from consideration since they would prove to be ineffectual in the determination of the mechanical properties. The data of force and elongation undergone by each of the tested specimens are as follows:

- Unfilled sample (0wt % graphene)

Table 5. Force and elongation for the unfilled sample

Specimen	Force (N)	Elongation (mm)
1	14.7	185.03
2	18.3	188.63
3	14.7	170

- 2.5wt % graphene sample (2.5wt % graphene)

Table 6. Force and elongation for 2.5wt % of the graphene sample

Specimen	Force (N)	Elongation (mm)
1	30	190
2	16.7	160
3	10.7	160
4	31.7	200

- 5wt % graphene sample (5wt % graphene)

Table 7. Force and elongation for 5wt % of the graphene sample

Specimen	Force (N)	Elongation (mm)
1	39.3	230
2	29	230
3	37	220

- 10wt % graphene sample (10wt % graphene)

Table 8. Force and elongation for 10wt % of the graphene sample

Specimen	Force (N)	Elongation (mm)
1	15	190
2	27	200
3	13	180
4	25.3	210
5	15.3	180

- 20wt % graphene sample (20wt % graphene)

Table 9. Force and elongation for 20wt % of the graphene sample

Specimen	Force (N)	Elongation (mm)
1	13.7	180
2	21	200
3	29.3	200
4	23	180

Based on the data for each sample, the tensile strength and elongation at break were determined to be:

- Unfilled sample (0wt % graphene)

Table 10. Tensile strength and elongation at break for the unfilled sample

Specimen	Tensile strength (MPa)	Elongation at break (%)
1	1.749	560.70
2	2.551	571.61
3	1.727	515.15

- 2.5wt % graphene sample (2.5wt % graphene)

Table 11. Tensile strength and elongation at break for 2.5wt % of the graphene sample

Specimen	Tensile strength (MPa)	Elongation at break (%)
1	3.450	575.76
2	2.092	484.85
3	1.346	484.85
4	3.658	606.06

- 5wt % graphene sample (5wt % graphene)

Table 12. Tensile strength and elongation at break for 5wt % of the graphene sample

Specimen	Tensile strength (MPa)	Elongation at break (%)
1	4.586	696.97
2	3.467	696.97
3	4.150	666.67

- 10wt % graphene sample (10wt % graphene)

Table 13. Tensile strength and elongation at break for 10wt % of the graphene sample

Specimen	Tensile strength (MPa)	Elongation at break (%)
1	1.860	575.76
2	3.400	606.06
3	1.649	545.45
4	2.993	636.36
5	1.872	545.45

- 20wt % of the graphene sample (20wt % graphene)

Table 14. Tensile strength and elongation at break for 20wt % of the graphene sample

Specimen	Tensile strength (MPa)	Elongation at break (%)
1	1.729	545.45
2	2.450	606.06
3	3.548	606.06
4	2.959	545.45

The mean mechanical properties of the NR-graphene nanocomposites prepared through latex mixing and acid-coagulation are shown in Table 15. From the data observed in Table 15, it is apparent that the tensile properties of the NR notably increases on the addition of the graphene nanofiller in comparison to pristine NR. It can be identified that on the addition of 5wt% graphene, the tensile

strength of NR is enhanced by almost 102% while the elongation at break exhibits an improvement by almost 25%.

Table 15. Average tensile properties for each sample tested

Test No.	Formulation	Tensile strength (MPa)	Elongation at break (%)
1	40g NR latex	2.01	549
2	40g NR latex + 2.5wt% graphene	2.64	538
3	40g NR latex + 5wt% graphene	4.07	687
4	40g NR latex + 10wt% graphene	2.35	582
5	40g NR latex + 20wt% graphene	2.67	576

The observed enhancements in the properties are likely attributed to the diffusion of the polymer particles between the particle-particle interfaces, in addition to the probable homogeneous dispersion of the nanofiller within the NR matrix.

However, once the loading of graphene is increased beyond 5wt%, a drop in the tensile properties after which no further improvement in properties seen at the 5wt%, loading can be observed. This is likely to be a result of aggregation of the graphene nanofiller at loadings greater than 5wt% Nanofiller aggregation results in an elevated difficulty for the interpenetration of the NR leading to relatively lacking tensile properties as seen in Figure 5.

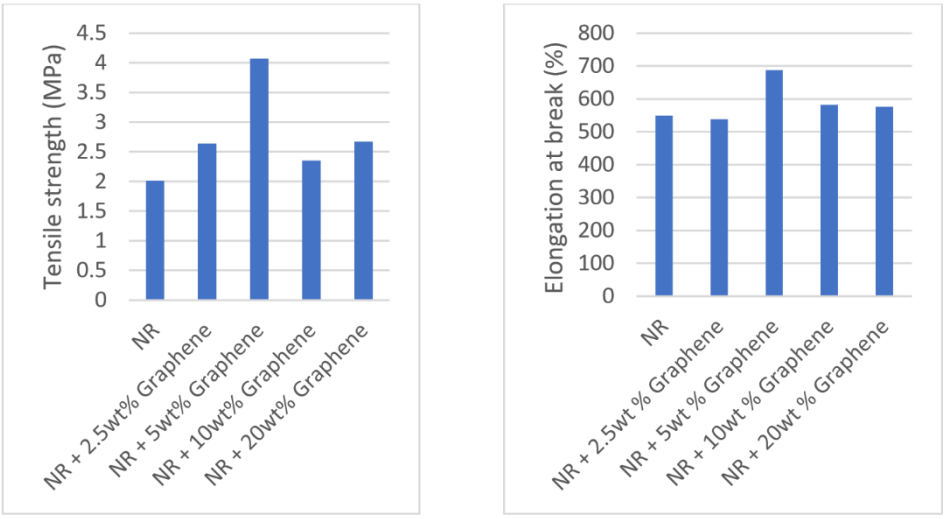

Figure 5. Graphical representation of tensile strength and elongation at break of the NR-graphene nanocomposites

4 CONCLUSIONS

In the following study, latex mixing was utilized for the dispersion of the graphene nanoparticles within the NR matrix at distinct loadings varying from 2.5 – 20 wt%. The curing methodology used for the sample preparation was acid-coagulation. Afterwards, the tensile properties of the nanocomposite samples were tested for. Through the obtained results, it was observed that the incorporation of the graphene nanofiller led to enhancements in the properties of the coagulated specimens when compared to the unfilled sample. The enhancements were likely a result of the interfacial interaction between the NR and graphene along with the likely uniform dispersion of the nanofiller within the NR matrix. From the samples tested, it was observed that the highest tensile strength and elongation at break were extracted at a graphene loading of 5wt%. This enhancement demonstrated that the incorporation of

graphene in the rubber matrix showed capability for the optimization of mechanical properties for future applications. Therefore, the improvements made to the tensile properties of the rubber encourage expansions in the field of application for the nanocomposite. Applications may include technical components in automobiles that require a higher degree of elasticity. They may also be implemented for the preparation of stronger latex gloves with better puncture resistance for use in healthcare and hygiene.

The results obtained in the study can be further optimized by refining the tested graphene loadings through the use of smaller incremental steps between 2.5wt %and 10wt %. This allows for the investigation of the rubber properties at much greater detail to refine the test results allowing a significantly precise optimum loading of graphene to be determined. The study can be further improved through modifications made to the specimen preparation procedure to ensure that the identified pre-coagulation can be minimized or eliminated. Additional considerations may include the testing of the other prevalent properties of rubber such as wear resistance, hysteresis, and dielectric properties.

5 ACKNOWLEDGEMENTS

The author expresses his gratitude to Mr. Chaminda Jayalath of Star Construction Pvt Ltd for his provision of laboratory facilities during the pandemic, thereby enabling the experimentation to be carried out.

REFERENCES

ASTM International. (2009). *Standard Test Methods for Vulcanized Rubber and Thermoplastic Elastomers - Tension.* Retrieved from UnivStrut: http://www.univstrut.com/uploadfiles/pdf/3.pdf

Bu, Q., Wang, J., Zhang, K., Lavorgna, M., & Xia, H. (2017). *Graphene-Rubber Nanocomposites: Preparation, Structure, and Properties.*

Erman, B., Mark, J. E., & Roland, C. (2013). *The Science and Technology of Rubber.* Oxford: Elsevier.

Jose, J., & Susamma, A. (2021). Studies on natural rubber nanocomposites by incorporating amine functionalised graphene oxide. *Plastics, Rubber and Composites*.

Liu, B., Pavlou, C., Wang, Z., Cang, Y., Galiotis, C., & Fytas, G. (2021). Determination of the elastic moduli of CVD graphene by probing graphene/polymer Bragg stacks. *2D Material*.

Oktriyedi, F., Dahlan, M. H., Irfannuddin, & Ngudiantoro. (2021). Impact of latex coagulant various from rubber industry in South Sumatera. *AIP Conference Proceeding 2344.*

Sur, U. K. (2012). Graphene: A Rising Star on the Horizon of Materials Science. *International Journal of Electrochemistry*.

Veerendra. (2020, December 22). *Which acid is used for coagulating rubber from latex?* Retrieved from https://www.aplustopper.com/acid-used-coagulating-rubber-latex/

Wang, Z., Liu, J., Wu, S., Wang, W., & Zhang, L. (2010). Novel percolation phenomena and mechanism of strengthening elastomers by nanofillers. *Physical Chemistry Chemical Physics*, 1-2.

Design and Dynamic Modelling of Knee Exoskeleton for Disabled People through ADAMS-Simulink Co-simulation

Jivindu P. Ranaweera[1]
[1]School of Civil and Mechanical Engineering, Faculty of Science and Engineering, Curtin University
Kent St, Bentley WA 6102, Australia

Malika Perera[2]
[2]Faculty of Engineering, Sri Lanka Institute of Information Technology
New Kandy Rd., Malabe 10115, Sri Lanka

ABSTRACT

This paper is written to outline the progress and findings of an undergraduate research project aimed at the designing and modelling of an exoskeleton design of the knee joint for rehabilitation and gait support. It focuses on the rehabilitation potential of the proposed exoskeleton design on patients with Hemiplegia and Monoplegia conditions with the objective of seeking a feasible, simple means of joint actuation to reduce the complexity of the design. Exoskeleton designs are able to provide rehabilitation and improve the overall quality of life of disabled people globally. However, a common issue found almost everywhere is the costly nature of the exoskeletons that are available in the market now as they are exclusive devices, which makes them inaccessible and impractical to the general public, especially in developing countries. Initially, the paper focuses on the review of relevant literature and previous research and evaluating the designs that have been developed as of now. A thorough analysis of the work done by previous researchers and companies was conducted to gather data on the underlying engineering principles and techniques used for the exoskeleton development as well as any limitations or restrictions to the process.

Conceptual designing of the possible solutions was developed using the understanding and knowledge gathered during the literature review. The selection of the best solution was based on the analysis of the pros and cons of all the solutions. The chosen design, utilising a 4-bar mechanism, was then modelled using SolidWorks software to provide a clear visualisation of the system. The kinematic and dynamic analysis of the mechanism was evaluated to analyse the possibility of using the proposed exoskeleton design by replicating the model in ADAMS multibody software. The dynamic analysis was conducted by using the co-simulation platform between ADAMS and Simulink to enable the addition and control of feedback loops within the system. The results of the analysis show that the design can achieve the required motions of the human gait cycle, especially during the swing phase of the gait cycle. The analysis of the actuation torques and reaction forces on the human body showed that an acceptable torque range was possible during the swing phase of the gait cycle.

KEYWORDS: *Exoskeleton, Walking-Aid, Rehabilitation, Multibody dynamics*

1 INTRODUCTION

As evident throughout history, physical disabilities have been a major cause of life-altering situations for people, irrespective of gender or social status. It is estimated that close to 10% of the world population suffers from disabilities. In fact, in developing countries, the prevalence of disability in working-age individuals is estimated to be from 3% to 16% (Mitra et al., 2013).

One main cause of physical disabilities worldwide is paralysis. Paralysis can be defined as the loss of motor or muscle function of a part of the body. In fact, studies have shown that, the number of patients suffering from various forms of paralysis can be over 1.4 million people in Sri Lanka alone (Peiris-John et al., 2014) . The main forms of paralysis are monoplegia and hemiplegia conditions. Monoplegia patients tend to lose muscle function in one limb or extremity of their body while hemiplegia patients usually lose the motor function of a complete side of their body.

Linkages are used in exoskeleton design to transfer the motion from an actuator to the exoskeleton in the desired way. Due to the nature of the linkages, they are promising in being able to reduce the torque required for the exoskeleton actuation and generate motion capable of mimicking the human gait.

As detailed in the research by (Zhang et al. 2019) it is possible to utilize linkage mechanisms, in this case a slider-crank, to provide the actuation torque of the exoskeleton. The actuation is used to generate the required range of motion of the knee joint of the user. It consists of a ball screw connected to a motor that can convert the rotary motion of the motor into a straight line motion. This moves the slider of the slider-crank mechanism which in turn actuates the crank which transfers the translational motion of the slider to the rotational movement required by the user's shank. In this particular design, the slider-crank mechanism is optimized to generate a larger torque at the necessary angles within the desired range of motion of the knee joint. It also discusses how gravity compensation was achieved using springs to reduce the torque requirement of the actuator.

In addition to this, research done by (Gilbert, Zhang, and Yin 2016) provides insight into an exoskeleton that utilizes slider-crank mechanisms at both the hip and knee joint for flexion/extension of the joints while another biped robot design by (Hamon, Aoustin, and Caro 2014) details a novel four-bar mechanism that is capable of allowing a more natural gait motion of the robot. In this case, the 4-bar mechanism is used to mimic the natural 4-bar mechanism found in the human knee joint.

While the motion of the knee joint is controlled through motor actuation, it is possible to drive the motion of the hip joint through passive actuation methods. This passive support could be either to reduce the peak power of the motor by utilising the energy-storing capabilities of springs as detailed in, (Wang, van Dijk, and van der Kooij 2011), by utilizing the springs either in parallel or series to the motor actuator, can allow the peak torque and power values required by the exoskeleton to be decreased. Additionally, spring mechanisms could also be used to counter the weight of certain links in a mechanism, which allows the actuation of that joint with less power. The gravity-balancing of links can be seen in (Arakelian 2016) where a detailed analysis is shown as to how springs can be used for this purpose and also its advantages over other mechanisms such as pulley systems.

Technological advancements and developments have led to the lives of disabled people being improved and the quality of life of these individuals has been retained. However, a common problem faced by many people in low or middle-income countries is the cost of these products. Complexity of the products has also contributed to reduced access to this technology in these countries.

Therefore, it is evident that there is an increasing need for exoskeleton designs that are more suited for these countries by devising designs that are simple, less expensive yet capable of ensuring the necessary assistance required by people with disabilities. The device also needs to use as few actuators as possible in order to reduce complexity and the cost of production.

The loss of muscle activity and strength due to medical conditions can come in two different forms. When the condition leads to weakness of the muscle it is termed as 'paresis' while complete loss of function or paralysis is termed as 'plegia'. When the loss of function is limited to one extremity or limb, it is called 'monoplegia' while the loss of function of one side of the body is called 'hemiplegia'.

This paper focuses on the development of a walking aid design focused on the rehabilitation and gait support of patients with lower-body paralysis, specifically conditions such as monoplegia and hemiplegia. The main objectives of the research are to seek a feasible, simple means of actuation of the exoskeleton, which leads to lower costs and less complexity of the design.

2 METHODOLOGY

2.1 Selection of design and determining linkage parameters

The study generated conceptual designs for the exoskeleton model. The designs were evaluated for their pros and cons to identify the best design for the exoskeleton. Once the design was selected, the viability of the proposed design to be used in an exoskeleton design was validated through the kinematic analysis of the proposed mechanism. The proposed mechanism and the alternative conceptual designs are illustrated in Figure 1 and Figure 2.

Alternative design concepts that were generated are shown in the following figure: -

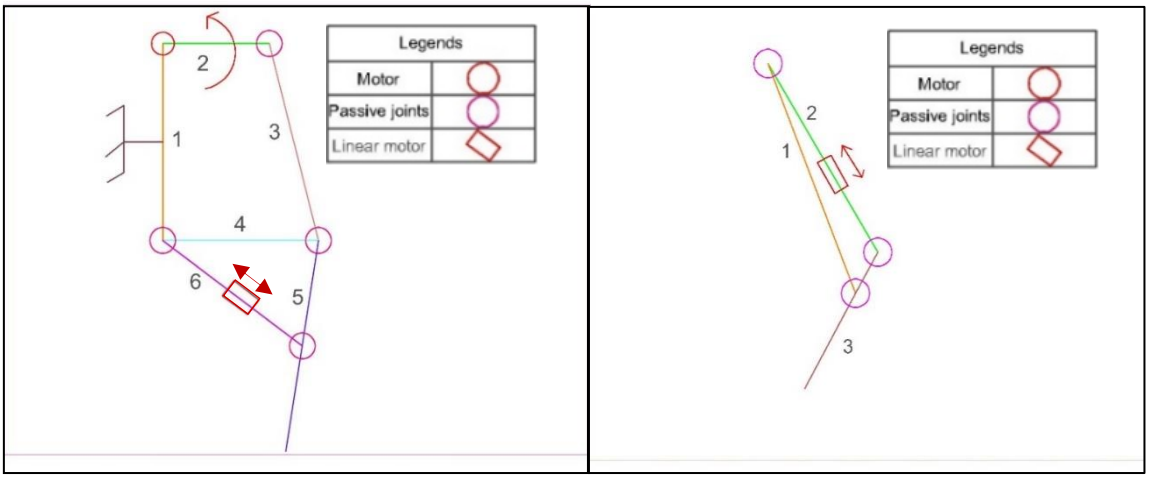

Figure 1: Alternative concept generations for the exoskeleton model

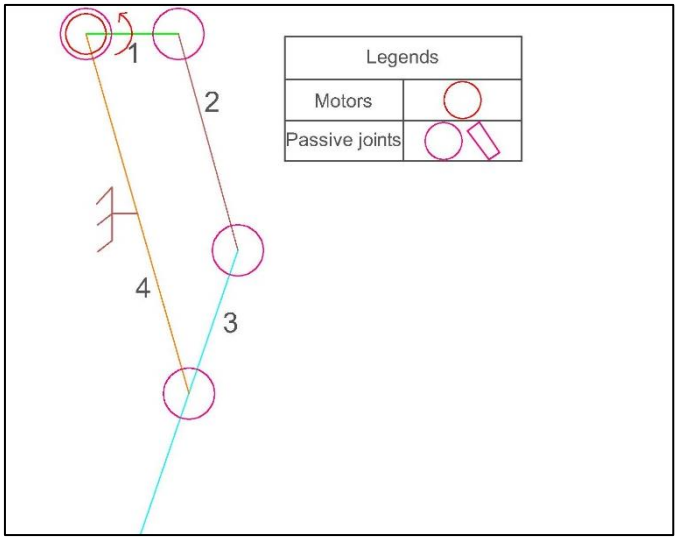

Figure 2: Selected conceptual design showing the linkage mechanism and joints

Figure 2 shows the selected conceptual design that is modelled as a modified 4-bar mechanism. The actuation of the linkage mechanism is generated at the crank arm (link 1). By using unequal lengths for the crank arm and rocker arm (link 3) it is possible to generate a larger torque at rocker arm using a lower torque at the crank arm, enabling the torque requirement of the linkage mechanism to be reduced.

Analysis using Grubler's equation (shown in equation 1) shows that the degrees of freedom of the proposed 4-bar mechanism are equal to 1 which means that the number of independent motions of the links in the mechanism is 1. Therefore, it is possible for the motion of the mechanism to be controlled through the motion of the crank arm.

$$F = 3(n-1) - 2l - h = 3(4-1) - (2 \times 4) - 0 = 1 \quad (31)$$

Where F is the number of degrees of freedom, n is the number of links, l is the number of lower pair joints and h is the number of higher pair joints.

The lengths of the linkage parts are determined to ensure that the exoskeleton is able to replicate the height and movement of the human user. Therefore, the selected link lengths must be assessed comparatively to the height of a user. The selected exoskeleton link lengths are shown in Table 1.

Table 5: The required lengths for the links of the exoskeleton to match the human user's height

Hip-knee length male (cm)	40.08
Knee-ankle length male (cm)	39.59
Total length at leg extended condition (cm)	79.67

The lengths of the proposed design of the 4-bar mechanism are selected accordingly and modelled in the ADAMS software interface as seen in the figure below: -

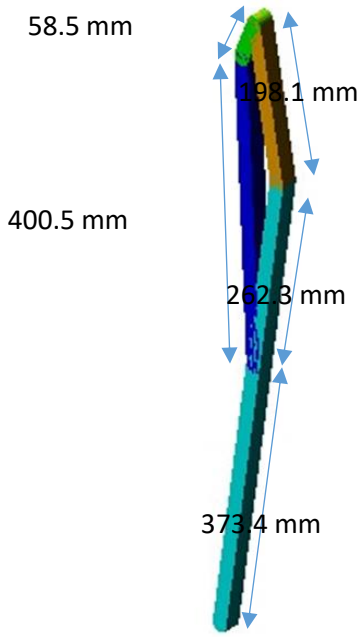

Figure 3: Lengths of the proposed 4-bar mechanism

2.2 Kinematic analysis

The kinematic analysis of the proposed 4-bar mechanism was conducted to generate the relationships between the angular velocities and angular displacements of the mechanism. This was done by applying motion functions to the crank arm (link 1) of the mechanism: -

$$STEP(time, 0.0, 0.0d, 5.0, 90.0d) + STEP(time, 10.0, 0.0d, 15.0, -90.0d) \quad (2)$$

This function induces a rotational displacement of 90° of the crank arm allowing the generation of the angular velocities of the rocker arm (link 3).

2.3 ADAMS modelling of exoskeleton and dynamic analysis

The exoskeleton design is then modelled in the ADAMS software by using the results of the kinematic analysis. The exoskeleton model is attached to a human body model to ensure that the system provides accurate results from the dynamic analysis. Actual weights of a 75kg user are added to the system to provide the necessary mass of the human body model. The weights of the individual body parts given to the human model are shown below in Table 2.

Table 6: The approximate weights of different body parts for a 75kg user

	Body segment % weight	**Appr. weight for 75kg user**
Thigh	9.88%	7.41kg
Shank	4.65%	3.49kg
Foot	1.45%	1.09kg
Torso	84.02%	63.01kg

The modified ADAMS model containing the exoskeleton and the human body model are shown in Figure 4. The 4-bar mechanism is connected to the human body model by the hip belt attachment which connects to the hip of the user.

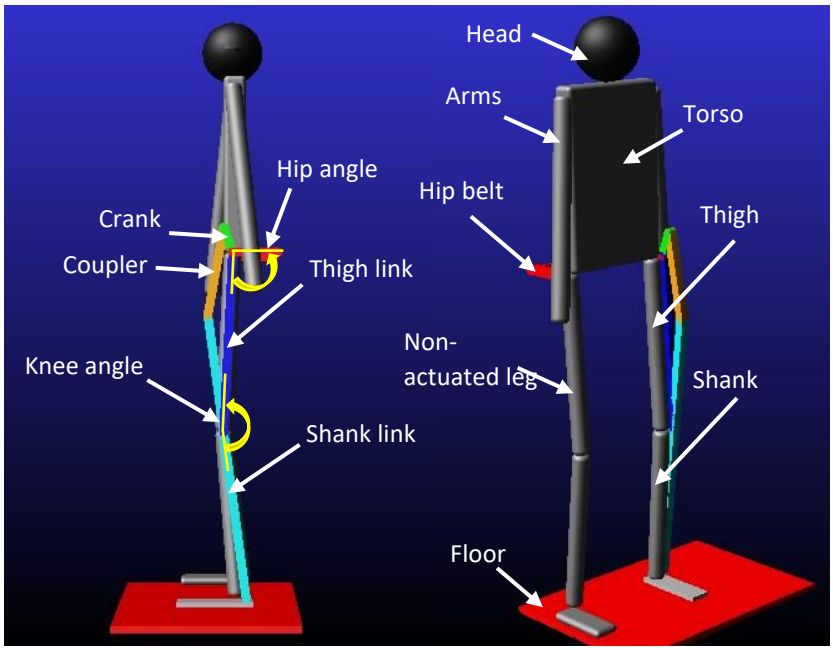

Figure 4: The modified ADAMS model showing the parts of the exoskeleton and the human body model with side-on and isometric views of the model

2.4 Addition of forces and ADAMS measures

The forces acting on the ADAMS model are defined within the system. The main forces applied to the system are the torque required at the crank arm (between the crank and hip belt), the reaction forces at the contact points of the users' legs and the floor, and the stability torque acting on the torso around a planar joint (within the sagittal plane) applied to the model to provide stability to the human body model. The movement of the model is restricted to the sagittal plane to balance the system.

The static and dynamic friction coefficients for the contact forces at the foot are given as 0.6 and 0.5 respectively. These values are consistent with the friction coefficients of the typical indoor floor surfaces. The crank torque and the stability torque of the model are controlled through feedback control loops using Simulink as the interface for the simulation. The addition of forces to the ADAMS model is shown in Figure 5.

Measures are introduced within the ADAMS software to measure the following parameters: -

1) Crank angular velocity
2) Shank link angular velocity
3) Thigh link angular velocity
4) Angular velocity of the torso

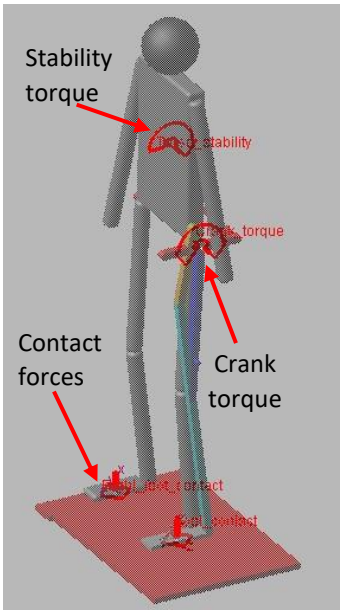

Figure 5: Figure showing the addition of forces to the model

The angular velocities of the crank and the torso are used as inputs to the Simulink model. By generating the error signal between the measured values and the desired values the feedback loop of the Simulink model provides the signals to the PI controllers. The thigh and shank link angular velocities are used to generate the angular displacement of the knee and hip joints of the human body model.

2.5 Control system design

The control system design is done using Simulink software. The model uses feedback control to generate the required responses to the system. The feedback loops use the measures generated through the ADAMS dynamic model to generate the error signal between the desired and the actual signals as the inputs to the PID controllers. The error signal is used by the PI controllers to generate the required torque for the ADAMS dynamic model to function. The desired angular velocity of the crank is shown below in Figure 6.

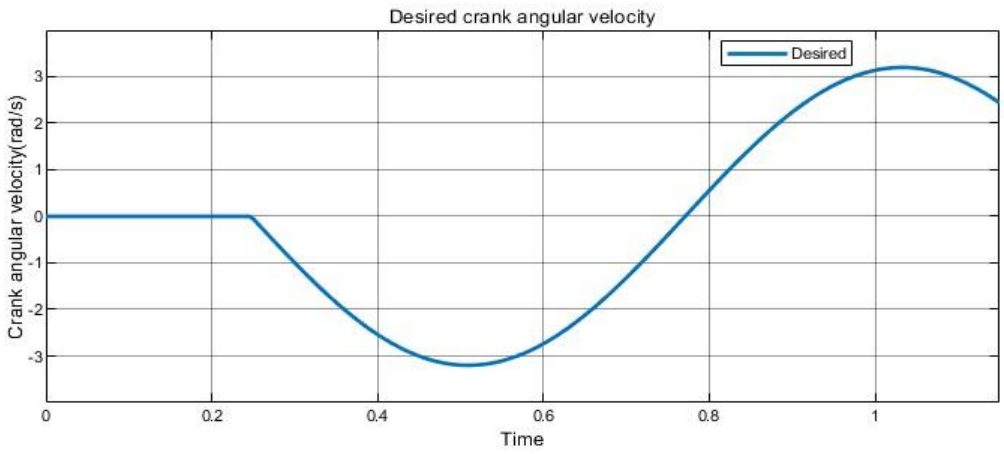

Figure 6: The desired crank angular velocity for the exoskeleton model

The PID control blocks used for the control of the crank and stability torque are shown in Figure 7.

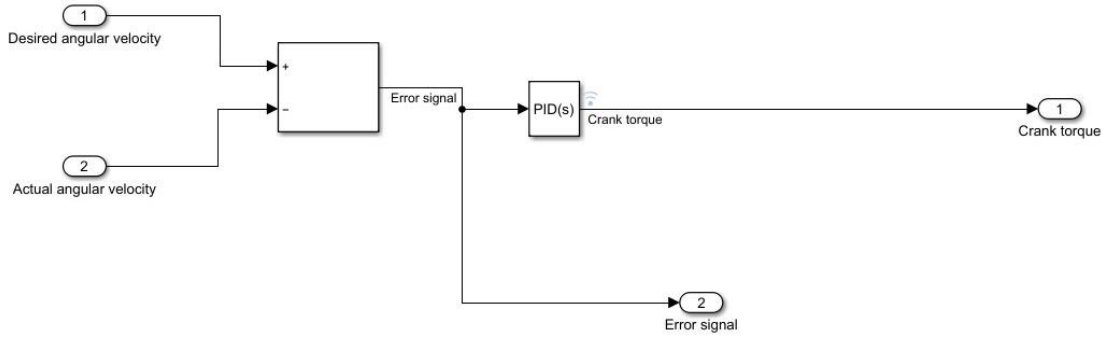

(a)

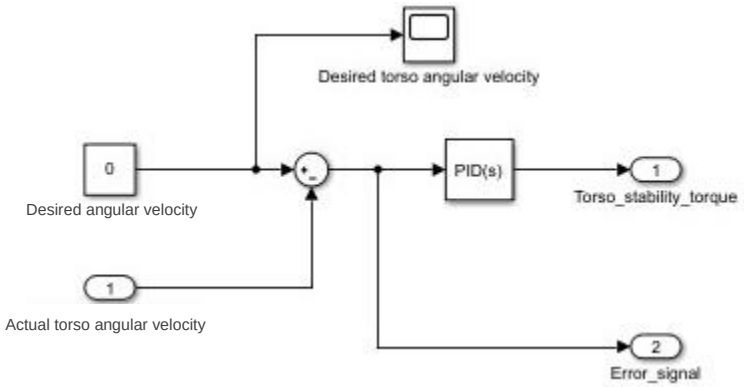

(b)

Figure 7: PID control blocks of the (a) crank torque and (b) the stability torque

2.6 Partial gravity balancing using spring

The proposed design of the 4-bar mechanism, although capable of actuating the exoskeleton, needs more support in order to actuate the hip joint of the user. Therefore, the addition of springs to balance the weight of the users' thighs is explored.

To calculate the parameters for the gravity balance springs, the mass of the body being considered must be assumed to act on one point and that the spring used is a zero-free length spring. This means that the spring exerts zero force when compressed fully. When these conditions are fulfilled (Arakelian, 2016) shows that by equaling the moment generated by the spring force and the moment due to the gravitational forces acting on the body, gravity compensation is possible. By using the following:-

$$Spring\ force\ (F_{spring}) = F_0 + k(l - l_0) \tag{3}$$

$$Potential\ energy\ (V) = mgs \sin\varphi \tag{4}$$

By balancing the moments of the spring force and the moment due to gravity,

$$V = \left(F_{spring} \times \frac{ar}{l}\right) \times \sin\varphi \tag{5}$$

Where m is the mass of the link, F_{spring} is the spring force, F_0 is the initial force of the spring, s is the length to the centre of mass of the link, a and r are the lengths from the pivot point to the spring connections and φ is the angle between the lengths a and r.

$$mgs = \left((F_0 + k(l - l_0)) \times \frac{ar}{l}\right) \tag{6}$$

For a zero-length spring, the relationship of $F_0 = kl_0$ is derived and therefore,

$$mgs = kl \times \frac{ar}{l} \tag{7}$$

$$k = \frac{mgs}{ar} \tag{8}$$

Equation 8 is used to calculate the spring stiffness required for a gravity balance spring. However, it must be noted that full gravity compensation is not required for this proposed design, therefore only partial gravity compensation is considered by reducing the mass to be lifted by the spring mechanism.

3 RESULTS AND DISCUSSION

The results of the kinematic analysis in Figure 8 show that the 4-bar actuates as expected, therefore the angular velocity of the rocker arm (shank link) would be proportional to the crank angular velocity. This means that due to the shank angular velocity being equal to the angular velocity of the knee joint, it is possible to control the knee joint motion by varying the crank angular velocity.

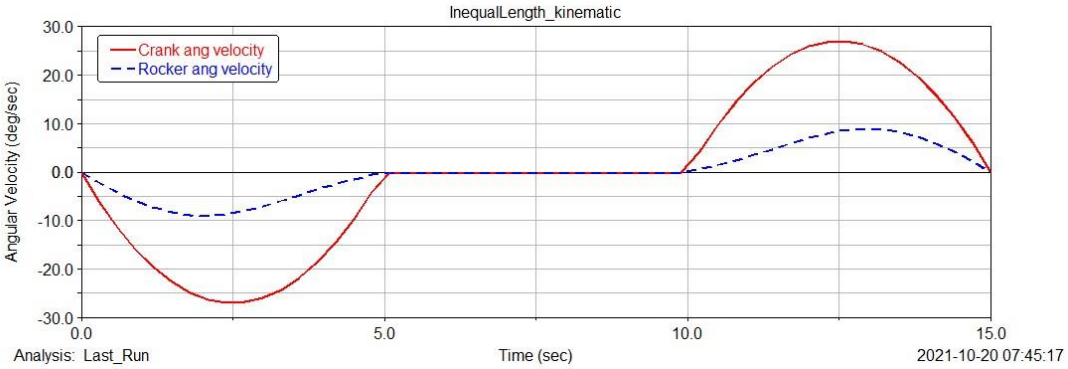

Figure 8: Rocker angular velocity with respect to the crank angular velocity

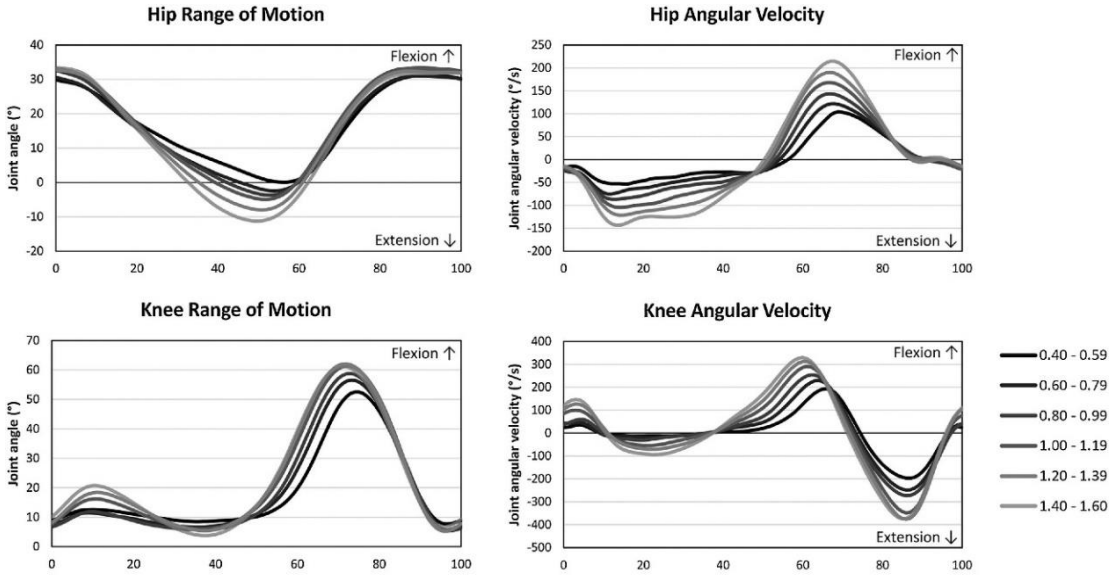

Figure 9: Natural range of motion of the human gait cycle (Mentiplay et al. 2018)

Initial dynamic analysis of the proposed design shows that the system is able to generate a good range of motion of the knee joint. The natural gait cycle of a person during the swing phase generates $30° - 50°$ of motion (Mentiplay et al. 2018), while the exoskeleton model induces a range of motion of around $20°$ By controlling the crank angular velocity, the required movement pattern of the knee joint was generated. The generated range of motion through Simulink is shown in Figure 10.

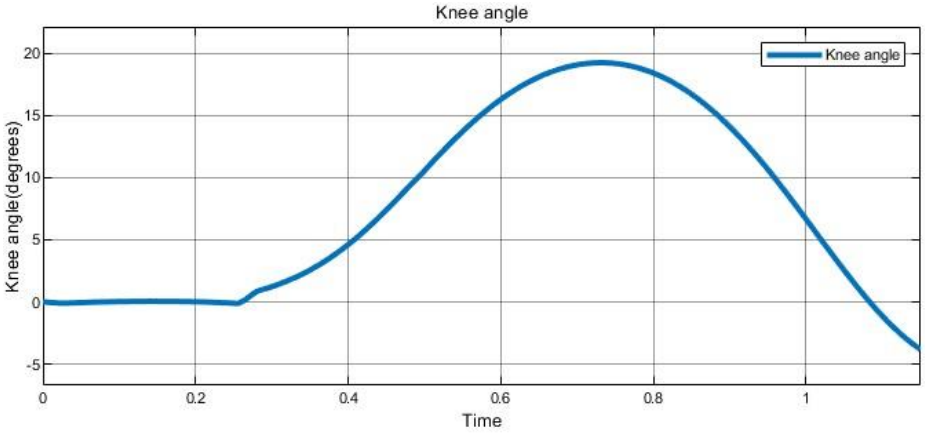

Figure 10: The knee range of motion generated through the initial simulations

However, the generated hip range of motion is relatively undesirable due to the dynamics of the proposed design as seen in Figure 11.

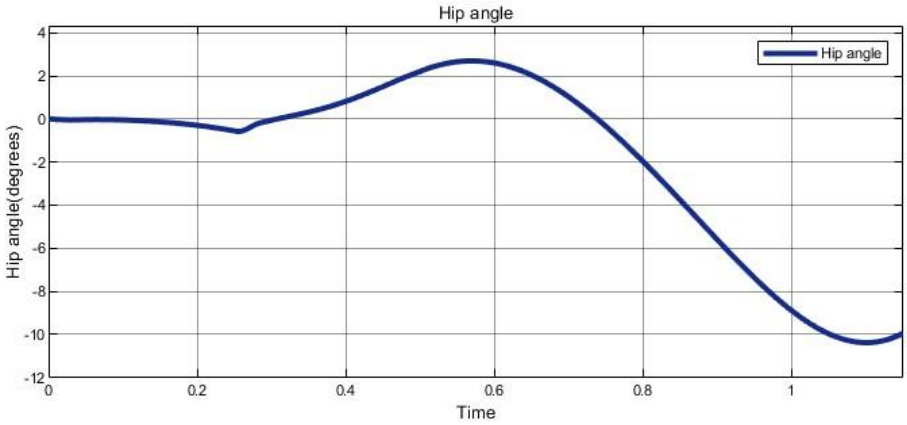

Figure 11: Undesired range of motion of the hip joint

This is due to the system inducing a negative range of motion of the hip joint as the exoskeleton rotates the user's legs backwards. The simulation results of the initial dynamic analysis shown in Figure 12 illustrates the dynamics of the simulation which show that the exoskeleton is able to generate the required motion of the knee joint at the halfway stage, even though at the simulation end, the user's legs move backwards due to the undesired hip range of motion. The undesired range of motion of the hip joint results in the need for an alternative actuation method to generate the desired range of motion of the hip joint. Therefore, the gravity balance spring is added to aid the 4-bar mechanism in actuating the hip joint of the user.

The addition of the gravity balance spring improves the range of motion of the hip joint up to $10°$ as shown in Figure 13. However, in comparison to the natural gait cycle of $30° - 40°$, the exoskeleton hip range of motion needs improvement. The simulation results from the final dynamic analysis shown in Figure 14 incorporating the gravity balance spring, illustrate the improved motions generated through the addition of the springs. The improved model is able to produce better motion of the exoskeleton to allow for the desired motion at the end of the gait cycle by inducing better motion of the hip joint.

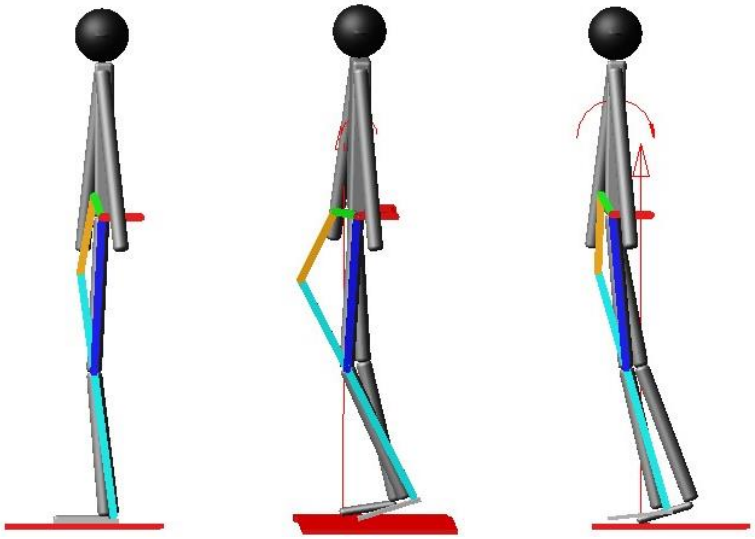

Figure 12: Simulation results of the initial dynamic analysis showing the movement pattern of the dynamic model at t = 0s, t = 0.6s, t = 1.2s respectively

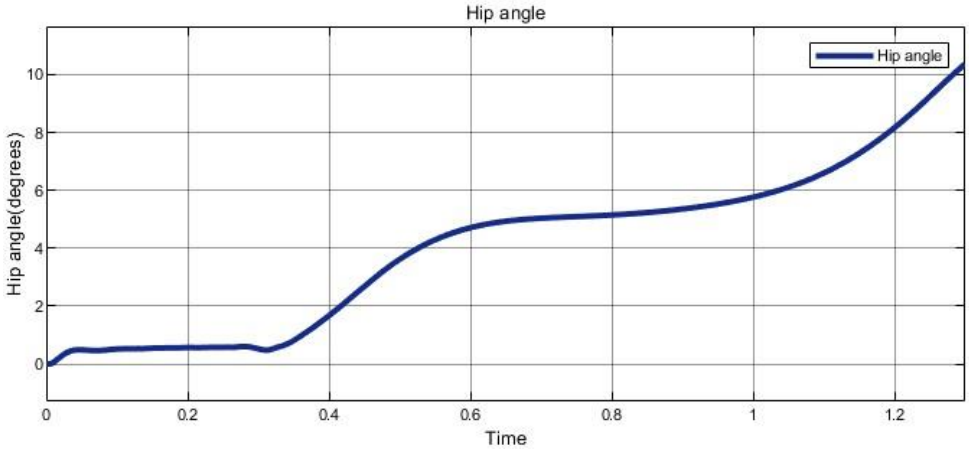

Figure 13: Improved hip range of motion through the addition of the spring mechanism

The torque requirement at the crank is generated through the Simulink interface. Figure 15 shows the crank torque requirement of the exoskeleton.

As seen in Figure 14, the crank torque peaks at around 14 Nm during the simulation. This torque is the torque required during the standing phase ($t = 0\ to\ t = 0.25s$) or when the exoskeleton bears the full weight of the model. During the swing phase ($t = 0.5s\ to\ t = 1.3s$) or during the flexion and extension of the knee joint, the crank torque can be seen to be below 1 Nm.

The reaction forces on the hip joint of the human body model are calculated to measure the impact of the exoskeleton on the users' body. The generated forces are shown in Figure 16. Through analysis of the forces, it is evident that the reaction force on the hip is generated due to both the crank torque and the moment of the spring force.

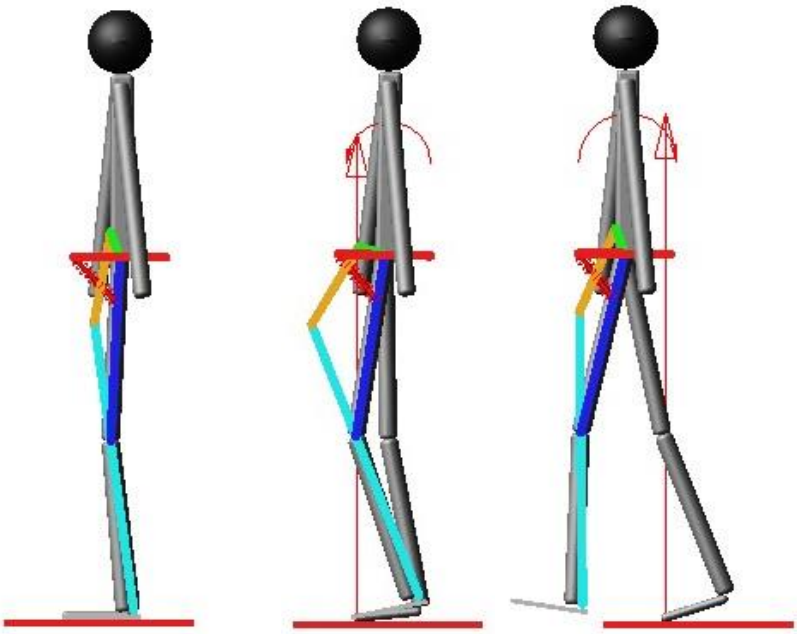

Figure 14: Simulation results of the final dynamic model with the addition of the gravity compensation springs at t = 0s, t = 0.6s, t = 1.2s respectively

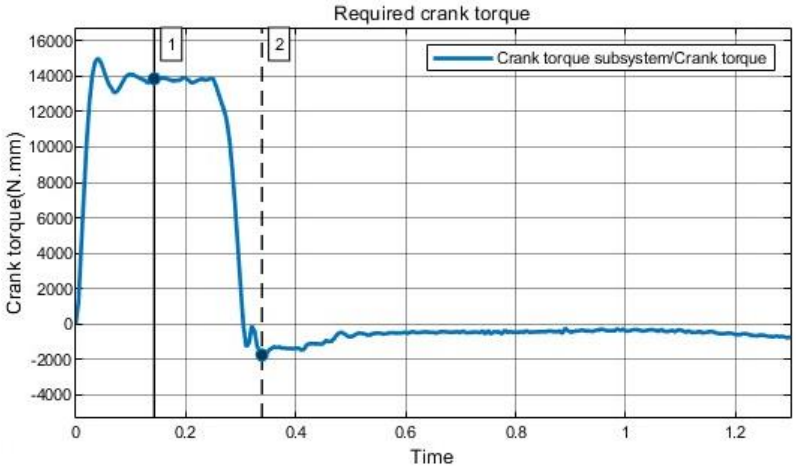

Figure 15: Crank torque required by the exoskeleton during the simulation

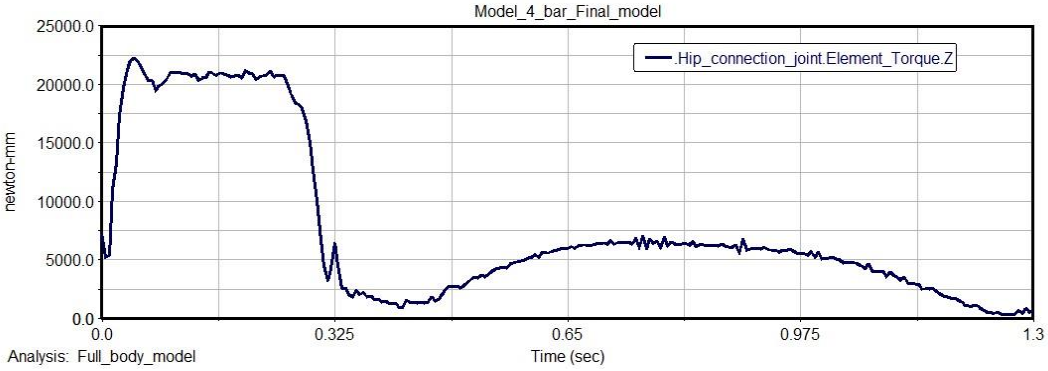

Figure 16: Reaction torque at the hip joint of the user due to the exoskeleton

4 CONCLUSIONS

The objective of this paper was to design and model an exoskeleton design that is cost effective and easy to manufacture but most importantly be usable for paralysis and stroke patients.

The exoskeleton is able to generate the required motions to allow the user to replicate the requirements of the walking cycle. The proposed design can actuate the knee joint of the user successfully using the single actuator of the 4-bar mechanism. The torque during the swing phase of the simulation is seen to be below 1 Nm without gravity compensation and under 2 Nm with gravity compensation. Improvements to the hip range of motion were done by the addition of the gravity balance springs to aid the motion of the exoskeleton. The spring mechanism was able to support the motion and enable the exoskeleton to generate a good range of motion for the hip joint. The overall system can induce a knee range of motion of 20 degrees and a hip range of motion of 10 degrees during the simulation. The feedback control system used for the system control was able to respond well to the requirements of the desired exoskeleton movements. The simplicity of the proposed 4-bar mechanism reduces the complexity of the exoskeleton to aid the manufacturing process.

Further improvements could be made to the exoskeleton design by optimizing the gravity balance spring mechanism and adding a framework to the exoskeleton to aid the user in withstanding the torque generated at the hip joint.

REFERENCES

Arakelian, V. (2016). Gravity compensation in robotics. *Advanced Robotics*, *30*(2), 79–96. https://doi.org/10.1080/01691864.2015.1090334

Mitra, S., Posarac, A., & Vick, B. (2013). Disability and Poverty in Developing Countries: A Multidimensional Study. *World Development*, *41*(1), 1–18. https://doi.org/10.1016/j.worlddev.2012.05.024

Peiris-John, R. J., Attanayake, S., Daskon, L., Wickremasinghe, A. R., & Ameratunga, S. (2014). Disability studies in Sri Lanka: Priorities for action. *Disability and Rehabilitation*, *36*(20), 1742–1748. https://doi.org/10.3109/09638288.2013.864714

Zhang, Zongwei, Yanhe Zhu, Tianjiao Zheng, Sikai Zhao, Shun Ma, Jizhuang Fan, and Jie Zhao. 2019. "Lower Extremity Exoskeleton for Stair Climbing Augmentation." In *ICARM 2018 - 2018 3rd International Conference on Advanced Robotics and Mechatronics*, 762–68. Institute of Electrical and Electronics Engineers Inc. https://doi.org/10.1109/ICARM.2018.8610718.

Hamon, A., Y. Aoustin, and S. Caro. 2014. "Two Walking Gaits for a Planar Bipedal Robot Equipped with a Four-Bar Mechanism for the Knee Joint." *Multibody System Dynamics* 31 (3): 283–307. https://doi.org/10.1007/s11044-013-9382-7.

Gilbert, Masengo, Xiaodong Zhang, and Gui Yin. 2016. "Modeling and Design on Control System of Lower Limb Rehabilitation Exoskeleton Robot." In *2016 13th International Conference on Ubiquitous Robots and Ambient Intelligence, URAI 2016*, 348–52. Institute of Electrical and Electronics Engineers Inc. https://doi.org/10.1109/URAI.2016.7734058.

Wang, Shiqian, Wietse van Dijk, and Herman van der Kooij. 2011. "Spring Uses in Exoskeleton Actuation Design." *IEEE International Conference on Rehabilitation Robotics*. https://doi.org/10.1109/ICORR.2011.5975471.

Mentiplay, Benjamin F., Megan Banky, Ross A. Clark, Michelle B. Kahn, and Gavin Williams. 2018. "Lower Limb Angular Velocity during Walking at Various Speeds." *Gait and Posture* 65 (September): 190–96. https://doi.org/10.1016/j.gaitpost.2018.06.162.


SLIIT
FACULTY OF ENGINEERING


SLIIT
SLIIT UNI
THE KNOWLEDGE UNIVERSITY